Convex formulations of inverse modeling problems on systems modeled by Hamilton-Jacobi equations: applications to traffic flow engineering

Christian Claudel

Electrical Engineering and Computer Sciences
University of California at Berkeley

Technical Report No. UCB/EECS-2011-5
http://www.eecs.berkeley.edu/Pubs/TechRpts/2011/EECS-2011-5.html

January 20, 2011

Acknowledgement

I gratefully acknowledge Professors Bayen (CEE) and Tomlin (EECS) for their guidance.

Convex formulations of inverse modeling problems on systems modeled by Hamilton-Jacobi equations: applications to traffic flow engineering

by

Christian G. Claudel

A dissertation submitted in partial satisfaction of the
requirements for the degree of
Doctor of Philosophy

in

Engineering - Electrical Engineering and Computer Sciences

in the

Graduate Division

of the

University of California, Berkeley

Committee in charge:

Professor Claire J. Tomlin, Chair
Associate Professor Alexandre M. Bayen
Professor Laurent El-Ghaoui

Fall 2010

Convex formulations of inverse modeling problems on systems modeled by Hamilton-Jacobi equations: applications to traffic flow engineering

Abstract

Convex formulations of inverse modeling problems on systems modeled by Hamilton-Jacobi equations. Applications to traffic flow engineering

by

Christian Claudel

Doctor of Philosophy in Engineering - Electrical Engineering and Computer Sciences

University of California, Berkeley

Professor Claire Jennifer Tomlin, Chair

This dissertation presents a new convex optimization-based estimation framework for systems modeled by scalar Hamilton-Jacobi equations. Leveraging the control framework of viability theory, we characterize the solutions to the Hamilton-Jacobi equation by a Lax-Hopf formula, and show that the solution satisfies an inf-morphism property. These two properties, enable us to construct a semi-analytic formula for the solution associated with piecewise affine initial, boundary and internal conditions. The semi-analytic solution is the first major contribution of the thesis. This enables the construction of a scheme which provides numerical solutions of the partial differential equation. In addition to being gridless, the semi-analytic numerical scheme has two main advantages over standard computational methods: it is both exact and very fast.

Using the semi-analytic formulation of the solution, we also prove that the Hamilton-Jacobi equation restricts the possible values that the piecewise affine initial, boundary and internal conditions can take, and that the corresponding set of possible values can be expressed in the form of convex constraints. This enables the creation of a framework for solving inverse modeling problems on systems modeled by Hamilton-Jacobi equations using linear programming, which is a contribution of the thesis. The formulation of these inverse modeling problems as convex programs was previously unknown. More generally, the thesis outlines a series of problems, which can now be cast in convex form, thanks to the semi-analytic solution proposed in the first part of the thesis. We apply this framework to solving several inverse modeling and estimation problems arising in transportation engineering, using experimental data from fixed sensors and mobile GPS devices. The problems that can be solved using linear programming include four classes of problems: data consistency verification, data assimilation, data reconciliation, and coefficient estimation. Data consistency verification is used to check if the measurements are compatible with the model assumptions, and are applied to sensor fault detection for instance. Data assimilation and data reconciliation techniques enable the estimation of the state of the system in situations for

which the model constraints are incompatible with the measurement constraints. When the model and data constraints are compatible, some quantities related to the state (for instance travel time in the context of transportation engineering) can be estimated using coefficient estimation.

To Coralie...

Contents

List of Figures

Acknowledgments

I would like first to express my deepest gratitude to my two advisors Professor Alexandre Bayen and Professor Claire Tomlin for their help and support ever since I arrived to Berkeley in 2007. I am forever indebted to Alexandre, who gave me the opportunity to join his research group. During these years of PhD studies, Alexandre has been an exceptional mentor, available to help me 24/7 in my research and sending me to the nicest conferences around. Alexandre also taught me more about myself than anybody else.

It has been an honor to be advised by Claire. Her vision and scientific achievements are an inspiration for all of us. Her outstanding teaching qualities motivated me to become a professor myself.

I would like to thank Professor Laurent El-Ghaoui for serving on my Dissertation Committee and Professors Murat Arcak and Jean Walrand for serving on my Qualifying Exam Committee.

Professors Jean-Pierre Aubin and Patrick Saint-Pierre are gratefully acknowledged for their vision and for their scientific generosity. Jean-Pierre suggested to me new ways of approaching an old problem. His expertise in Hamilton-Jacobi equations was extremely helpful for deriving my results. Patrick's advice on numerical computations was also invaluable.

I would also like to thank Professor Carlos Daganzo, who was the first to formulate the traffic flow model used in this thesis as a Hamilton-Jacobi equation.

The Mobile Millennium gang was a fantastic team to work with. I would like to thank the French connection (Aude, Julie, Pierre-Emmanuel, Sébastien, Timothy), the Chicago syndicate (Dan, Matthieu, Olli-Pekka) and numerous other gangsters: Andrew, Mohammad, Ryan, Samitha, Saurabh and Tarek, for being so nice to work with. I will miss you all!

The support staff of the CCIT was also wonderful. Saneesh Apte, Joe Butler, Daniel Edwards and Tom West have been working hard during the last three years to make Mobile Millennium a success.

On a more personal note, I would like to thank my parents Jacques and Anne-Marie, and my sisters Aurélia and Anne-Claire who always offered me their love, support and help.

Finally, my wife Coralie offered me her endless love during all these years at UC Berkeley, and the strength to overcome difficulties. I want to dedicate my thesis to her.

Chapter 1

Introduction

‘

1.1 Background

Traffic congestion is a major issue in urban environments. Regardless of its cause, it creates both delays and increased fuel consumption, which has a major impact on the economy. In the United States alone, the cost traffic congestion is approximately $500 per driver per year and the total annual cost of traffic congestion represents 0.5% of the GDP [43]. Since congestion occurs when user demand exceeds the infrastructure capacity, congestion can be solved by either increasing the infrastructure capacity (for instance building new roads), or reducing user demand (for instance through better traffic information systems). With the decreasing cost of sensors and the increasing number of computational platforms (for instance GPS-enabled smartphones) that can act as sensors [101] themselves, there is now an unprecedented amount of traffic data, which can be leveraged to provide better traffic information. This information in turn could be used to help reduce congestion, by providing traffic management authorities with the proper tools to spread used demand over the day more efficiently.

While increasing quantities of traffic measurement data become available, the problem of estimating traffic from significantly different data sources is very complex. The highway network is usually modeled as a distributed parameter system, which means that it can be viewed as an infinite dimensional system. In addition, the physics of traffic are known to be nonlinear. Finally, measurement data comes from different types of sensors which do not necessarily measure the same physical quantities. The main goal of this dissertation is to address the problem of integrating the constraints of the traffic model in a tractable manner, using a convex-optimization based framework. This framework is applied to solve various estimation problems arising in transportation engineering, using experimental data.

1.2 Partial differential equation models of large scale infrastructure systems

Large scale infrastructure systems, such as transportation networks, networked water channels, or air transportation networks are *distributed parameter systems*, that is, their state is usually described by a function of space and time, in contrast to a finite dimensional vector. Another way to think about this would be as an "infinite dimensional" vector. A common mathematical tool for modeling such systems is *partial differential equations* (PDEs). They provide an efficient way of representing physical phenomena in a mathematically compact manner, which integrates the distributed features of the systems of interest [44].

Among PDEs, a specific class stands out, *conservation laws* [71, 19], which model phenomena in which a balance equation governs the physics (for example mass balance, momentum balance, charge balance, etc.). Water channels for instance can be modeled using the *Saint-Venant PDE* [73], obtained from the conservation of water mass and momentum. Examples of applications of such models can be found in [34, 84, 74, 34]. Ground [72, 86] and air transportation networks [92] can both be modeled by the *Lighthill-Whitham-Richards* (LWR) PDE, which is based on the conservation of vehicles. Alternatively, traffic flow can also be modeled using *second order models* [33, 11, 81, 17, 100], which are non-scalar conservation laws. All these PDEs and others used to describe distributed parameter systems are not necessarily conservation laws however. In structural engineering for instance, beam deformation can be modeled by the *Euler-Bernoulli beam* PDE [66], which is not a conservation law. In electrical engineering, the *Telegraph equation* [50] can be used to model wave propagation in telecommunication lines, and is also not a conservation law.

1.3 Control and estimation of partial differential equations

1.3.1 Filtering based methods

State estimation and control for PDE-based systems is more complex than for their *ordinary differential equation* (ODE) based counterparts, because of the distributed nature of the state.

The tools available for estimating [90] and controlling [66] the states of an ODE can be extended to systems modeled by a PDE, for instance using variations of *Kalman Filtering* (KF), originally derived for systems modeled by linear ODEs [15]. *Extended Kalman Filtering* (EKF) [3] is a modification of Kalman filtering for nonlinear systems. EKF techniques have been applied to water channels state estimation problems in [46], and in traffic flow estimation problems in [96, 3] for instance.

The EKF can however perform poorly for specific nonlinear systems, for which *Monte*

Carlo techniques are a possible alternative. For example, when the dynamics exhibits nonsmoothness or nondifferentiability, EKF is known to have problems [97]. Monte Carlo methods involve estimating the current probable value of the state, computing the state evolution, and comparing it against new measurement data to obtain a current estimate. By their nature, Monte-Carlo based methods can apply to any model, albeit with some computational cost penalty. *Ensemble Kalman Filtering* (EnKF) [47] is a Monte-Carlo based method that can be used for systems modeled by nonlinear PDEs, for instance the LWR [97] PDE, without approximating the model around the current estimate as done in EKF. Other examples of application of EnKF include Shallow Water Equations [94], or meteorology [62]. The EnKF samples the possible current states of the system according to a probability distribution, computes the evolution of these samples, and combine these evolutions with new measurements to obtain the best estimate of the state. The *Mobile Millennium* system [101] is an example of operational implementation of the EnKF for traffic flow modeling using the LWR PDE. More generally, the state of distributed parameter systems can be estimated using *Particle Filtering* (PF), which can be used for general nonlinear systems, albeit with a higher computational cost [26].

1.3.2 Other methods

Backstepping methods [66] are control design methods that can be applied to some classes of nonlinear systems. They involve designing a controller for a known-stable system and "back out" new controllers that progressively stabilize each outer supersystem.

The theory of *differential flatness*, which was originally developed in [49], consists in a parametrization of the trajectories of a system by one of its outputs, called the "flat output" [82, 1]. It can be used to control the state of water channels [85] for instance.

Lyapunov methods [65] are based the extension of the Lyapunov theory for ODE-based systems to the PDE case. Similarly to ODE-based systems, they involve the use of a *Lyapunov function* associated with the state of the system, and which is either bounded or decreasing.

Machine learning methods [63] in contrast rely on experimental datasets to learn how the state evolves. One of the main focuses of machine learning methods is to automatically learn to recognize specific patterns using statistical methods [2]. Machine learning methods can be applied to very different problems, including estimation problems [59] on systems modeled by PDEs.

Finally, spectral methods [99, 27] use modal decomposition techniques to transform dynamic constraints into static constraints in the frequency domain, and subsequently obtain a static inverse modeling problem, which is easier to solve.

One of the major difficulties arising when dealing with sensing problems on systems modeled by PDEs is the integration of the model constraints into the estimation problem. The PDEs investigated in this dissertation are nonlinear. Their solutions can be nonsmooth and even discontinuous, which makes the model constraints difficult to derive. One of the

contributions of this dissertation is to express the model constraints as convex inequalities, which are both explicit and computationally tractable.

1.4 Hamilton-Jacobi equations

In one dimensional systems (for example to model the highway network), hyperbolic scalar conservation laws have a direct counterpart in *Hamilton-Jacobi* (HJ) theory [44], which is the subject of this dissertation. HJ PDEs [12] have a particular importance in optimal control, and more generally in variational problems, for which they were originally derived.

Because of their structure, the solutions to a given HJ PDE satisfy the HJ PDE in a generalized sense, and are thus called *weak solutions*. Several classes of weak solutions to HJ PDEs exist. Historically, *viscosity solutions* [36, 35] were the first class of weak solutions identified for HJ PDEs. They were initially discovered by taking the limit of the solutions to a modified HJ PDE in which a viscosity term is added, when the value of this term converges to zero, leading to the term of "vanishing viscosity", initially used to describe them. Viscosity solutions are continuous, but not necessarily differentiable everywhere. *Barron-Jensen/Frankowska* (BJ-F) solutions [14, 52] generalize the concept of viscosity solutions by allowing the solution to be discontinuous. A third concept of solutions is sometimes used, so called "nonsmooth solutions", based on nonsmooth analysis [28].

HJ PDEs also integrated the framework of *differential games* [45, 22, 23], which model problems containing two actors, a pursuer and an evader, with conflicting goals. They can for instance be used to solve aircraft safety problems [78] by computing the set in which an evader aircraft is always safe from a pursuer aircraft that attempts to collide with it.

The solutions used in the present work are obtained using a *Lax-Hopf* [68] formula, which expresses the solution at any given point as a minimization (or maximization) problem.

1.5 Numerical analysis for Hamilton-Jacobi equations

The solutions to HJ PDEs (and their conservation laws counterparts) can be computed numerically using various methods, relying either on the structure of the PDE (finite difference schemes), the structure of their solutions (wave-front tracking methods), a different expression of the problem (level set methods), or the Lax-Hopf formula (dynamic programming, Lax-Hopf algorithm). The most basic numerical schemes that can be thought of are *finite difference schemes*, such as the Godunov scheme [54], or the Lax-Friedrichs method [64]. Finite difference methods require the approximation of the PDE as a finite difference equation on a computational grid. The finite difference equation is then solved numerically. Finite difference schemes compute approximate solutions, and are often subject to stability conditions, such as the *Courant-Friedrichs-Levy* (CFL) condition, which constrains the

computational grid [71].

Level set methods [77, 76] rely on finite difference schemes to numerically approximate the solution with subgrid accuracy and avoid their high cost of grid refinement. They can be extended in some cases by *fast marching methods* [89], which are computationally efficient (but have specific restrictions in their possible applications).

Wave-front tracking methods [19, 38] in contrast rely on the structure of the mathematical solutions to hyperbolic conservation laws, which feature *shockwaves* and *expansion waves*. Wave-front tracking methods are event-based numerical methods that compute the location of these waves, and thus derive the expression of the solution everywhere because of its structure.

Finally, the Lax-Hopf formula used in the present work can be solved numerically to compute the solution as a minimization problem. Possible solution methods include *dynamic programming* [44, 41] or the Lax-Hopf algorithm derived in this dissertation, adapted from [8].

1.6 Contributions

The first contribution of this dissertation is the construction of a new grid-free solution procedure known as the *Lax-Hopf algorithm* for solving Hamilton-Jacobi equations and their associated scalar conservation laws. This numerical scheme exhibits two main benefits with respect to standard first-order schemes. Firstly, the solutions computed using the Lax-Hopf algorithm are exact, *i.e.* do not exhibit error aside from the error due to numerical accuracy of the numerical software used to compute them. Secondly, the solution can be computed at any time without requiring intermediate computations, unlike (first-order) finite difference schemes which have to do so because of the *Courant-Friedrich-Lewy* (CFL) conditions.

The second contribution of the thesis is the construction of a convex-optimization based framework for computing solutions to various estimation problems on systems modeled by HJ PDEs. For this, we first establish the relationship between the physics of the problem and the value of the initial, boundary or internal conditions which are required to solve the PDE. However, it is in general impossible given our measurement data to establish the value of the initial, boundary and internal conditions univocally, because of sensor errors, coefficients that cannot be measured and constants of integration that are unknown. The measurement data constraints the possible values that the initial, boundary and internal conditions can take. Similarly the HJ PDE model also constraints the possible values that the initial, boundary and internal conditions can take. While the derivation of the data constraints is usually easy if we know how the sensors perform, deriving these model constraints is very difficult in general because of the nonlinearity of the model and the nonsmoothness of its solutions. In this dissertation, we show that the model constraints can be reduced to a set of convex inequalities, which is a desirable property. Estimation problems associated with convex objectives and constraints are usually tractable, even if the dimensionality of the problem (the number of unknown coefficients to estimate) is very high.

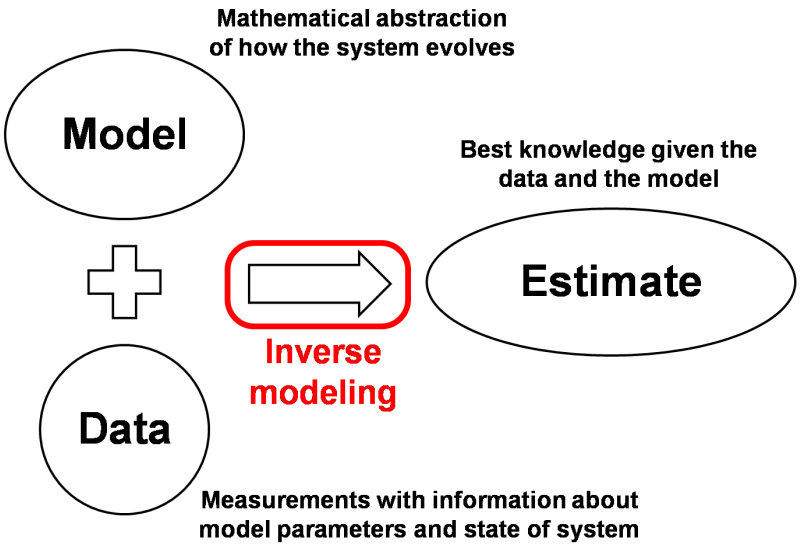

Figure 1.1: **Illustration of the state estimation procedure.**

The third contribution is the numerical implementation of this estimation framework illustrated in Figure 1.1 for solving various transportation engineering problems using experimental traffic data. The same framework can be used for very different problems, such as estimation problems (for instance travel time estimation), sensor fault detection problems, or user privacy analysis. All these problems are posed as *Linear Programs* (LPs), a particular class of convex-optimization problems for which numerous solvers exist [18].

1.7 Structure of the dissertation

The rest of this dissertation is organized as follows. We construct the Lax-Hopf algorithm introduced as the backbone of our method, and present some of its benefits and applications in chapter 2. For this, section 2.1 introduces the HJ PDE model investigated in this dissertation. Section 2.2 presents the notion of *value condition*, which encompasses the traditional concepts of initial and boundary as well as a new concept of internal conditions. We then derive a possible method for solving the HJ PDE using the control framework of *Viability Theory* in section 2.3. This method enables us to define a *Lax-Hopf formula*, which characterizes the solution. In section 2.4, we describe the mathematical properties of the solution, derived from the structure of the Lax-Hopf formula. In particular, the inf-morphism property enables us to decompose a complex problem involving multiple initial, boundary and internal conditions into more tractable subproblems. We then show in section 2.5 that the subproblems, namely the problems of computing the solutions associated with affine initial, boundary and internal conditions can be solved exactly and explicitly. Using these solutions

and the inf-morphism property derived earlier, we build in section 2.6 a semi-analytic numerical scheme for solving the HJ PDE exactly and without requiring a computational grid. We also show in section 2.7 that a similar numerical scheme can be used to solve the corresponding scalar conservation laws. Numerical illustrations and a comparison with standard first-order numerical schemes are performed in section 2.8.

The derivation of the model constraints as convex inequalities on systems modeled by HJ PDEs is presented in Chapter 3. We derive the model constraints in section 3.1 and present some important properties of the model constraints in section 3.2. Using the Lax-Hopf formula, we show that the model constraints are convex, and can be written explicitly. The nature of the model constraints also imply an important monotonicity property with respect to new data, which states that adding new data into the estimation problem can only increase the accuracy of the solution.

The applications of this framework to practical problems are presented in Chapter 4. We first establish the relationship between measurement data and initial, boundary and internal conditions in section 4.1. We then instantiate the model compatibility constraints explicitly for triangular Hamiltonians in section 4.2. We also derive the corresponding measurement data constraints explicitly (in section 4.3). In section 4.4, we introduce two fundamental convex feasibility problems that can be used to determine if the model and data constraints are compatible and if the measurement data is consistent with the physics of the problem. This is used in section 4.5 to present different estimation problems that can be solved using LPs obtained by direct instantiation of the convex problems derived earlier. We show in particular that some nonconvex estimation problems such as the travel time estimation problem can still be decomposed as a series of LPs and thus are computationally tractable. In section 4.6, we define two important inverse modeling problems for situations in which the data and model constraints are incompatible. These problems are respectively known as *data assimilation* and *data reconciliation*, and are obtained by relaxing model and data constraints respectively. We then proceed to solve different problems of interest for transportation engineering. The examples presented in this dissertation involve experimental highway traffic data sets, obtained from the *Performance Measurement System* (PeMS) and the *Mobile Century* experiment in California. Some of the resulting algorithms have been implemented in the *Mobile Millennium* system [101], in particular a sensor fault detection algorithm detailed in section 4.7 that runs in real time, every $30s$ for all highways in northern California.

Chapter 2

Fast and exact semi-analytic schemes for scalar Hamilton-Jacobi partial differential equations

2.1 Macroscopic highway traffic modeling

2.1.1 State of the art

Traffic flow models can be separated into at least two distinct classes, depending on the scale at which they describe traffic. *Microscopic models* such as the *car following model* [51], describe traffic at the individual vehicle level as a flow of particles. Their objective is to provide a relationship between the velocity of a given vehicle and its environment. In contrast, *macroscopic models* [56, 72, 86] describe traffic flow as a continuous medium and are related to fluid mechanics models. In this dissertation, we focus on the *Lighthill-Whitham-Richards* [72, 86] (LWR) model, which is a first order macroscopic flow model. Owing to its simplicity and its robustness, the LWR model and its related *cell transmission model* [39, 40] are commonly used in transportation engineering [95, 41, 3, 97]. Note that macroscopic models are not necessarily first order models, see for instance [17]. Traffic flow can also be described at an intermediate scale using *mesoscopic models* [21]. Mesoscopic models follow methods of statistical mechanics, and express the solution using an integro-differential equation such as the *Boltzmann equation* [25].

Similarly to other large scale infrastructure systems such as the water channel network, the highway transportation network is a very complex graph containing highway sections connected by junctions or splits. In this dissertation, we do not consider the effects of the network and solely focus on the description of traffic flow on a highway section. Extending this framework to the whole transportation network [20, 53] requires the computation of boundary conditions of each highway section, and is out of the scope of this thesis. It is still a somewhat open problem which will require the generalization of weak boundary

conditions [13, 70], commonly used in traffic engineering [91, 97, 58].

2.1.2 First order scalar conservation laws

We define the physical (and computational) domain as the one-dimensional set $X := [\xi, \chi] \subset \mathbb{R}$, where ξ represents the *upstream boundary* and χ represents the *downstream boundary* of the domain. The upstream and downstream boundaries represent the locations at which traffic enters and exits the road section respectively.

Two macroscopic functions are used to describe the state of traffic flow on the highway section: the *density function* and *flow function*, defined as follows. The density $\rho(t, x)$ corresponds to the number of vehicles per unit distance at location x and time t. The flow $q(t, x)$ is defined as the number of vehicles that cross the point x per unit time, at time t. Both functions are related by a conservation equation expressing the fact that vehicles do not appear or disappear inside the highway section:

$$\frac{\partial \rho(t,x)}{\partial t} + \frac{\partial q(t,x)}{\partial x} \;=\; 0 \tag{2.1}$$

Equation (2.1) alone cannot be solved since it involves two different functions. In order to compute the evolution of $\rho(\cdot,\cdot)$ and $q(\cdot,\cdot)$, one needs an additional equation relating these two functions. Greenshields [56] was one of the first to identify a direct relationship between density and flow of the form $q(\cdot,\cdot) = \psi(\rho(\cdot,\cdot))$, where $\psi(\cdot)$ is a function identified since as *Fundamental Diagram* [83]. The fundamental diagram translates the fact that drivers adapt their speed to the density of vehicles that surround them. Adding this relationship into equation (2.1) yields a first order scalar conservation law involving the density function, known as *Lighthill-Whitham-Richards* [72, 86] PDE:

$$\frac{\partial \rho(t,x)}{\partial t} + \frac{\partial \psi(\rho(t,x))}{\partial x} \;=\; 0 \tag{2.2}$$

2.1.3 Hamilton Jacobi equations with concave Hamiltonians

Instead of describing traffic flow in terms of a density function [71, 91], a possible alternate formulation known as the *Moskowitz function* uses a Hamilton-Jacobi equation for describing the evolution of an integral of the function $\rho(\cdot,\cdot)$ [29, 8, 31, 32]. The Moskowitz function is physically defined as follows.

Definition 1. [Moskowitz function] Let consecutive integer labels be assigned to vehicles entering the highway at location $x = \xi$. The Moskowitz function $\mathbf{M}(\cdot,\cdot)$ is a continuous function satisfying $\lfloor \mathbf{M}(t,x) \rfloor = n$ where n is the label of the vehicle located in x at time t [41, 42, 79]. Hence, $\mathbf{M}(t,x)$ represents the label of the vehicle located at x at time t, counted from the reference point $(0,\xi)$ corresponding to the vehicle numbered 0.

The properties of the Moskowitz function have been extensively studied, for instance in the famous Newell trilogy [80]. The formal link between the density function $\rho(\cdot,\cdot)$, the flow function $q(\cdot,\cdot)$ and the Moskowitz function $\mathbf{M}(\cdot,\cdot)$ is given by:

$$\mathbf{M}(t_2,x_2) - \mathbf{M}(t_1,x_1) = \int_{x_1}^{x_2} -\rho(t_1,x)dx + \int_{t_1}^{t_2} q(t,x_2)dt \tag{2.3}$$

Conversely, the flow and density functions $q(\cdot,\cdot)$ and $\rho(\cdot,\cdot)$ are related to the spatial and temporal derivatives of the Moskowitz function $\mathbf{M}(\cdot,\cdot)$:

$$q(t,x) = \tfrac{\partial \mathbf{M}(t,x)}{\partial t} \quad \rho(t,x) = -\tfrac{\partial \mathbf{M}(t,x)}{\partial x} \tag{2.4}$$

The Moskowitz function $\mathbf{M}(\cdot,\cdot)$ solves the following equation, obtained by combining (2.4) and the LWR PDE (2.2):

$$\frac{\partial \mathbf{M}(t,x)}{\partial t} - \psi\left(-\frac{\partial \mathbf{M}(t,x)}{\partial x}\right) \;=\; 0 \tag{2.5}$$

Equation (2.5) is an *Hamilton-Jacobi* (HJ) PDE [35, 8]. In the context of HJ PDEs, the parameter $\psi(\cdot)$ is known as *Hamiltonian*, while it is known as fundamental diagram in the context of the LWR PDE (2.2) and traffic engineering [39].

2.1.4 Hamiltonian

The LWR PDE (2.2) and its associated HJ PDE (2.5) are both characterized by a Hamiltonian $\psi(\cdot)$, which describes the relationship between density and flow. For low densities, the average velocity of traffic $v(\cdot,\cdot) = \frac{q(\cdot,\cdot)}{\rho(\cdot,\cdot)}$ is close to maximal velocity allowed on the road section, denoted by $\nu^\flat$. As the density increases, traffic velocity progressively drops and vanishes for the maximal density ω that the highway section can contain and known as *jam density*. Hence, the Hamiltonian $\psi(\cdot)$ satisfies the following properties:

- $\lim\limits_{\rho\to 0} \dfrac{\psi(\rho)}{\rho} = \nu^\flat$
- the function $\rho \to \frac{\psi(\rho)}{\rho}$ is decreasing
- $\psi(\omega) = 0$

An example of flow-density plot using experimental data from the *Performance Measurement System* (PeMS) [103] is shown in Figure 2.1.

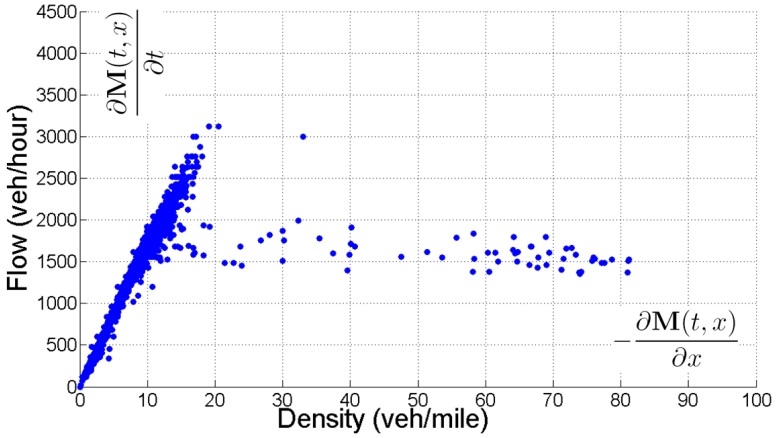

Figure 2.1: **Illustration of the flow-density relationship.**
The horizontal axis represents the density of vehicles, while the vertical axis corresponds to the flow of vehicles. Each point of this plot corresponds to a simultaneous measurement of flow and density at a fixed location, using an inductive loop detector [103].

For mathematical reasons, the Hamiltonian is often assumed to be either concave or convex [35, 8] in the HJ PDE theory, though this requirement is not dictated by the physics of the problem. In this dissertation, we assume *once and for all* that the Hamiltonian is a concave and upper semicontinuous function defined on $[0, \omega]$, where ω is called *jam density* and that $\psi(0) = \psi(\omega) = 0$. We also assume that $\psi(\cdot)$ satisfies $\psi'(0) = \nu^\flat$ and $\psi'(\omega) = -\nu^\sharp$, where $\nu^\flat > 0$ and $\nu^\sharp > 0$, which implicitly assumes that $\psi(\cdot)$ is differentiable at 0 and ω. However, we do not assume that $\psi(\cdot)$ is differentiable on $]0, \omega[$ and construct our analysis for this general set of concave $\psi(\cdot)$ functions.

Different choices of Hamiltonians satisfying these properties are possible, including the two examples presented below.

Example 1. [Greenshields Hamiltonian] [56, 5]. One of the first Hamiltonian identified in the context of traffic-flow modeling is the *Greenshields Hamiltonian* [56], defined by:

$$\forall\, \rho \in \mathbb{R}, \quad \psi(\rho) := \frac{\nu}{\omega}\rho\,(\omega - \rho) \tag{2.6}$$

where ω and ν are model parameters, respectively referred to as *jam density* and *free flow velocity* in the transportation literature. Note that the Greenshields Hamiltonian depends only on two parameters, which makes it compact and easy to calibrate. The Greenshields Hamiltonian is however not used very often in practice, since it predicts unrealistically high maximal flows.

Another example of Hamiltonian is the *Trapezoidal Hamiltonian*, widely used in traffic flow modeling [39].

Example 2. [**Trapezoidal Hamiltonian**] [39, 40, 93]. The trapezoidal Hamiltonian is commonly used to model the hybrid nature of traffic flow propagation:

$$\psi(\rho) = \begin{cases} \nu^\flat \rho & \text{if} \quad \rho \leq \gamma^\flat \\ \delta & \text{if} \quad \rho \in [\gamma^\flat, \gamma^\sharp] \\ \nu^\sharp(\omega - \rho) & \text{if} \quad \rho \geq \gamma^\sharp \end{cases}$$

where $\nu^\flat$, $\nu^\sharp$, ω, δ, $\gamma^\flat$ and $\gamma^\sharp$ are constants and satisfy the following relations: $\delta \leq \frac{\omega \nu^\flat \nu^\sharp}{\nu^\flat + \nu^\sharp}$ (called capacity in the transportation engineering literature),$\gamma^\flat := \frac{\delta}{\nu^\flat}$ (called lower critical density in the transportation engineering literature) and $\gamma^\sharp := \frac{\nu^\sharp \omega - \delta}{\nu^\sharp}$ (called upper critical density in the transportation engineering literature). When $\gamma^\flat = \gamma^\sharp$, the Hamiltonian is triangular, as used in the applications of Chapter 4.

The Greenshields and trapezoidal Hamiltonians are illustrated in Figure 2.2.

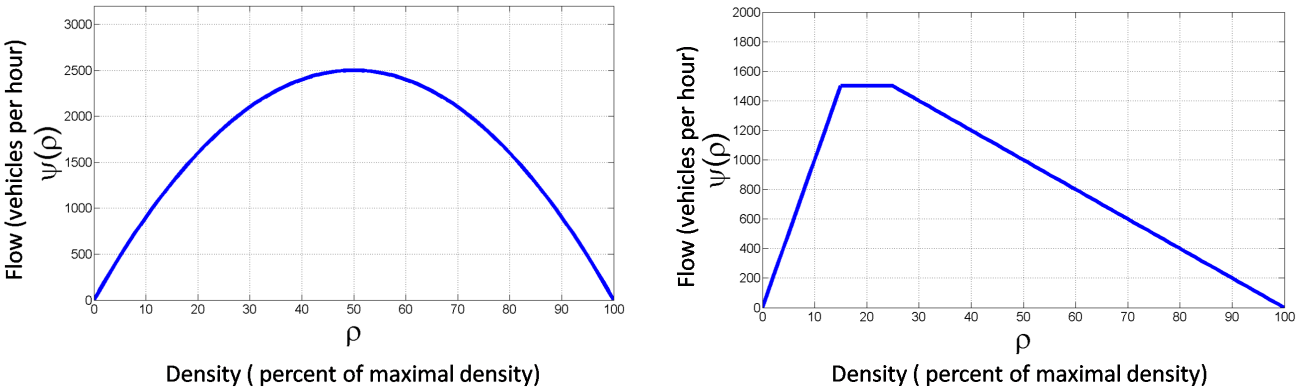

Figure 2.2: **Illustration of the Greenshields and trapezoidal Hamiltonians.** Numerical values are represented in the context of transportation, *i.e.* the variable ρ is homogeneous to the vehicle density (in percent of the maximal density). The Hamiltonian $\psi(\rho)$ is represented in vehicles per hour. **Left:** representation of a Greenshields Hamiltonian. **Right:** representation of a trapezoidal Hamiltonian.

Solving the HJ PDE (2.5) requires the definition of *value conditions*, which we now define.

2.2 Value conditions

2.2.1 General definition

Value conditions encompass the traditional concepts of initial, boundary and internal conditions and are defined as follows.

Definition 2. [**Value condition**] A value condition $\mathbf{c}(\cdot,\cdot)$ is a lower semicontinuous function defined on a subset of $[0, t_{\max}] \times X$.

By convention, a value condition $\mathbf{c}(\cdot,\cdot)$ as defined in definition 2 satisfies $\mathbf{c}(t,x) = +\infty$ if $(t,x) \notin \mathrm{Dom}(\mathbf{c})$. The domain of definition of a value condition represents the subset of the space time domain $\mathbb{R}_+ \times X$ in which we want the value condition to apply. Different types of value condition exist, including the traditional initial, upstream and downstream boundary conditions [8, 39]. More complex value conditions do exist however. Internal conditions consist in value condition whose domains of definition are connected and of empty interior [41, 69]. Hybrid conditions [29] are the most general type of value condition, but are out of the scope of this dissertation.

2.2.2 Initial, boundary and internal conditions

Initial, boundary are common in problems involving PDEs. Internal conditions are specific to the problem introduced in this thesis, though it applies to numerous other fields. These value conditions are defined as follows.

Definition 3. [**Initial condition**] An *initial condition* is a value condition $\mathbf{c}(\cdot,\cdot)$ defined on $\mathrm{Dom}(\mathbf{c}) := \{0\} \times X$.

Note that the traditional *Cauchy problem* consists in finding the solution to (2.5) associated with a value condition defined on $\{0\} \times \mathbb{R}$, *i.e.* an initial condition defined on an infinite spatial domain.

In contrast, the upstream and downstream boundary conditions are related to the value of the state on the boundaries of the physical domain.

Definition 4. [**Upstream and downstream boundary conditions**] An *upstream boundary condition* is a value condition $\mathbf{c}(\cdot,\cdot)$ defined on the set $\mathrm{Dom}(\mathbf{c}) := [0, t_{\max}] \times \{\xi\}$. A *downstream boundary condition* is a value condition $\mathbf{c}(\cdot,\cdot)$ defined on $\mathrm{Dom}(\mathbf{c}) := [0, t_{\max}] \times \{\chi\}$.

Note that the traditional *mixed Initial-Boundary conditions problem* [91] consists in finding the solution to (2.5) associated with a value condition defined on $\{0\} \times X \cup \mathbb{R}_+ \times \{\xi\} \cup \mathbb{R}_+ \times \{\chi\}$, *i.e.* an initial condition, an upstream boundary condition and a downstream boundary condition defined on an infinite temporal domain.

Note that the initial, upstream and downstream boundary conditions are all defined at the boundary of the computational domain $[0, t_{\max}] \times X$. Since probe measurements originate from the interior of the computational domain, a specific type of value condition, known as *internal condition* has to be defined as follows.

Definition 5. [**Internal condition**] An *internal condition* is a value condition $\mathbf{c}(\cdot,\cdot)$ defined on a domain of the form $\mathrm{Dom}(\mathbf{c}) := \{(t, x_v(t)),\ t \in \mathrm{Dom}(x_v)\}$, where $x_v(\cdot)$ is a function of $[0, t_{\max}]$.

In definition 5, the function $x_v(\cdot)$ represents the *velocity function* associated with the internal condition. The set $\{(t, x_v(t)),\ t \in \mathrm{Dom}(x_v)\}$ is the *trajectory* associated with the internal condition.

Note that in the applications of this dissertation, measurement data alone is not sufficient to define the value conditions unambiguously, since some of coefficients used to build these value conditions are impossible to measure, or are not perfectly known due to measurement errors.

We now present a characterization of the solutions to the HJ PDE (2.5) associated with the value conditions defined earlier. This characterization uses *Viability theory*, an area of optimal control studying the evolution of dynamical systems evolving under state constraints [6, 7] known as *viability constraints*.

2.3 Viability formulation of the solution

2.3.1 Barron-Jensen/Frankowska solutions

As mentioned earlier, several classes of solutions to HJ PDEs exist. *Viscosity solutions* [35] to HJ PDEs are continuous functions. The specific type of solutions to (2.5) that we consider in the present work is the *Barron-Jensen/Frankowska* (B-J/F) solutions [14, 52]. B-J/F solutions extend the concept of viscosity solutions by allowing the solution to be lower semicontinuous. Note that both concepts are identical for mixed initial-boundary conditions problems involving Lipschitz-continuous initial and boundary conditions [52].

The B-J/F solutions to (2.5) can be derived using the control framework of Viability theory [6], presented in the following section.

2.3.2 Viability characterization of Barron-Jensen/Frankowska solutions

We now introduce some tools used in the context of viability theory [6, 7], which are essential building blocks for the work presented here.

Definition 6. [6, 7] **[Capture basin]** Given a dynamical system F and two sets $\mathcal{K}$ (called the constraint set) and $\mathcal{C}$ (called the target set) satisfying $\mathcal{C} \subset \mathcal{K}$, the capture basin $\mathrm{Capt}_F(\mathcal{K}, \mathcal{C})$ is the subset of states of $\mathcal{K}$ from which there exists at least one evolution solution to F reaching the target $\mathcal{C}$ in finite time while remaining in $\mathcal{K}$.

Note that the capture basin associated with a given dynamical system, constraint and target set can be numerically computed using the *Capture Basin Algorithm* [22, 23, 88]. In order to properly define the dynamical system used to construct B-J/F solutions to (2.5), we first need to define a convex transform $\varphi^*(\cdot)$ of the Hamiltonian $\psi(\cdot)$ as follows.

Definition 7. [Convex transform] Given a concave and upper semicontinuous function $\psi(\cdot)$ with domain $\mathrm{Dom}(\psi)$, we define the convex transform $\varphi^*(\cdot)$ of $\psi(\cdot)$ as follows:

$$\varphi^*(u) \;:=\; \sup_{p\in \mathrm{Dom}(\psi)} [p\cdot u + \psi(p)] \tag{2.7}$$

The inverse transform of a convex and lower semicontinuous function $\varphi^*(\cdot)$ is defined [8] by:

$$\psi(p) \;:=\; \inf_{u\in \mathrm{Dom}(\varphi^*)} [\varphi^*(u) - p\cdot u] \tag{2.8}$$

Note that equation (2.7) in definition 7 differs from the traditional definition of the Legendre-Fenchel transform by a sign change.

The function $\varphi^*(\cdot)$ defined by (2.7) is convex as the pointwise supremum of affine functions [18, 87] and is defined on the interval $\mathrm{Dom}(\varphi^*) := [-\nu^\flat, \nu^\sharp]$. Since $\varphi^*(\cdot)$ is convex, it is subdifferentiable [18] on $[-\nu^\flat, \nu^\sharp]$ and its subderivative satisfies the Legendre-Fenchel inversion formula [8]:

$$u \in -\partial_+\psi(\rho) \quad \text{if and only if} \quad \rho \in \partial_-\varphi^*(u) \tag{2.9}$$

in which, following [18], we use the following definition of the subderivative $\partial_-(\cdot)$ and the superderivative $\partial_+(\cdot)$:

$$v \in \partial_-\mathcal{F}(x_0) \;\text{ if and only if }\; \forall x \in \mathrm{Dom}\,(\mathcal{F}),\;\; \mathcal{F}(x) \geq \mathcal{F}(x_0) + v(x - x_0) \tag{2.10}$$

$$v \in \partial_+\mathcal{F}(x_0) \;\text{ if and only if }\; \forall x \in \mathrm{Dom}\,(\mathcal{F}),\;\; \mathcal{F}(x) \leq \mathcal{F}(x_0) + v(x - x_0) \tag{2.11}$$

Note that any convex (respectively concave) function $\mathcal{F}(\cdot)$ is subdifferentiable (respectively superdifferentiable) on its domain of definition [18].

The convex transform satisfies $\varphi^*(-\nu^\flat) := \sup_{p\in\mathrm{Dom}(\psi)}[-p\nu^\flat + \psi(p)] = 0$ since $\psi(\cdot)$ is concave and satisfies $\psi'(0) = \nu^\flat$. In addition, it is positive by (2.7) since $\psi(0) = 0$ and $0 \in [0, \omega]$.

The convex transforms associated with Greenshields and trapezoidal Hamiltonians defined in section 2.1.4 are represented in Figure 2.3.

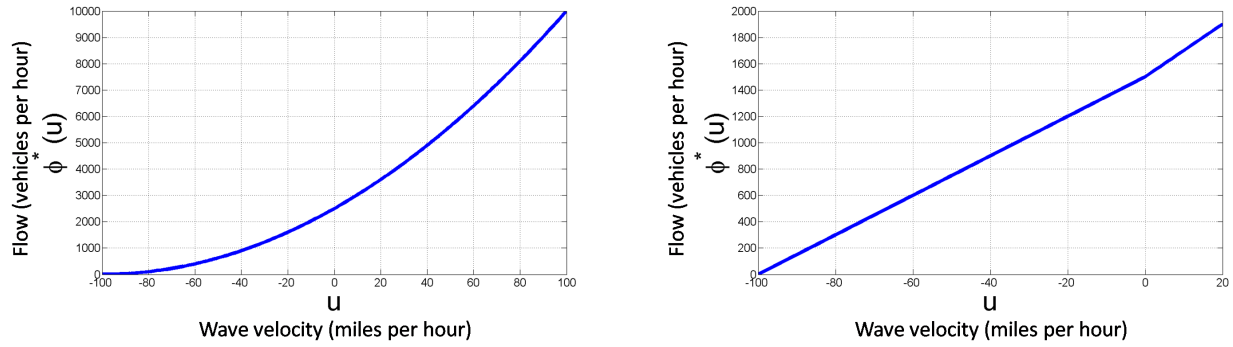

Figure 2.3: **Illustration of the convex transforms associated with the Greenshields and trapezoidal Hamiltonians.**
Left: representation of the function φ^* associated with a Greenshields Hamiltonian. **Right:** representation of the function $\varphi^*(\cdot)$ associated with a trapezoidal Hamiltonian.

The convex transform $\varphi^*(\cdot)$ enables the definition of an auxiliary dynamical system, which will be used to characterize the solutions to (2.5) as capture basins.

Definition 8. [Auxiliary dynamical system] We define an auxiliary dynamical system F associated with the HJ PDE (2.5):

$$F := \left\{ \begin{array}{rcll} \tau'(t) & = & -1 & \\ x'(t) & = & u(t) & \text{where } u(t) \in \text{Dom}(\varphi^*) \\ y'(t) & = & -\varphi^*(u(t)) & \end{array} \right. \tag{2.12}$$

The function $u(\cdot)$ is called *auxiliary control* of the dynamical system F.

The dynamical system (2.12) is both Marchaud and Lipschitz [8]. To be rigorous, we have to mention *once and for all* that the controls $u(\cdot)$ are measurable integrable functions with values in $\text{Dom}(\varphi^*)$, and thus, ranging $L^1(0, +\infty; \text{Dom}(\varphi^*))$ and that the above system of differential equations is valid for almost all $t \geq 0$. We illustrate the auxiliary dynamical system in Figure 2.4.

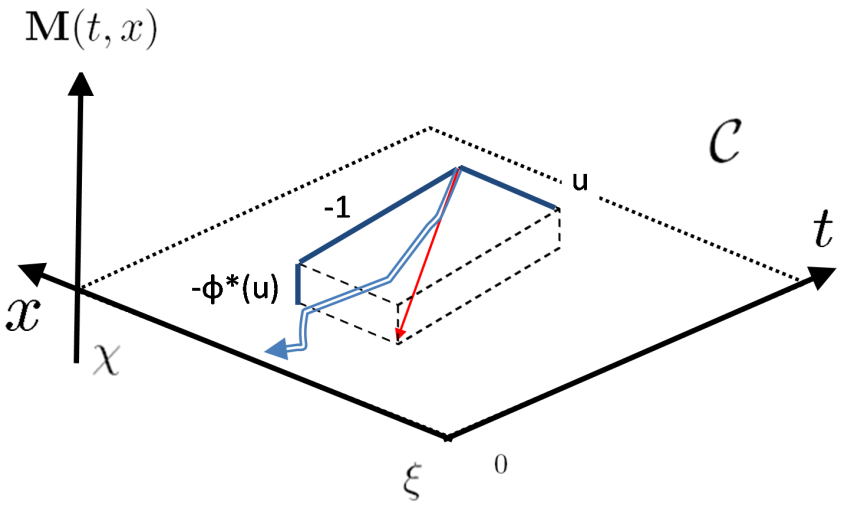

Figure 2.4: **Illustration of the auxiliary dynamical system used to construct the solutions to the HJ PDE.**
The auxiliary dynamical system (2.12) is illustrated by a box. The compound line represents a possible evolution of this dynamical system.

The environment set $\mathcal{K}$ is defined in epigraphical form as $\mathcal{K} := \mathcal{E}pi(\mathbf{b}(\cdot,\cdot))$, where $\mathbf{b}(\cdot,\cdot)$ is a lower semicontinuous function. $\mathbf{b}(\cdot,\cdot)$ represents a lower bound that we impose on the solution to the HJ PDE (2.5). The problem of finding a solution to (2.5) under lower bound constraints is extensively studied in [8]. In the present dissertation, we do not impose a lower bound on the solution and thus choose the following environment set:

Definition 9. [**Environment set**] We define the environment $\mathcal{K}$ as $\mathcal{K} := \mathbb{R}_+ \times [\xi, \chi] \times \mathbb{R}$.

The target set is also defined in epigraphical form as $\mathcal{C} := \mathcal{E}pi(\mathbf{c}(\cdot,\cdot))$, where $\mathbf{c}(\cdot,\cdot)$ represents an upper bound that we impose on the solution to the HJ PDE (2.5).

Definition 10. [**Target set**] Let a value condition $\mathbf{c}(\cdot,\cdot)$ be given. The epigraphical target set associated with $\mathbf{c}(\cdot,\cdot)$ is defined as $\mathcal{C} := \mathcal{E}pi(\mathbf{c})$.

Note that the target set $\mathcal{C} = \mathcal{E}pi(\mathbf{c})$ associated with a value condition $\mathbf{c}(\cdot,\cdot)$ is closed, since it is the epigraph of a lower semicontinuous function.

Using the above definitions of auxiliary dynamical system F, environment set $\mathcal{K}$ and target set $\mathcal{C}$, we can now represent the capture basin $\mathrm{Capt}_F(\mathcal{K},\mathcal{C})$ as in definition 6. We illustrate the construction of $\mathrm{Capt}_F(\mathcal{K},\mathcal{C})$ in Figure 2.5.

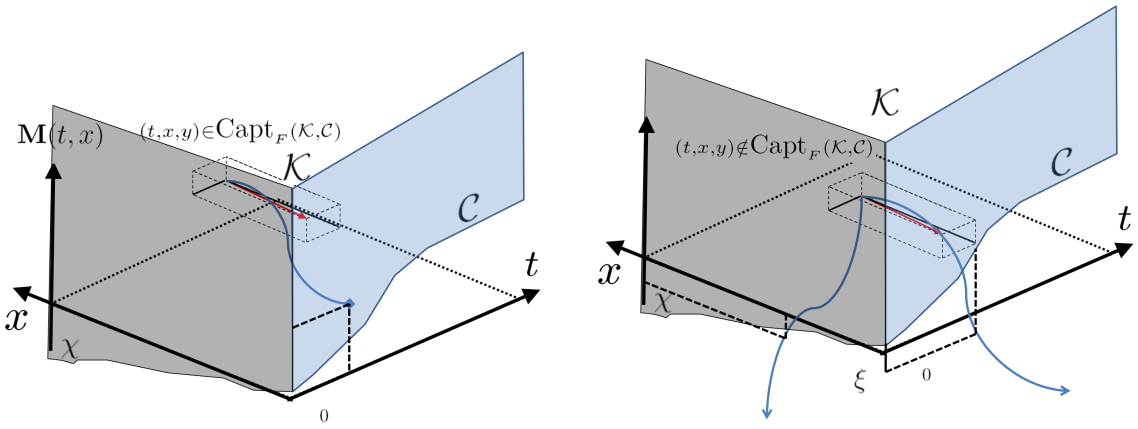

Figure 2.5: **Illustration of a capture basin associated with an epigraphical target. Left:** element (t, x, y) of the capture basin $\mathrm{Capt}_F(\mathcal{K}, \mathcal{C})$: there exists an evolution starting from (t, x, y) and reaching $\mathcal{C}$ in finite time while remaining in $\mathcal{K} := \mathbb{R}_+ \times X \times \mathbb{R}$. **Right:** element (t, x, y) not belonging to the capture basin $\mathrm{Capt}_F(\mathcal{K}, \mathcal{C})$: all evolutions starting from (t, x, y) exit the set $\mathcal{K}$ before reaching $\mathcal{C}$ (only two evolutions are represented for clarity).

Definition 11. [Viability episolution] The *viability episolution* $\mathbf{M_c}(\cdot, \cdot)$ associated with the epigraphical target $\mathcal{C} = \mathbf{c}(\cdot, \cdot)$ is defined by

$$\mathbf{M_c}(t, x) \ := \inf_{(t,x,y) \in \mathrm{Capt}_F(\mathcal{K},\mathcal{C})} y \tag{2.13}$$

Remark 1. The capture basin $\mathrm{Capt}_F(\mathcal{K}, \mathcal{C})$ of a target $\mathcal{C}$ viable in the environment $\mathcal{K}$ is the subset of initial states (t, x, y) for which there exists a measurable control $u(\cdot)$ such that its associated evolution

$$s \mapsto \left(t - s, x + \int_0^s u(\tau) d\tau, y - \int_0^s \varphi^*(u(\tau)) d\tau \right) \tag{2.14}$$

is viable in $\mathcal{K}$ (*i.e.* remains in $\mathcal{K}$ at all times) until it reaches the target $\mathcal{C}$ in finite time.

Remark 2. The capture basin $\mathrm{Capt}_F(\mathcal{K}, \mathcal{C})$ is actually the epigraph of the function $\mathbf{M_c}(\cdot, \cdot)$ defined by (2.13). Indeed, let $(t, x, y) \in \mathrm{Capt}_F(\mathcal{K}, \mathcal{C})$. We thus have that (2.14) is an evolution viable in $\mathcal{K}$ reaching $\mathcal{C}$ in finite time. Since $\mathcal{K}$ and $\mathcal{C}$ are epigraphs, we have for any $y' \geq y$ that the evolution

$$s \mapsto \left(t - s, x + \int_0^s u(\tau) d\tau, y' - \int_0^s \varphi^*(u(\tau)) d\tau \right) \tag{2.15}$$

also remains in $\mathcal{K}$ at all times until it reaches the target $\mathcal{C}$. Hence, (t, x, y') also belongs to $\mathrm{Capt}_F(\mathcal{K}, \mathcal{C})$, which proves that $\mathrm{Capt}_F(\mathcal{K}, \mathcal{C}) = \mathcal{E}pi(\mathbf{M_c})$.

We illustrate the viability episolution associated with a given value condition in Figure 2.6.

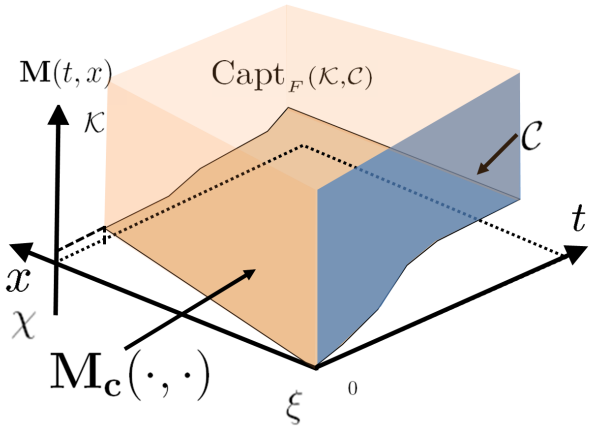

Figure 2.6: **Illustration of a viability episolution.**
We represent on the same figure a target $\mathcal{C}$ and its associated viability episolution $\mathbf{M_c}(\cdot,\cdot)$. The episolution is the lower boundary of the capture basin $\mathrm{Capt}_{_F}(\mathcal{K},\mathcal{C})$, shaded in this figure.

The viability episolution $\mathbf{M_c}(\cdot,\cdot)$ defined by equation (2.13) is shown in theorem 1 to be a B-J/F solution to equation (2.5). If furthermore $\mathbf{M_c}(\cdot,\cdot)$ is differentiable, it is a classical solution to equation (2.5).

The work [8] defines the B/J-F solution in hypographical form for a function $\mathbf{N}(\cdot,\cdot)$ satisfying an inhomogeneous HJ PDE:

$$\frac{\partial \mathbf{N}(t,x)}{\partial t} + \psi\left(\frac{\partial \mathbf{N}(t,x)}{\partial x}\right) \;=\; \psi(v(t)) \tag{2.16}$$

The following theorem is identical to the main existence and uniqueness theorem of [8] modulo the variable change $\mathbf{M}(t,x) = -\mathbf{N}(t,x) + \int_0^t \psi(v(u))du$, the translation of hypographs into epigraphs and the corresponding change on epi/hypo derivatives and differentials.

Theorem 1. [Barron-Jensen/Frankowska solution] [8] For any lower semicontinuous value condition $\mathbf{c}_i$, the associated solution $\mathbf{M}_{\mathbf{c}_i}$ is the **unique** lower semicontinuous function lower than $\mathbf{c}_i$ satisfying:

$$\left\{\begin{array}{ll} (i) & \forall (t,x) \in \mathrm{Dom}(\mathbf{M}_{\mathbf{c}_i}) \backslash \mathrm{Dom}(\mathbf{c}_i),\ \forall (p_t,p_x) \in d_{-}\mathbf{M}_{\mathbf{c}_i}(t,x),\ \ p_t - \psi(-p_x) \;=\; 0 \\ (ii) & \forall (t,x) \in \mathrm{Dom}(\mathbf{M}_{\mathbf{c}_i}) \backslash \mathrm{Dom}(\mathbf{c}_i),\ \forall (p_t,p_x) \in (\mathrm{Dom}(D_{\uparrow}\mathbf{M}_{\mathbf{c}_i}(t,x)))^{+},\ \ p_t - \sigma(\mathrm{Dom}(\varphi^*),p_x) \;=\; 0 \end{array}\right. \tag{2.17}$$

where the epiderivative $D_{\uparrow}$ is defined by its epigraph:

$$\mathcal{E}p(D_{\uparrow}\mathbf{M}_{\mathbf{c}_i}(t,x)) \;:=\; T_{\mathcal{E}p(\mathbf{M}_{\mathbf{c}_i})}(t,x,\mathbf{M}_{\mathbf{c}_i}(t,x)) \tag{2.18}$$

where in the formulae (2.18) and (2.17) $T_{\mathcal{Z}}(z)$ represents the contingent cone to $\mathcal{Z}$ at z (see [10]), $\sigma(\cdot,\cdot)$ is the support function (see [6, 10, 9]), the + superscript denotes the normal cone (see [8]) and where the subdifferential d_- of a function $u : X \to \mathbb{R} \cup \{+\infty\}$ is defined by $d_-u(x) = \{p \in X^* | \forall v \in X,\ \ \langle p, v\rangle \leq D_\uparrow u(x)(v)\}$.

Theorem 1 ensures that $\mathbf{M}_{\mathbf{c}_i}$ is a solution to the HJ PDE (2.5) in the B-J/F sense. In particular, since $d_-\mathbf{M}_{\mathbf{c}_i}(t,x) = \{(\frac{\partial \mathbf{M}_{\mathbf{c}_i}(t,x)}{\partial t}, \frac{\partial \mathbf{M}_{\mathbf{c}_i}(t,x)}{\partial x})\}$ whenever $\mathbf{M}_{\mathbf{c}_i}(t,x)$ is differentiable, equation (2.17) implies the following property:

$$\forall (t,x) \in \mathrm{Dom}(\mathbf{M}_{\mathbf{c}_i}) \backslash \mathrm{Dom}(\mathbf{c}_i) \text{ such that } \mathbf{M}_{\mathbf{c}_i} \text{ is differentiable, } \frac{\partial \mathbf{M}_{\mathbf{c}_i}(t,x)}{\partial t} - \psi\left(-\frac{\partial \mathbf{M}_{\mathbf{c}_i}(t,x)}{\partial x}\right) = 0 \tag{2.19}$$

The construction of the B-J/F solution to (2.5) as a capture basin enables the definition of a *Lax-Hopf formula*.

2.3.3 The Lax-Hopf formula

The viability episolution $\mathbf{M}_{\mathbf{c}}(\cdot,\cdot)$ associated with a general value condition $\mathbf{c}(\cdot,\cdot)$ can be computed using the following generalized Lax-Hopf formula. The classical Lax-Hopf formulae can be found in [8] for initial and upstream boundary conditions.

Theorem 2. [Generalized Lax Hopf formula] The viability episolution $\mathbf{M}_{\mathbf{c}}(\cdot,\cdot)$ associated with a target $\mathcal{C} := \mathcal{E}pi(\mathbf{c})$, for a given lower semicontinuous function $\mathbf{c}(\cdot,\cdot)$ and defined by equation (2.13) can be expressed as:

$$\mathbf{M}_{\mathbf{c}}(t,x) = \inf_{(u,T)\in \mathrm{Dom}(\varphi^*)\times\mathbb{R}_+} (\mathbf{c}(t-T, x+Tu) + T\varphi^*(u)) \tag{2.20}$$

Proof — We fix $(t,x) \in \mathbb{R}_+ \times X$ and define R as the set of elements $(u(\cdot), T, y)$ belonging to $L^1(0,\infty; \mathrm{Dom}(\varphi^*)) \times \mathbb{R}_+ \times \mathbb{R}$ and satisfying viability property (2.21):

$$\forall s \in [0,T] \left(t-s, x + \int_0^s u(\tau)d\tau, y - \int_0^s \varphi^*(u(\tau))d\tau\right) \in \mathcal{K} \tag{2.21}$$

Equations (2.13) and (2.14) thus imply the following formula:

$$\mathbf{M}_{\mathbf{c}}(t,x) = \inf_{(u(\cdot),T,y)\in R \text{ such that } \left(t-T, x+\int_0^T u(\tau)d\tau, y-\int_0^T \varphi^*(u(\tau))d\tau\right)\in \mathcal{E}pi(\mathbf{c})} y \tag{2.22}$$

Since the graph of the value condition $\mathbf{c}(\cdot,\cdot)$ (denoted $\mathrm{Graph}(\mathbf{c})$) is the lower boundary of $\mathcal{E}pi(\mathbf{c})$, we have that

$$\left.\begin{array}{l} \left(t-T, x+\int_0^T u(\tau)d\tau, y-\int_0^T \varphi^*(u(\tau))d\tau\right) \in \mathcal{E}pi(\mathbf{c}) \\ \text{and } \left(t-T, x+\int_0^T u(\tau)d\tau, z-\int_0^T \varphi^*(u(\tau))d\tau\right) \in \mathrm{Graph}(\mathbf{c}) \end{array}\right\} \Rightarrow z \leq y \tag{2.23}$$

Hence, we can (without any further assumption) write equation (2.22) as:

$$\mathbf{M_c}(t,x) = \inf_{(u(\cdot),T,y)\in R \text{ such that } \left(t-T,x+\int_0^T u(\tau)d\tau,y-\int_0^T \varphi^*(u(\tau))d\tau\right)\in \text{Graph}(\mathbf{c})} y \tag{2.24}$$

Since $\mathbf{c}$ is infinite outside of its domain of definition and given the definition of Graph($\mathbf{c}$), equation (2.24) can be expressed as follows:

$$\mathbf{M_c}(t,x) = \inf_{(u(\cdot),T,y)\in R} \left[\mathbf{c}\left(t-T, x+\int_0^T u(\tau)d\tau\right) + \int_0^T \varphi^*(u(\tau))d\tau\right] \tag{2.25}$$

We consider a fixed element $(u(\cdot),T,y) \in R$ and define the following constant control function $\widehat{u}$ on the time interval $[0,T]$ as:

$$\widehat{u} := \frac{1}{T}\int_0^T u(\tau)d\tau \tag{2.26}$$

The control function $\widehat{u}$ is the average value of the control function $u(\cdot)$ on the time interval $[0,T]$. Note that by convexity of $\mathcal{K}$, $(\widehat{u},T,y) \in R$ if $(u(\cdot),T,y) \in R$. In the following, we slightly abuse the notation by calling $\widehat{u}(\cdot)$ the constant function $t \to \widehat{u}$.

We define $y(u(\cdot),T)$ and $y(\widehat{u}(\cdot),T)$ respectively as the values of the term minimized in (2.25) obtained for the control functions $u(\cdot)$ and $\widehat{u}(\cdot)$ and for the capture time T:

$$\begin{cases} y(u(\cdot),T) = \mathbf{c}(t-T, x+\int_0^T u(\tau)d\tau) + \int_0^T \varphi^*(u(\tau))d\tau \\ y(\widehat{u}(\cdot),T) = \mathbf{c}(t-T, x+T\widehat{u}) + T\varphi^*(\widehat{u}) \end{cases} \tag{2.27}$$

Since φ^* is convex and lower semicontinuous, Jensen's inequality implies

$$\varphi^*\left(\frac{1}{T}\int_0^T u(\tau)d\tau\right) \;\leq\; \frac{1}{T}\int_0^T \varphi^*(u(\tau))d\tau \tag{2.28}$$

and thus, since $\widehat{u}T = \int_0^T u(\tau)d\tau$

$$y(\widehat{u}(\cdot),T) \leq y(u(\cdot),T) \tag{2.29}$$

Equation (2.29) thus implies that one can replace the search of the infimum over the class of measurable functions $u(\cdot)$ by the search of the infimum over the set of constant functions $\widehat{u}(\cdot)$.

Hence, we can write equation (2.25) as:

$$\mathbf{M_c}(t,x) = \inf_{(u,T)\in \text{Dom}(\varphi^*)\times\mathbb{R}_+} \left(\mathbf{c}(t-T, x+Tu) + T\varphi^*(u)\right) \tag{2.30}$$

which enables us to restrict ourselves to the set of constant controls and completes the proof. ■

Remark 3. Given a constant control function u, the coefficient T used for the minimization in equation (2.20) can be restricted to the elements of the set $S_{\mathbf{c}}(t,x,u)$ defined by formula (2.31):

$$S_{\mathbf{c}}(t,x,u) := \{s \in \mathbb{R}_+ \text{ such that } (t-s, x+su) \in \mathrm{Dom}(\mathbf{c})\} \tag{2.31}$$

Indeed, when $T \notin S_{\mathbf{c}}(t,x,u)$, $\mathbf{c}(t-T, x+Tu)$ is infinite.

We could also alternatively define for any (t,x) the set $R_{\mathbf{c}}(t,x)$ as $R_{\mathbf{c}}(t,x) := \{(u,T) \in \mathrm{Dom}(\varphi^*) \times \mathbb{R}_+ \text{ s. t. } (t-T, x+Tu) \in \mathrm{Dom}(\mathbf{c})\}$. Note that the coefficients (u,T) used for the minimization in equation (2.20) can also be restricted to the elements of $R_{\mathbf{c}}$ (when $(u,T) \notin R_{\mathbf{c}}(t,x)$, $\mathbf{c}(t-T, x+Tu)$ is infinite).

Remark 4. When $\forall u \in \mathrm{Dom}(\varphi^*)$, $S_{\mathbf{c}}(t,x,u) = \emptyset$, equation (2.30) involves a minimization on an empty set and $\mathbf{M}_{\mathbf{c}}(t,x)$ is infinite.

Remark 5. Since $\mathbf{c}(t-T, x+Tu) = +\infty$ when $(t-T, x+Tu) \notin \mathrm{Dom}(\mathbf{c})$, we can write equation (2.30) as:

$$\mathbf{M}_{\mathbf{c}}(t,x) = \inf_{\{(u,T) \in \mathrm{Dom}(\varphi^*)\times\mathbb{R}_+ \text{ such that } T \in S_{\mathbf{c}}(t,x,u)\}} (\mathbf{c}(t-T, x+Tu) + T\varphi^*(u)) \tag{2.32}$$

or alternatively as:

$$\mathbf{M}_{\mathbf{c}}(t,x) = \inf_{\{(u,T) \in R_{\mathbf{c}}(t,x)\}} (\mathbf{c}(t-T, x+Tu) + T\varphi^*(u)) \tag{2.33}$$

Specific forms of the Lax-Hopf formula (2.20) associated with affine initial, boundary and internal conditions are presented in section 2.5.

2.4 Properties of the Barron-Jensen/Frankowska solutions to Hamilton-Jacobi equations

2.4.1 Domain of definition

Proposition 1. [Domain of definition] For a given value condition $\mathbf{c}(\cdot,\cdot)$, the domain of definition of $\mathbf{M}_{\mathbf{c}}(\cdot,\cdot)$, also called *domain of influence of* $\mathbf{c}(\cdot,\cdot)$, is defined by the following formula:

$$\mathrm{Dom}(\mathbf{M}_{\mathbf{c}}) = \bigcup_{(t,x)\in\mathrm{Dom}(\mathbf{c})} \left(\bigcup_{T\in\mathbb{R}_+} \{t+T\} \times [x - \nu^\sharp T, x + \nu^\flat T] \right) \tag{2.34}$$

Proof — The generalized Lax Hopf formula (2.20) implies that

$$\begin{aligned}\mathrm{Dom}(\mathbf{M}_\mathbf{c}) = \; & \{(t,x) \in \mathbb{R}_+ \times X \text{ such that } \exists (T,u) \in \mathbb{R}_+ \times \mathrm{Dom}(\varphi^*) \\ & \text{and } (t-T, x+Tu) \in \mathrm{Dom}(\mathbf{c})\}\end{aligned}$$

Equation (2.34) is derived from the previous formula, observing that u ranges in $\mathrm{Dom}(\varphi^*) := [-\nu^\flat, \nu^\sharp]$. ■

Remark 6. The domain of influence of $\mathbf{c}(\cdot,\cdot)$ is the union of the cones originating at $(t,x) \in \mathrm{Dom}(\mathbf{c})$ and limited by the minimal $-\nu^\flat$ and maximal $\nu^\sharp$ slopes of the Hamiltonian. This property is illustrated in Figure 2.7.

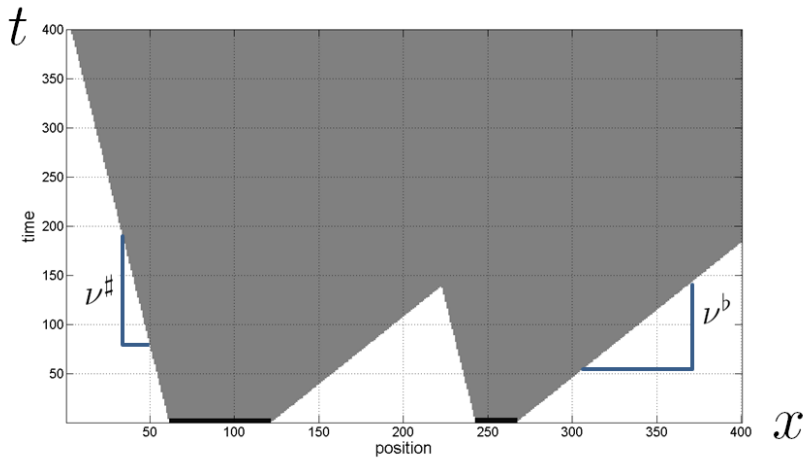

Figure 2.7: **Illustration of the domain of influence of a value condition.** We define a value condition $\mathbf{c}(\cdot)$ on a domain represented by two black segments at $t = 0$. The domain of influence of $\mathbf{c}(\cdot,\cdot)$ is highlighted in gray.

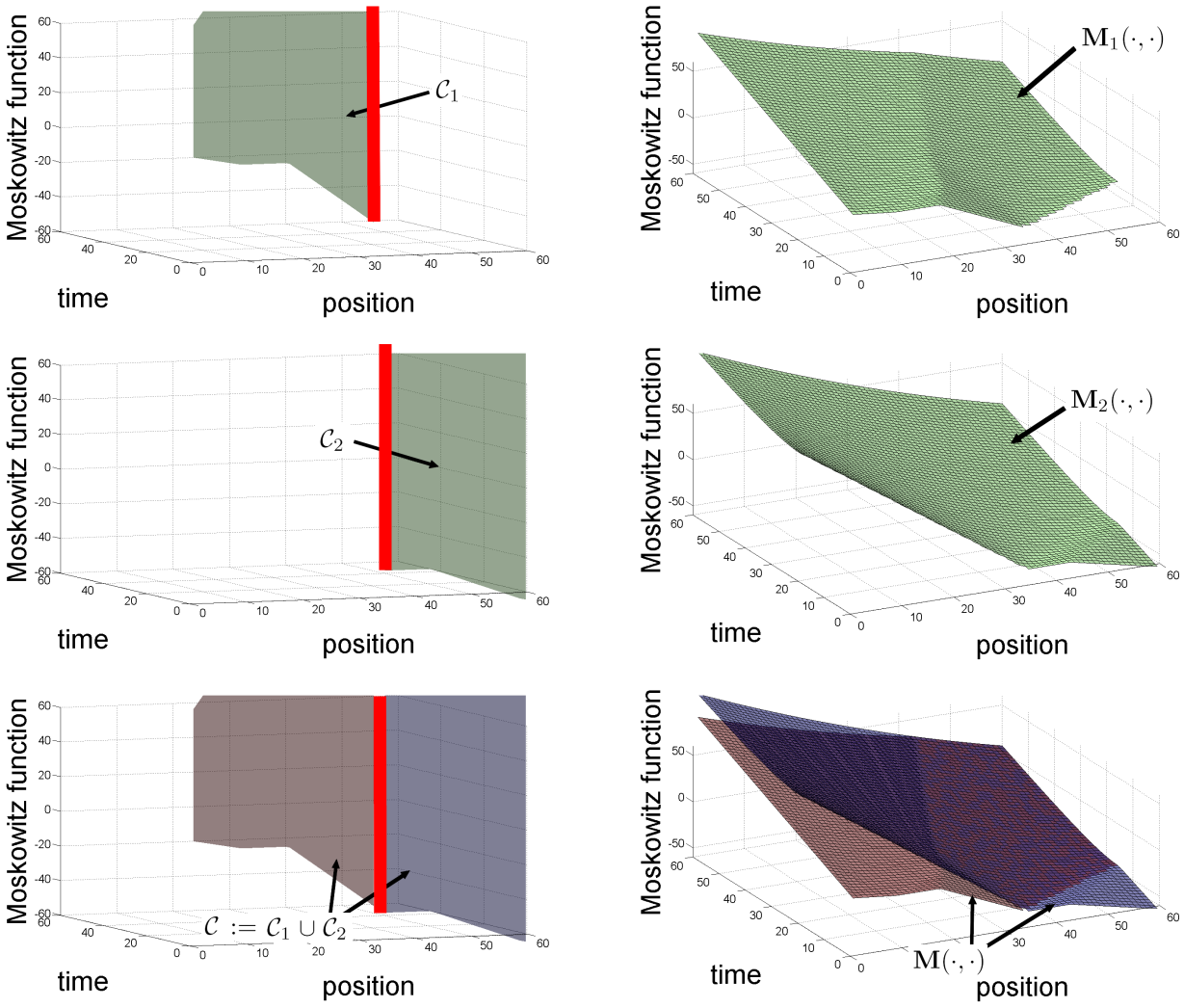

Figure 2.8: **Illustration of the inf-morphism property.**
Top: representation of the target $\mathcal{C}_1 := \mathcal{E}pi(\mathbf{c}_1)$ **(left)**, representation of the corresponding episolution $\mathbf{M}_1(\cdot,\cdot)$ **(right)**. **Center:** representation of the target $\mathcal{C}_2 := \mathcal{E}pi(\mathbf{c}_2)$ **(left)**, representation of the corresponding episolution $\mathbf{M}_2(\cdot,\cdot)$ **(right)**. **Bottom:** Representation of the target $\mathcal{C} := \mathcal{C}_1 \bigcup \mathcal{C}_2$ **(left)**. The episolution $\mathbf{M}(\cdot,\cdot)$ associated with the target $\mathcal{C}$ **(right)** is the minimum of the episolutions $\mathbf{M}_1(\cdot,\cdot)$ and $\mathbf{M}_2(\cdot,\cdot)$ associated with $\mathcal{C}_1$ and $\mathcal{C}_2$.

2.4.2 The inf-morphism property

It is well known [6, 7, 8] that for a given environment $\mathcal{K}$, the capture basin of a finite union of targets is the union of the capture basins of these targets.

$$\mathrm{Capt}_F\left(\mathcal{K}, \bigcup_{i\in I}\mathcal{C}_i\right) = \bigcup_{i\in I}\mathrm{Capt}_F(\mathcal{K}, \mathcal{C}_i) \tag{2.35}$$

This property can be translated in epigraphical form as follows.

Proposition 2. [**Inf-morphism property**] [8] Let $\mathbf{c}_i$ (i belongs to a finite set I) be a family of functions whose epigraphs are the targets $\mathcal{C}_i$. Since the epigraph of the minimum of the functions $\mathbf{c}_i$ is the union of the epigraphs of the functions $\mathbf{c}_i$, the target $\mathcal{C} := \bigcup_{i\in I}\mathcal{C}_i$ is the epigraph of the function $\mathbf{c} := \min_{i\in I}\mathbf{c}_i$. Hence, equation (2.35) implies the following property, known as *inf-morphism property*:

$$\forall\, t \geq 0,\ x \in X,\ \ \mathbf{M}_{\mathbf{c}}(t,x) \ = \ \min_{i\in I}\mathbf{M}_{\mathbf{c}_i}(t,x) \tag{2.36}$$

Remark 7. The inf-morphism property enables us to decompose a complex problem into more tractable subproblems. For instance, a piecewise affine initial condition can be decomposed as the minimum of a finite number of affine initial conditions. Hence, the solution associated with a piecewise affine initial condition is the minimum of a finite number of solutions associated with affine initial conditions.

The inf-morphism property is illustrated in Figure 2.8.

Note that in the context of traffic flow engineering, this property was identified but not proved mathematically by Newell in [80].

2.4.3 Convexity property of the solutions associated with convex value conditions

We now show an important convexity property of the solution to (2.5) associated with convex value conditions. Let a convex value condition $\mathbf{c}(\cdot,\cdot)$ be defined defined on a compact and nonempty domain $\mathrm{Dom}(\mathbf{c}) \subset [0, t_{\max}] \times X$. Since $\mathbf{c}(\cdot,\cdot)$ is convex and defined on a compact set, it is bounded below. In order to prove the convexity of the solution $\mathbf{M}_{\mathbf{c}}(\cdot,\cdot)$ associated with $\mathbf{c}(\cdot,\cdot)$, we first need to define a variable change as follows.

Definition 12. [**Variable change for the auxiliary control**] We define a new variable v as $v = Tu$ and define the cone $\mathcal{D} := \left\{[-\nu^\flat t, \nu^\sharp t] \times \{t\} \mid t \in \mathbb{R}_+\right\}$.

Note that definition 12 implies that $(u,T) \in \mathrm{Dom}(\varphi^*) \times \mathbb{R}_+$ if and only if $(v,T) \in \mathcal{D}$. We now define an auxiliary objective function $f(\cdot,\cdot,\cdot,\cdot)$, which is the argument of the Lax-Hopf formula (2.20) with the variable change $v = Tu$.

Definition 13. [**Auxiliary objective function**] We define the function $f(\cdot,\cdot,\cdot,\cdot)$ as:

$$\begin{array}{l}\forall (t,x,v,T) \in \mathbb{R}_+ \times X \times \mathcal{D},\\ f(t,x,v,T) := \mathbf{c}(t-T, x+v) + T\varphi^*\left(\frac{v}{T}\right)\end{array}$$

Note that $f(\cdot,\cdot,\cdot,\cdot)$ is bounded below since the value condition $\mathbf{c}(\cdot,\cdot)$ is bounded below and the function $\varphi^*(\cdot)$ is positive. By definition of $f(\cdot,\cdot,\cdot,\cdot)$, we can rewrite equation (2.20) as:

$$\mathbf{M_c}(t,x) = \inf_{(v,T)\in\mathcal{D}} f(t,x,v,T) \tag{2.37}$$

Equation (2.37) implies:

$$\mathcal{E}pi(\mathbf{M_c}) = \{(t,x,y) \mid \exists (v,T) \in \mathcal{D} \text{ s.t. } (t,x,v,T,y) \in \mathcal{E}pi(f)\} \tag{2.38}$$

The above variable change enables us to prove the following convexity property.

Proposition 3. [Convexity property of solutions associated with convex value conditions] The solution $\mathbf{M_c}(\cdot,\cdot)$ associated with a convex value condition $\mathbf{c}(\cdot,\cdot)$ is convex.

Proof — Since $\varphi^*(\cdot)$ is convex, its associated *perspective function* $(v,T) \to T\varphi^*(\frac{v}{T})$ is also convex [18] for $T > 0$. Since the function $(t,x,v,T) \to (t-T, x+v)$ is affine and $\mathbf{c}(\cdot,\cdot)$ is convex, the function $(t,x,v,T) \to \mathbf{c}(t-T,x+v)$ is convex [87, 18]. Hence the function $f(\cdot,\cdot,\cdot,\cdot)$ is convex as the sum of two convex functions.

Since the function $f(\cdot,\cdot,\cdot,\cdot)$ is convex, its epigraph $\mathcal{E}pi(f)$ is also convex. Since the set $\mathcal{E}pi(\mathbf{c})$ is nonempty, the epigraph of $\mathbf{M_c}(\cdot,\cdot)$ is nonempty by the inclusion $\mathcal{E}pi(\mathbf{c}) \subset \mathrm{Capt}_F(\mathcal{K}, \mathcal{E}pi(\mathbf{c})) := \mathcal{E}pi(\mathbf{M_c})$ (see [6] for a proof of this property).

Hence, equation (2.38) implies that the epigraph of $\mathbf{M_c}$ is convex, since it is the projection of a convex set on a subspace [87, 18]. ■

In particular, proposition 3 implies that the solutions associated with affine initial, boundary and internal conditions are convex. We now prove that they can also be computed explicitly for general concave Hamiltonians.

2.5 Analytic solutions associated with affine initial, boundary and internal conditions

In this section, we compute the solutions associated with affine initial, boundary and internal conditions analytically. For each type of value condition, we follow the procedure outlined below.

1. Write the Lax-Hopf formula associated with the corresponding affine value condition. Because of the structure of the affine value condition, we can compute the set $S_{\mathbf{c}}(t,x,u)$ defined by (2.31) explicitly, which enables us to express (2.32) as a minimization over a single variable.

2. Write the minimization problem associated with this instantiation of the Lax-Hopf formula as a convex optimization problem (convex objective and convex constraints).

3. Analytically find a minimizer of the convex optimization problem, using subderivatives (2.10).

2.5.1 Analytic Lax-Hopf formula associated with an affine initial condition

Definition 14. [**Affine initial condition**] We consider the following affine initial condition $\mathcal{M}_{0,i}(0,x)$, where i is an integer:

$$\mathcal{M}_{0,i}(0,x) = \begin{cases} a_i x + b_i & \text{if } \ x \in [\overline{\alpha}_i, \overline{\alpha}_{i+1}] \\ +\infty & \text{otherwise} \end{cases} \tag{2.39}$$

The following formula expresses the Lax-Hopf formula (2.20) for the specific initial condition (2.39).

Proposition 4. [**Lax-Hopf formula for an affine initial condition**] The Lax-Hopf formula associated with the initial condition (2.39) can be expressed as:

$$\mathbf{M}_{\mathcal{M}_{0,i}}(t,x) \ = \inf_{u \in \mathrm{Dom}(\varphi^*) \cap \left[\frac{\overline{\alpha}_i - x}{t}, \frac{\overline{\alpha}_{i+1} - x}{t}\right]} \left(a_i(x+tu) + b_i + t\varphi^*(u)\right), \ \ \forall (t,x) \in \mathbb{R}_+^* \times X \tag{2.40}$$

and

$$\forall x \times X, \ \ \mathbf{M}_{\mathcal{M}_{0,i}}(0,x) \ = \inf_{(T,u) \in \mathrm{Dom}(\varphi^*) \times [0,0]} \left(a_i(x+0u) + b_i + 0\varphi^*(u)\right) \ = \ a_i x + b_i \tag{2.41}$$

Proof — The Lax-Hopf formula associated with an initial condition reads:

$$\mathbf{M}_{\mathcal{M}_{0,i}}(t,x) \;=\; \inf_{(T,u)\in \mathrm{Dom}(\varphi^*)\times[0,t] \text{ such that } (x+Tu)\in[\overline{\alpha}_i,\overline{\alpha}_{i+1}] \text{ and } t-T=0} (a_i(x+tu)+b_i+T\varphi^*(u)) \tag{2.42}$$

This formula is valid for all $(t,x)\in\mathbb{R}_+\times X$. Since $t-T=0$, we have $T=t$. Since $t>0$, the condition $(x+tu)\in[\overline{\alpha}_i,\overline{\alpha}_{i+1}]$ is equivalent to $u\in[\frac{\overline{\alpha}_i-x}{t},\frac{\overline{\alpha}_{i+1}-x}{t}]$, which in turn implies equation (2.40). ■

The domain of definition of the solution can be explicitly characterized as follows.

Proposition 5. [Domain of influence of an affine initial condition] The domain of definition of $\mathbf{M}_{\mathcal{M}_{0,i}}(\cdot,\cdot)$ is given by the following formula:

$$\mathrm{Dom}(\mathbf{M}_{\mathcal{M}_{0,i}}) = \left\{(t,x)\in\mathbb{R}_+^*\times X \text{such that } \overline{\alpha}_i-\nu^\sharp t\le x\le \overline{\alpha}_{i+1}+\nu^\flat t\right\} \tag{2.43}$$

Proof — The Lax-Hopf formula (2.40) implies:

$$\mathrm{Dom}(\mathbf{M}_{\mathcal{M}_{0,i}}) := \left\{(t,x)\in\mathbb{R}_+^*\times X \text{such that } \exists u\in\mathrm{Dom}(\varphi^*)\cap\left[\tfrac{\overline{\alpha}_i-x}{t},\tfrac{\overline{\alpha}_{i+1}-x}{t}\right]\right\}$$

Equation (2.43) is obtained using the above formula and noting that $\mathrm{Dom}(\varphi^*)=[-\nu^\flat,\nu^\sharp]$. ■

The solution can be computed analytically by minimizing an auxiliary function, which we now define.

Definition 15. [Auxiliary objective function] For all $(a_i,b_i,t,x)\in\mathbb{R}^2\times\mathrm{Dom}(\mathbf{M}_{\mathcal{M}_{0,i}})$, we define an objective function $\zeta_{a_i,b_i,t,x}(\cdot)$ by the following formula:

$$\forall u\in\mathrm{Dom}(\varphi^*),\;\; \zeta_{a_i,b_i,t,x}(u) := a_i(x+tu)+b_i+t\varphi^*(u) \tag{2.44}$$

Given this definition, equation (2.40) becomes:

$$\forall (t,x)\in\mathbb{R}_+^*\times X,\; \mathbf{M}_{\mathcal{M}_{0,i}}(t,x) \;=\; \inf_{u\in\mathrm{Dom}(\varphi^*)\cap\left[\frac{\overline{\alpha}_i-x}{t},\frac{\overline{\alpha}_{i+1}-x}{t}\right]} \zeta_{a_i,b_i,t,x}(u) \tag{2.45}$$

The function $\zeta_{a_i,b_i,t,x}(\cdot)$ is convex as the sum of two convex functions and thus subdifferentiable on $\mathrm{Dom}(\varphi^*)$ in the sense of (2.10). The subderivative of $\zeta_{a_i,b_i,t,x}(\cdot)$ is given by:

$$\begin{aligned}\forall u\in\mathrm{Dom}(\varphi^*),\; \partial_-\zeta_{a_i,b_i,t,x}(u) &= \{w \mid \exists v\in\partial_-\varphi^*(u),\;\; w=a_it+vt\}\\ &:= t\cdot(\{a_i\}+\partial_-\varphi^*(u))\end{aligned} \tag{2.46}$$

with a slight abuse of notation for the summation of the two sets in the second equality. This last expression can now be used to analytically compute the minimizer.

Proposition 6. [Explicit minimization of $\zeta_{a_i,b_i,t,x}(\cdot)$] We now assume that a_i in the value condition $\mathcal{M}_{0,i}$ given by (2.39) satisfies the condition $-a_i \in \mathrm{Dom}(\psi) := [0,\omega]$. Since $\psi(\cdot)$ is concave, it is also superdifferentiable on its domain of definition and thus $\forall \rho \in [0,\omega],\ \partial_+\psi(\rho) \neq \emptyset$.

Let $u_0(a_i)$ be an element of $-\partial_+\psi(-a_i) \neq \emptyset$. Note that the Legendre-Fenchel inversion formula (2.9) implies that $u_0(a_i) \in \mathrm{Dom}(\varphi^*)$ and $-a_i \in \partial_-\varphi^*(u_0(a_i))$. Using this definition of $u_0(a_i)$, the function $\zeta_{a_i,b_i,t,x}(\cdot)$ has the following minimizer over $\mathrm{Dom}(\varphi^*) \cap [\frac{\overline{\alpha}_i - x}{t}, \frac{\overline{\alpha}_{i+1}-x}{t}]$:

$$\begin{cases} u = u_0(a_i) & \text{if } \ u_0(a_i) \in [\frac{\overline{\alpha}_i - x}{t}, \frac{\overline{\alpha}_{i+1}-x}{t}] \\ u = \frac{\overline{\alpha}_i - x}{t} & \text{if } \ u_0(a_i) \leq \frac{\overline{\alpha}_i - x}{t} \\ u = \frac{\overline{\alpha}_{i+1}-x}{t} & \text{if } \ u_0(a_i) \geq \frac{\overline{\alpha}_{i+1}-x}{t} \end{cases} \tag{2.47}$$

Proof — The function $\zeta_{a_i,b_i,t,x}(u)$ is minimal for a given $u \in \mathrm{Dom}(\varphi^*)$ if and only if $0 \in \partial_-\zeta_{a_i,b_i,t,x}(u)$ by [18]. By equation (2.46), this happens if and only if for this u, $-a_i \in \partial_-\varphi^*(u)$. Using the Legendre-Fenchel inversion formula (2.9), we can rewrite $u := u_0(a_i) \in -\partial_+\psi(-a_i)$ as $-a_i \in \partial_-\varphi^*(u_0(a_i))$ and thus $u_0(a_i)$ minimizes $\zeta_{a_i,b_i,t,x}(\cdot)$ over $\mathrm{Dom}(\varphi^*)$. Hence, since $\zeta_{a_i,b_i,t,x}(\cdot)$ is convex, $\zeta_{a_i,b_i,t,x}(u)$ is decreasing for $u \leq u_0(a_i)$ and increasing for $u \geq u_0(a_i)$, which implies equation (2.47). ■

Proposition 7. [Computation of $\mathbf{M}_{\mathcal{M}_{0,i}}(\cdot,\cdot)$] Let $u_0(a_i)$ be defined as in proposition 6. For all $(t,x) \in \mathrm{Dom}(\mathbf{M}_{\mathcal{M}_{0,i}})$, the expression $\mathbf{M}_{\mathcal{M}_{0,i}}(t,x)$ can be computed using the following formula:

$$\mathbf{M}_{\mathcal{M}_{0,i}}(t,x) = \begin{cases} (i) & t\psi(-a_i) + a_i x + b_i \\ & \text{if } \ u_0(a_i) \in [\frac{\overline{\alpha}_i - x}{t}, \frac{\overline{\alpha}_{i+1}-x}{t}] \\ (ii) & a_i\overline{\alpha}_i + b_i + t\varphi^*(\frac{\overline{\alpha}_i - x}{t}) \\ & \text{if } \ u_0(a_i) \leq \frac{\overline{\alpha}_i - x}{t} \\ (iii) & a_i\overline{\alpha}_{i+1} + b_i + t\varphi^*(\frac{\overline{\alpha}_{i+1}-x}{t}) \\ & \text{if } \ u_0(a_i) \geq \frac{\overline{\alpha}_{i+1}-x}{t} \end{cases} \tag{2.48}$$

Proof — The cases (ii) and (iii) of equation (2.48) are trivially obtained by combining equations (2.40) and (2.47). Since the function $-\psi(\cdot)$ is convex, it is identical [18] to its Fenchel biconjugate:

$$\forall \rho \in [0,\omega],\ \ \psi(\rho) = \inf_{u \in \mathrm{Dom}(\varphi^*)} (-\rho u + \varphi^*(u))$$

The function $g : u \to a_i u + \varphi^*(u)$ is convex and thus subdifferentiable on $\mathrm{Dom}(\varphi^*)$. By definition of $u_0(a_i)$, $0 \in \partial_- g(u_0(a_i))$. This last property implies that $u_0(a_i)$ minimizes $g(\cdot)$ over $\mathrm{Dom}(\varphi^*)$ and thus that $\psi(-a_i) = a_i u_0(a_i) + \varphi^*(u_0(a_i))$. Hence, the case (i) of equation (2.48) is obtained by combining equations (2.40), (2.47) and the property $\psi(-a_i) = a_i u_0(a_i) + \varphi^*(u_0(a_i))$. ■

Figure 2.9 illustrates the different domains of equation (2.48) for the solution associated with an affine initial condition defined by equation (2.39).

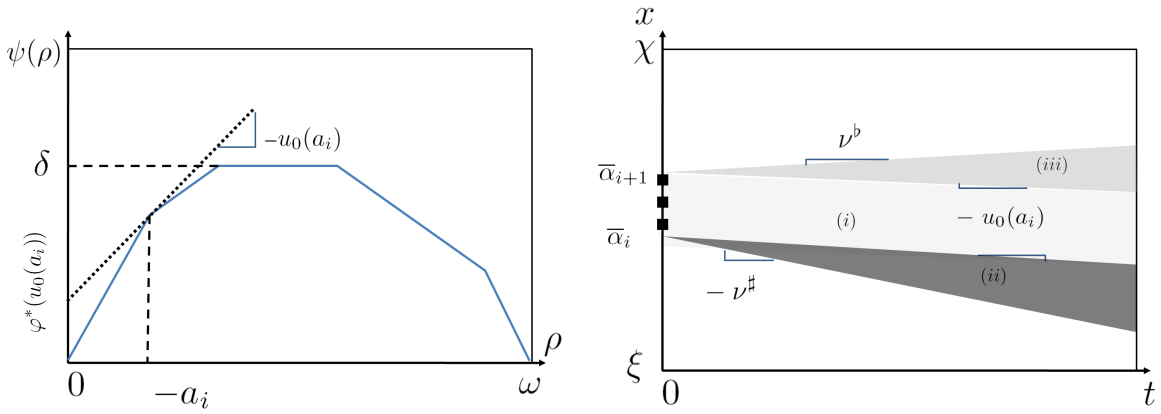

Figure 2.9: **Construction of the solution associated with an affine initial condition. Left:** Illustration of the construction of a $u_0(a_i)$ from the knowledge of a_i. The transform $\varphi^*(u_0(a_i))$ corresponds to the value intercepted on the vertical axis by the tangent line of slope $-u_0(a_i)$ to the graph of ψ in $-a_i$. **Right:** The (t, x) domain of the solution corresponding to the affine initial condition (2.39) can be separated in three different areas. The domain highlighted in light gray corresponds to the case (i) in equation (2.48). The domain highlighted in medium gray corresponds to the case (iii) and the remaining domain in dark gray corresponds to the case (ii). The domain of the initial condition is represented by a dashed line.

2.5.2 Analytic Lax-Hopf formula associated with an affine upstream boundary condition

Definition 16. [Affine upstream boundary condition] We consider the following upstream boundary condition $\gamma_j(t, \xi)$ of $\gamma_j(t, x)$:

$$\gamma_j(t,\xi) = \begin{cases} c_j t + d_j & \text{if } \ t \in [\overline{\gamma}_j, \overline{\gamma}_{j+1}] \\ +\infty & \text{otherwise} \end{cases} \tag{2.49}$$

In the following derivation, we consider that $x > \xi$. We also assume that the value condition (2.49) satisfies the condition $c_j \in \mathrm{Im}(\psi) = [0, \delta]$.

Proposition 8. [Lax-Hopf formula for an affine upstream boundary condition] The Lax-Hopf formula (2.50) associated with the upstream boundary condition (2.49) can be expressed as:

$$\mathbf{M}_{\gamma_j}(t,x) \ = \inf_{T \in \left[-\frac{\xi-x}{\nu^\flat}, +\infty\right[\cap \left[t-\overline{\gamma}_{j+1}, t-\overline{\gamma}_j\right]} \left(c_j(t-T) + d_j + T\varphi^*\left(\frac{\xi - x}{T}\right)\right) \quad \forall (t,x) \in \mathbb{R}_+^* \times X \backslash \{\xi\} \tag{2.50}$$

Proof — The Lax-Hopf formula (2.32) associated with the upstream boundary condition reads:

$$\mathbf{M}_{\gamma_j}(t,x) \;=\; \inf_{(u,T)\in \mathrm{Dom}(\varphi^*)\times\mathbb{R}_+ \text{ such that } x+Tu=\xi \text{ and } \overline{\gamma}_j\leq t-T\leq\overline{\gamma}_{j+1}} (c_j(t-T)+d_j+T\varphi^*(u)) \tag{2.51}$$

We define the variable change $T := \frac{\xi-x}{u} > 0$, which represents the capture time using the control u (see [31]). Since $T = \frac{\xi-x}{u} > 0$ and $x > \xi$, we have $u < 0$. The constraint $u \in \mathrm{Dom}(\varphi^*) := [-\nu^\flat, \nu^\sharp]$ thus implies $T \in [-\frac{\xi-x}{\nu^\flat}, +\infty[$. The additional constraint $t - \frac{\xi-x}{u} \in [\overline{\gamma}_j, \overline{\gamma}_{j+1}]$ results from the definition of $\gamma_j(\cdot,\cdot)$ and implies $T \in [t-\overline{\gamma}_{j+1}, t-\overline{\gamma}_j]$, which yields equation (2.50). ■

Proposition 9. [Domain of influence of an affine upstream boundary condition] The domain of definition of $\mathbf{M}_{\gamma_j}(\cdot,\cdot)$ is given by the following formula:

$$\mathrm{Dom}(\mathbf{M}_{\gamma_j}) = \left\{(t,x)\in\mathbb{R}_+\times X \;\text{ such that }\; x\leq \xi+\nu^\flat(t-\overline{\gamma}_j)\right\} \tag{2.52}$$

Proof — The Lax-Hopf formula (2.51) implies:

$$\mathrm{Dom}(\mathbf{M}_{\gamma_j}) := \left\{(t,x)\in\mathbb{R}_+\times X \;\text{ such that }\; \exists T\in\left[-\frac{\xi-x}{\nu^\flat},+\infty\right[\cap\left[t-\overline{\gamma}_{j+1},t-\overline{\gamma}_j\right]\right\}$$

Hence, $(t,x)\in\mathrm{Dom}(\mathbf{M}_{\gamma_j})$ if and only if $-\frac{\xi-x}{\nu^\flat}\leq t-\overline{\gamma}_j$, which in turn implies equation (2.52). ■

Definition 17. [Auxiliary objective function] For all $(t,x)\in\mathrm{Dom}(\mathbf{M}_{\gamma_j})$, we define an objective function $\eta_{c_j,d_j,t,x}(\cdot)$ by the following formula:

$$\forall T\in\mathbb{R}_+^*\;\; \eta_{c_j,d_j,t,x}(T) := c_j(t-T)+d_j+T\varphi^*\left(\frac{\xi-x}{T}\right) \tag{2.53}$$

Given this definition, equation (2.50) becomes:

$$\mathbf{M}_{\gamma_j}(t,x) \;=\; \inf_{T\in\left[-\frac{\xi-x}{\nu^\flat},+\infty\right[\cap\left[t-\overline{\gamma}_{j+1},t-\overline{\gamma}_j\right]} \eta_{c_j,d_j,t,x}(T) \tag{2.54}$$

Since $\varphi^*(\cdot)$ is convex, its associated perspective function $T\to T\varphi^*(\frac{\xi-x}{T})$ is also convex [18] for $T>0$. Hence the function $\eta_{c_j,d_j,t,x}(\cdot)$ is convex as the sum of two convex functions. The subderivative of $\eta_{c_j,d_j,t,x}(\cdot)$ is given by:

$$\begin{aligned}\forall T\in[-\tfrac{\xi-x}{\nu^\flat},+\infty[,\quad \partial_-\eta_{c_j,d_j,t,x}(T) \;&=\left\{w\mid \exists v\in\partial_-\varphi^*(\tfrac{\xi-x}{T}),\;\; w=-c_j+\varphi^*(\tfrac{\xi-x}{T})-\tfrac{\xi-x}{T}v\right\}\\ &:=\left\{-c_j+\varphi^*(\tfrac{\xi-x}{T})\right\}-\tfrac{\xi-x}{T}\partial_-\varphi^*(\tfrac{\xi-x}{T})\end{aligned} \tag{2.55}$$

with a slight abuse of notation for the second line as previously.

Definition 18. [Density associated with c_j] Recalling that $\mathrm{Im}\,(\psi) := [0, \delta]$, we define ρ_c as:

$$\rho_c = \inf_{\rho \in [0,\omega] \text{ such that } \psi(\rho) = \delta} \rho$$

Since $c_j \in \mathrm{Im}(\psi) = [0, \delta]$, there exists $\rho_j \in [0, \rho_c]$ such that $\psi(\rho_j) = c_j$. Note that since $\psi(\cdot)$ is concave and $\delta > 0$, $\psi(\cdot)$ is increasing on $[0, \rho_c]$ and thus $\partial_+\psi(\rho_j) \cap \mathbb{R}_+ \neq \emptyset$.

- Let $u_0(\rho_j)$ be an element of $-\partial_+\psi(\rho_j) \cap \mathbb{R}_- \neq \emptyset$.
- Let $T_0(\rho_j, x)$ be defined as

$$T_0(\rho_j, x) := \begin{cases} \frac{\xi - x}{u_0(\rho_j)} & \text{if } \ u_0(\rho_j) \neq 0 \\ +\infty & \text{if } \ u_0(\rho_j) = 0 \end{cases} \tag{2.56}$$

We have by the Legendre-Fenchel inversion formula that $u_0(\rho_j) \in \mathrm{Dom}(\varphi^*)$ and $\rho_j \in \partial_-\varphi^*(u_0(\rho_j))$.

Proposition 10. [Explicit minimization of $\eta_{c_j,d_j,t,x}(\cdot)$] Let $T_0(\rho_j, x)$ be given by definition 18. For all $(t, x) \in \mathrm{Dom}(\mathbf{M}_{\gamma_j})$, the function $\eta_{c_j,d_j,t,x}(\cdot)$ has the following minimizer over $[-\frac{\xi - x}{\nu^\flat}, \infty[\cap [t - \overline{\gamma}_{j+1}, t - \overline{\gamma}_j]$:

$$\begin{cases} T_0(\rho_j, x) & \text{if } \ T_0(\rho_j, x) \in [t - \overline{\gamma}_{j+1}, t - \overline{\gamma}_j] \\ t - \overline{\gamma}_j & \text{if } \ t - \overline{\gamma}_j \leq T_0(\rho_j, x) \\ t - \overline{\gamma}_{j+1} & \text{if } \ T_0(\rho_j, x) \leq t - \overline{\gamma}_{j+1} \end{cases} \tag{2.57}$$

Proof — The function $\eta_{c_j,d_j,t,x}(\cdot)$ is minimal for a given $T > 0$ if and only if $0 \in \partial_-\eta_{c_j,d_j,t,x}(T)$ by [18]. Since $u_0(\rho_j) \in -\partial_+\psi(\rho_j) \cap \mathbb{R}_-$, we have by the Legendre-Fenchel inversion formula that $\rho_j \in \partial_-\varphi^*(u_0(\rho_j))$. This last formula implies $0 \in \partial_- \left(\varphi^*(\cdot) - \cdot\rho_j\right)(u_0(\rho_j))$ and thus that:

$$\psi(\rho_j) = \inf_{u \in \mathrm{Dom}(\varphi^*)} [\varphi^*(u) - \rho_j u] = \varphi^*(u_0(\rho_j)) - \rho_j u_0(\rho_j)$$

The property $c_j = \psi(\rho_j)$ implies that $-c_j + \varphi^*\left(u_0(\rho_j)\right) = \rho_j u_0(\rho_j)$ by the previous formula. Equation (2.55) thus implies:

$$\begin{aligned} \partial_-\eta_{c_j,d_j,t,x}(\tfrac{\xi - x}{u_0(\rho_j)}) &= \{w \mid \exists v \in \partial_-\varphi^*\left(u_0(\rho_j)\right), \ \ w = \rho_j u_0(\rho_j) - u_0(\rho_j)v\} \\ &:= \{\rho_j u_0(\rho_j)\} - u_0(\rho_j)\partial_-\varphi^*\left(u_0(\rho_j)\right) \end{aligned} \tag{2.58}$$

Since $\rho_j \in \partial_-\varphi^*\left(u_0(\rho_j)\right)$, this last property implies that $0 \in \partial_-\eta_{c_j,d_j,t,x}(\frac{\xi - x}{u_0(\rho_j)})$. Hence, $T_0(\rho_j, x) := \frac{\xi - x}{u_0(\rho_j)}$ minimizes the convex function $\eta_{c_j,d_j,t,x}(\cdot)$ over $\mathbb{R}_+^*$.

Since $\eta_{c_j,d_j,t,x}(\cdot)$ is convex, it is decreasing for $T \leq T_0(\rho_j, x)$ and increasing for $T \geq T_0(\rho_j, x)$. The values of the capture time T which minimize $\eta_{c_j,d_j,t,x}(T)$ over $[-\frac{\xi-x}{\nu^\flat}, \infty[\cap[t - \overline{\gamma}_{j+1}, t - \overline{\gamma}_j]$ are thus given by equation (2.57). Note that the property $u_0(\rho_j) \in [-\nu^\flat, 0]$ implies $-\frac{\xi-x}{\nu^\flat} \leq T_0(\rho_j, x)$. Note also that since $(t, x) \in \mathrm{Dom}(\mathbf{M}_{\gamma_j})$, we have $-\frac{\xi-x}{\nu^\flat} \leq t - \overline{\gamma}_j$. ■

Proposition 11. [Computation of $\mathbf{M}_{\gamma_j}(\cdot,\cdot)$] For all $(t, x) \in \mathrm{Dom}(\mathbf{M}_{\gamma_j})$, the solution $\mathbf{M}_{\gamma_j}(t, x)$ can be computed using the following formula:

$$\mathbf{M}_{\gamma_j}(t,x) = \begin{cases} (i) & t\psi(\rho_j) + \rho_j(\xi - x) + d_j & \text{if } T_0(\rho_j, x) \in [t - \overline{\gamma}_{j+1}, t - \overline{\gamma}_j] \\ (ii) & \psi(\rho_j)\overline{\gamma}_j + d_j + (t - \overline{\gamma}_j)\varphi^*(\frac{\xi-x}{t-\overline{\gamma}_j}) & \text{if } t - \overline{\gamma}_j \leq T_0(\rho_j, x) \\ (iii) & \psi(\rho_j)\overline{\gamma}_{j+1} + d_j + (t - \overline{\gamma}_{j+1})\varphi^*(\frac{\xi-x}{t-\overline{\gamma}_{j+1}}) & \text{if } T_0(\rho_j, x) \leq t - \overline{\gamma}_{j+1} \end{cases} \tag{2.59}$$

Proof — The cases (ii) and (iii) in equation (2.59) are trivially obtained by combining equations (2.54) and (2.57). The case (i) in equation (2.59) is obtained by combining (2.53), (2.57) and observing that $\varphi^*\left(\frac{\xi-x}{T_0(\rho_j,x)}\right) = \psi(\rho_j) + \frac{\xi-x}{T_0(\rho_j,x)}\rho_j$. ■

Remark 8. Equation (2.59) can also be obtained from equation (2.83), observing that the affine upstream boundary condition (2.49) can be viewed as an affine internal condition of the form (2.73), where:

$$\begin{cases} \overline{\delta}_l = \overline{\gamma}_j \\ \overline{\delta}_{l+1} = \overline{\gamma}_{j+1} \\ x_l = \xi \\ v_l = 0 \\ g_l = c_j \\ h_l = c_j\overline{\gamma}_j + d_j \end{cases} \tag{2.60}$$

Figure 2.10 illustrates the different domains of equation (2.59) for the solution associated with an affine upstream condition defined by equation (2.49).

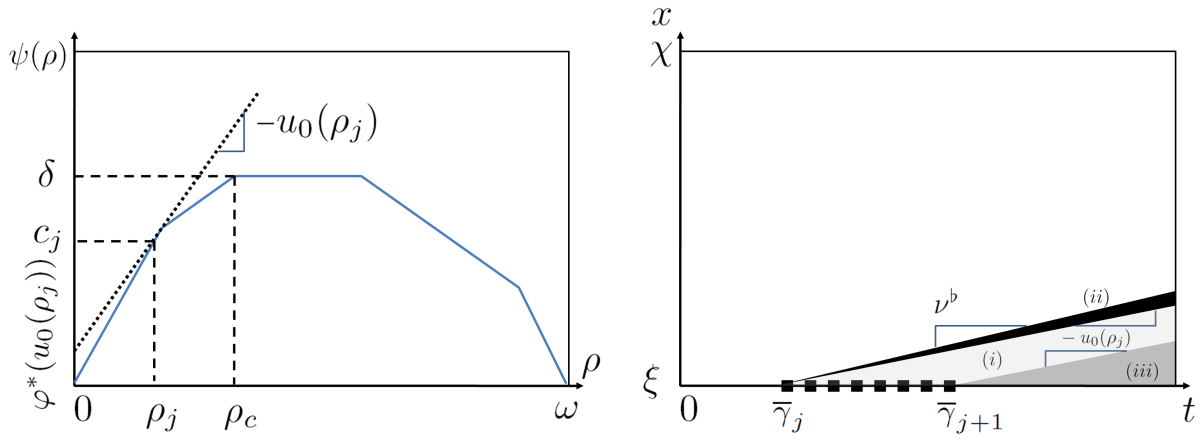

Figure 2.10: **Construction of the solution associated with an affine upstream boundary condition.**
Left: Illustration of the construction of a $u_0(\rho_j)$ from a known c_j. The transform $\varphi^*(u_0(\rho_j))$ corresponds to the value intercepted on the vertical axis by the tangent line of slope $-u_0(\rho_j)$ to the graph of ψ in ρ_j. **Right:** The (t, x) domain of the solution corresponding to the affine upstream boundary condition (2.49) can be separated in three different areas. The domain highlighted in light gray corresponds to the case (i) in equation (2.59). The domain highlighted in dark gray corresponds to the case (ii) and the remaining domain in medium gray corresponds to the case (iii). The domain of the upstream boundary condition is represented by a dashed line.

2.5.3 Analytic Lax-Hopf formula associated with an affine downstream boundary condition

Definition 19. [Affine downstream boundary condition] We consider the following downstream boundary condition $\beta_k(t, \chi)$ of $\beta(t, x)$:

$$\beta_k(t,x) = \begin{cases} e_k t + f_k & \text{if } t \in [\overline{\beta}_k, \overline{\beta}_{k+1}] \\ +\infty & \text{otherwise} \end{cases} \tag{2.61}$$

In the following computation, we consider that $x < \chi$. We also assume that the value condition (2.61) satisfies the condition $e_k \in \mathrm{Im}(\psi) = [0, \delta]$.

Proposition 12. [Lax-Hopf formula for an affine downstream boundary condition] The Lax-Hopf formula (2.62) associated with the downstream boundary condition (2.61) can

be expressed as:

$$\mathbf{M}_{\beta_k}(t,x) \;=\; \inf_{T\in\left[\frac{\chi-x}{\nu^\sharp},+\infty\right[\cap\left[t-\overline{\beta}_{k+1},t-\overline{\beta}_k\right]} \left(e_k(t-T)+f_k+T\varphi^*\left(\frac{\chi-x}{T}\right)\right) \quad \forall (t,x)\in\mathbb{R}_+^*\times X \tag{2.62}$$

Proof — The Lax-Hopf formula (2.32) associated with the affine downstream boundary condition can be written as:

$$\mathbf{M}_{\beta_k}(t,x) \;=\; \inf_{(u,T)\in \mathrm{Dom}(\varphi^*)\times\mathbb{R}_+ \text{ such that } x+Tu=\chi \text{ and } \overline{\beta}_k\le t-T\le\overline{\beta}_{k+1}} (e_k(t-T)+f_k+T\varphi^*(u)) \tag{2.63}$$

We define the variable change $T := \frac{\chi-x}{u}$, which represents the capture time using the control u. Since $T=\frac{\chi-x}{u}>0$ and $x<\chi$, we have $u>0$. The constraint $u\in\mathrm{Dom}(\varphi^*):=[-\nu^\flat,\nu^\sharp]$ implies $T\in[\frac{\chi-x}{\nu^\sharp},+\infty[$. The additional constraint $t-\frac{\chi-x}{u}\in[\overline{\beta}_k,\overline{\beta}_{k+1}]$ can be expressed as $T\in[t-\overline{\beta}_{k+1},t-\overline{\beta}_k]$, which yields equation (2.62). ■

Proposition 13. [Domain of influence of a downstream boundary condition] The domain of definition of $\mathbf{M}_{\beta_k}(\cdot,\cdot)$ is given by the following formula:

$$\mathrm{Dom}(\mathbf{M}_{\beta_k}) = \{(t,x)\in\mathbb{R}_+\times X \;\text{ such that }\; x\ge\chi-\nu^\sharp(t-\overline{\beta}_k)\} \tag{2.64}$$

Proof — The Lax-Hopf formula (2.63) implies:

$$\mathrm{Dom}(\mathbf{M}_{\beta_k}) := \left\{(t,x)\in\mathbb{R}_+\times X \;\text{ such that }\; \exists T\in\left[\frac{\chi-x}{\nu^\sharp},+\infty\right[\cap\left[t-\overline{\beta}_{k+1},t-\overline{\beta}_k\right]\right\}$$

Hence, $(t,x)\in\mathrm{Dom}(\mathbf{M}_{\beta_k})$ if and only if $\frac{\chi-x}{\nu^\sharp}\le t-\overline{\beta}_k$, which in turn implies equation (2.64). ■

Definition 20. [Auxiliary objective function] For all $(t,x)\in\mathrm{Dom}(\mathbf{M}_{\beta_k})$, we define an objective function $\theta_{e_k,f_k,t,x}(\cdot)$ by:

$$\forall T\in\mathbb{R}_+^* \;\; \theta_{e_k,f_k,t,x}(T) := e_k(t-T)+f_k+T\varphi^*\left(\frac{\chi-x}{T}\right) \tag{2.65}$$

Given this definition, equation (2.62) becomes:

$$\mathbf{M}_{\beta_k}(t,x) \;=\; \inf_{T\in\left[\frac{\chi-x}{\nu^\sharp},+\infty\right[\cap\left[t-\overline{\beta}_{k+1},t-\overline{\beta}_k\right]} \theta_{e_k,f_k,t,x}(T) \tag{2.66}$$

Since $\varphi^*(\cdot)$ is convex, its associated perspective function $T\to T\varphi^*(\frac{\chi-x}{T})$ is also convex [18] for $T>0$. Hence the function $\theta_{e_k,f_k,t,x}(\cdot)$ is convex as the sum of two convex functions. The subderivative of $\theta_{e_k,f_k,t,x}(\cdot)$ is given by:

$$\forall T \in [\tfrac{\chi-x}{\nu^\sharp}, +\infty[, \quad \partial_- \theta_{e_k,f_k,t,x}(T) \begin{array}{l} = \left\{ w \mid \exists v \in \partial_- \varphi^*(\tfrac{\chi-x}{T}),\ \ w = -e_k + \varphi^*(\tfrac{\chi-x}{T}) - \tfrac{\chi-x}{T} v \right\} \\ := \left\{ -e_k + \varphi^*(\tfrac{\chi-x}{T}) \right\} - \tfrac{\chi-x}{T} \partial_- \varphi^*(\tfrac{\chi-x}{T}) \end{array} \tag{2.67}$$

with a slight abuse of notation for the second line as in the previous two sections.

Definition 21. [Density associated with e_k] Recalling that $\mathrm{Im}(\psi) = [0, \delta]$, we define ρ_c as:

$$\rho_c = \sup_{\rho \in [0,\omega] \text{ such that } \psi(\rho) = \delta} \rho$$

Since $e_k \in \mathrm{Im}(\psi) = [0, \delta]$, there exists $\rho_k \in [\rho_c, \omega]$ such that $\psi(\rho_k) = e_k$. Note that since $\psi(\cdot)$ is concave and $\delta > 0$, $\psi(\cdot)$ is decreasing on $[\rho_c, \omega]$ and thus $\partial_+ \psi(\rho_k) \cap \mathbb{R}_- \neq \emptyset$.

- Let $u_0(\rho_k)$ be an element of $-\partial_+ \psi(\rho_k) \cap \mathbb{R}_+$
- Let $T_0(\rho_k, x)$ be defined as

$$T_0(\rho_k, x) := \begin{cases} \frac{\xi - x}{u_0(\rho_k)} & \text{if } \ u_0(\rho_k) \neq 0 \\ +\infty & \text{if } \ u_0(\rho_k) = 0 \end{cases} \tag{2.68}$$

We have by the Legendre-Fenchel inversion formula that $\rho_k \in \partial_- \varphi^*(u_0(\rho_k))$, which implies that $u_0(\rho_k) \in \mathrm{Dom}(\varphi^*)$.

Remark 9. Note that the definition of ρ_c differs from the previous section for functions $\psi(\cdot)$ which are not strictly concave. This is sometimes referred as "lower critical density" (section 2.5.2) and "upper critical density" (section 2.5.3), but we have kept the same notation since the two corresponding densities are only intermediate variables in our derivations.

Proposition 14. [Explicit minimization of $\theta_{e_k,f_k,t,x}(\cdot)$] For all $(t, x) \in \mathrm{Dom}(\mathbf{M}_{\beta_k})$, the function $\theta_{e_k,f_k,t,x}(\cdot)$ has the following minimizer over $[\tfrac{\chi-x}{\nu^\sharp}, +\infty[\cap [t - \overline{\beta}_{k+1}, t - \overline{\beta}_k]$:

$$\begin{cases} T_0(\rho_k, x) & \text{if } \ T_0(\rho_k, x) \in [t - \overline{\beta}_{k+1}, t - \overline{\beta}_k] \\ t - \overline{\beta}_k & \text{if } \ t - \overline{\beta}_k \leq T_0(\rho_k, x) \\ t - \overline{\beta}_{k+1} & \text{if } \ T_0(\rho_k, x) \leq t - \overline{\beta}_{k+1} \end{cases} \tag{2.69}$$

Proof — The function $\theta_{e_k,f_k,t,x}(\cdot)$ is minimal for a given $T > 0$ if and only if $0 \in \partial_- \theta_{e_k,f_k,t,x}(T)$ by [18]. Since $u_0(\rho_k) \in -\partial_+ \psi(\rho_k)$, we have by the Legendre-Fenchel inversion formula that $\rho_k \in \partial_- \varphi^*(u_0(\rho_k))$. In the exact same way as the previous section, this last formula implies that $0 \in \partial_- \left(\varphi^*(\cdot) - \cdot \rho_k\right)(u_0(\rho_k))$ and thus that:

$$\psi(\rho_k) = \inf_{u \in \mathrm{Dom}(\varphi^*)} \left[\varphi^*(u) - \rho_k u\right] = \varphi^*(u_0(\rho_k)) - \rho_k u_0(\rho_k)$$

The property $e_k = \psi(\rho_k)$ implies that $-e_k + \varphi^*(u_0(\rho_k)) = \rho_k u_0(\rho_k)$. Equation (2.67) thus implies:

$$\begin{array}{ll} \partial_- \theta_{e_k,f_k,t,x}(\frac{\chi-x}{u_0(\rho_k)}) & = \{w \mid \exists v \in \partial_- \varphi^*\left(u_0(\rho_k)\right), \;\; w = \rho_k u_0(\rho_k) - u_0(\rho_k) v\} \\ & := \{\rho_k u_0(\rho_k)\} - u_0(\rho_k) \partial_- \varphi^*\left(u_0(\rho_k)\right) \end{array} \tag{2.70}$$

with the same abuse of notation for the second line.

Since $\rho_k \in \partial_- \varphi^*\left(u_0(\rho_k)\right)$, this last property implies that $0 \in \partial_- \theta_{e_k,f_k,t,x}(\frac{\chi-x}{u_0(\rho_k)})$. Hence, $T_0(\rho_k, x) := \frac{\chi-x}{u_0(\rho_k)}$ minimizes the convex function $\theta_{e_k,f_k,t,x}(\cdot)$ over $\mathbb{R}_+^*$.

Since $\theta_{e_k,f_k,t,x}(\cdot)$ is convex, it is decreasing for $T < T_0(\rho_k, x)$ and increasing for $T > T_0(\rho_k, x)$. The values of the capture time T which minimize $\theta_{e_k,f_k,t,x}(T)$ over $[\frac{\chi-x}{\nu^\sharp}, +\infty[\cap [t - \overline{\beta}_{k+1}, t - \overline{\beta}_k]$ are thus given by equation (2.69). Note that the property $u_0(\rho_k) \in [0, \nu^\sharp]$ implies $\frac{\chi-x}{\nu^\sharp} \leq T_0(\rho_k, x)$. Note also that since $(t, x) \in \mathrm{Dom}(\mathbf{M}_{\beta_k})$, we have $\frac{\chi-x}{\nu^\sharp} \leq t - \overline{\beta}_k$. ■

Proposition 15. [Computation of $\mathbf{M}_{\beta_k}(\cdot,\cdot)$] For all $(t, x) \in \mathrm{Dom}(\mathbf{M}_{\beta_k})$, the expression $\mathbf{M}_{\beta_k}(t, x)$ can be computed using the following formula:

$$\mathbf{M}_{\beta_k}(t,x) = \left\{ \begin{array}{lll} (i) & t\psi(\rho_k) + \rho_k(\chi - x) + f_k & \text{if } \; T_0(\rho_k, x) \in [t - \overline{\beta}_{k+1}, t - \overline{\beta}_k] \\ (ii) & \psi(\rho_k)\overline{\beta}_k + f_k + (t - \overline{\beta}_k)\varphi^*(\frac{\chi-x}{t-\overline{\beta}_k}) & \text{if } \; t - \overline{\beta}_k \leq T_0(\rho_k, x) \\ (iii) & \psi(\rho_k)\overline{\beta}_{k+1} + f_k + (t - \overline{\beta}_{k+1})\varphi^*(\frac{\chi-x}{t-\overline{\beta}_{k+1}}) & \text{if } \; T_0(\rho_k, x) \leq t - \overline{\beta}_{k+1} \end{array} \right. \tag{2.71}$$

Proof — The cases (ii) and (iii) in equation (2.71) are trivially obtained by combining equations (2.66) and (2.69). The case (i) in equation (2.71) is obtained by combining (2.66), (2.69) and observing that $\varphi^*\left(\frac{\chi-x}{T_0(\rho_k,x)}\right) = \psi(\rho_k) + \frac{\chi-x}{T_0(\rho_k,x)}\rho_k$. ■

Remark 10. Equation (2.71) can be obtained from equation (2.84), observing that the affine downstream boundary condition (2.61) can be viewed as an affine internal condition of the form (2.73), where:

$$\left\{ \begin{array}{l} \overline{\delta}_l = \overline{\beta}_k \\ \overline{\delta}_{l+1} = \overline{\beta}_{k+1} \\ x_l = \chi \\ v_l = 0 \\ g_l = e_k \\ h_l = e_k\overline{\beta}_k + f_k \end{array} \right. \tag{2.72}$$

Figure 2.11 illustrates the different domains of equation (2.71) for the solution associated with an affine downstream boundary condition defined by equation (2.61).

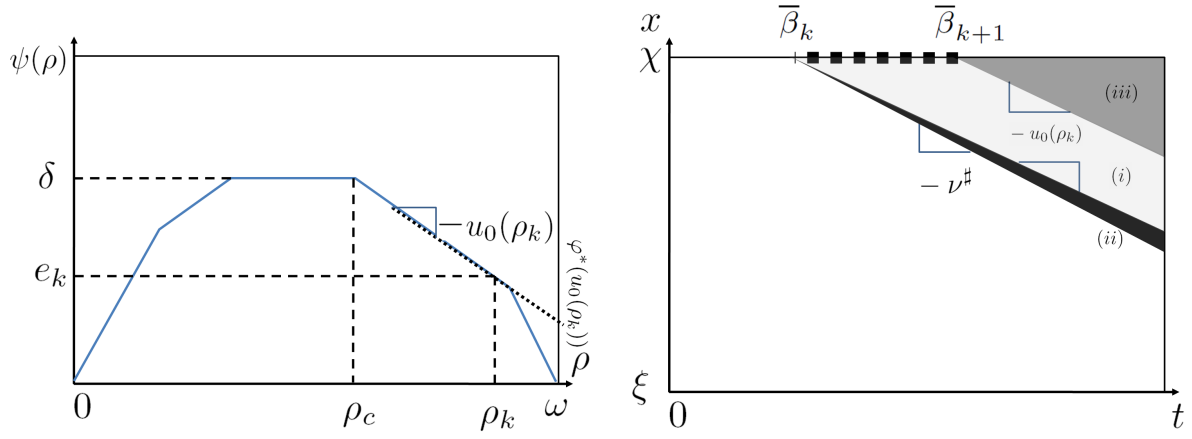

Figure 2.11: **Construction of the solution associated with an affine downstream boundary condition.**
Left: Illustration of the construction of a $u_0(\rho_k)$ from a known e_k. The transform $\varphi^*(u_0(\rho_k))$ corresponds to the value intercepted on the vertical axis by the tangent line of slope $-u_0(\rho_k)$ to the graph of ψ in ρ_k. **Right:** The (t,x) domain of the solution corresponding to the affine downstream boundary condition (2.61) can be separated in three different areas. The domain highlighted in light gray corresponds to the case (i) in equation (2.71). The domain highlighted in dark gray corresponds to the case (ii) and the remaining domain in medium gray corresponds to the case (iii). The domain of the downstream boundary condition is represented by a dashed line.

2.5.4 Analytic Lax-Hopf formula associated with an affine internal condition

The previous section explained how to compute the solution to affine initial and boundary conditions. We now treat the problem of internal conditions using a similar approach. As will appear in this section, the algebra involved in doing this mathematical construction is more involved than the previous case.

Definition 22. [Affine internal condition] We consider the following affine internal condition $\mu_l(\cdot,\cdot)$, where l is an integer:

$$\mu_l(t,x) = \begin{cases} g_l(t-\overline{\delta}_l)+h_l & \text{if } x = x_l + v_l(t-\overline{\delta}_l) \\ & \text{and } t \in [\overline{\delta}_l, \overline{\delta}_{l+1}] \\ +\infty & \text{otherwise} \end{cases} \tag{2.73}$$

For the computation of the corresponding solution $\mathbf{M}_{\mu_l}(t,x)$, we assume that (t,x) satisfy $x \neq x_l + v_l(t-\overline{\delta}_l)$. In addition, we assume that the constants g_l and v_l satisfy $0 \leq g_l \leq \varphi^*(-v_l)$.

Proposition 16. [Lax-Hopf formula for affine internal condition] The Lax-Hopf formula (2.74) associated with the internal boundary condition (2.73) can be expressed as:

$$\mathbf{M}_{\mu_l}(t,x) = \inf_{T\in\mathbb{R}_+\cap[t-\overline{\delta}_{l+1},t-\overline{\delta}_l]} \left(g_l(t-T-\overline{\delta}_l) + h_l + T\varphi^*\left(\frac{x_l+v_l(t-\overline{\delta}_l-T)-x}{T}\right)\right) \quad (2.74)$$

Proof — The Lax-Hopf formula (2.32) associated with an affine internal condition reads:

$$\mathbf{M}_{\mu_l}(t,x) \; = \inf_{(u,T)\in \mathrm{Dom}(\varphi^*)\times\mathbb{R}_+ \text{ such that } x+Tu=x_l+v_l(t-T-\overline{\delta}_l) \text{ and } \overline{\delta}_l\le t-T\le\overline{\delta}_{l+1}} \big(g_l(t-T-\overline{\delta}_l)+h_l+T\varphi^*(u)\big) \quad (2.75)$$

Since $x+Tu = x_l+v_l(t-T-\overline{\delta}_l)$, we have $u=\frac{x_l+v_l(t-T-\overline{\delta}_l)-x}{T}$. In addition, the constraint $\overline{\delta}_l \le t-T\le\overline{\delta}_{l+1}$ can be written as $T\in[t-\overline{\delta}_{l+1},t-\overline{\delta}_l]$, which yields (2.74). ■

The solution to the affine internal condition has a domain of definition, which can be computed analytically as follows.

Proposition 17. [Domain of influence of an affine internal condition] The domain of definition of $\mathbf{M}_{\mu_l}(\cdot,\cdot)$ is given by the following formula:

$$\mathrm{Dom}(\mathbf{M}_{\mu_l}) = \{(t,x)\in\mathbb{R}_+\times X \text{ such that } \; t\ge\overline{\delta}_l \;\text{ and }\; x_l-\nu^\sharp(t-\overline{\delta}_l)\le x\le x_l+\nu^\flat(t-\overline{\delta}_l)\} \quad (2.76)$$

Proof — The Lax-Hopf formula (2.74) implies:

$$\mathrm{Dom}(\mathbf{M}_{\mu_l}) := \Big\{(t,x)\in\mathbb{R}_+\times X \;\text{ s.t. }\; \exists T\in\mathbb{R}_+^*\cap[t-\overline{\delta}_{l+1},t-\overline{\delta}_l] \text{ and } \tfrac{x_l+v_l(t-\overline{\delta}_l-T)-x}{T}\in\mathrm{Dom}(\varphi^*)\Big\}$$

Since $T>0$, the condition $\frac{x_l+v_l(t-\overline{\delta}_l-T)-x}{T}\in\mathrm{Dom}(\varphi^*)=[-\nu^\flat,\nu^\sharp]$ is equivalent to $T\ge\frac{x_l+v_l(t-\overline{\delta}_l)-x}{\nu^\sharp+v_l}$ and $T\ge\frac{x_l+v_l(t-\overline{\delta}_l)-x}{-\nu^\flat+v_l}$. Hence, $(t,x)\in\mathrm{Dom}(\varphi^*)$ if and only if the set $\mathbb{R}_+^*\cap[t-\overline{\delta}_{l+1},t-\overline{\delta}_l]\cap[\frac{x_l+v_l(t-\overline{\delta}_l)-x}{\nu^\sharp+v_l},+\infty[\cap[\frac{x_l+v_l(t-\overline{\delta}_l)-x}{-\nu^\flat+v_l},+\infty[$ is not empty, which implies

$$\max\left(0,\frac{x_l+v_l(t-\overline{\delta}_l)-x}{-\nu^\flat+v_l},\frac{x_l+v_l(t-\overline{\delta}_l)-x}{\nu^\sharp+v_l}\right)\le t-\overline{\delta}_l$$

This last inequality implies equation (2.76). ■

The method followed next also makes use of an auxiliary objective function, which is later used to explicitly find the minimizer.

Definition 23. [Auxiliary objective function] For all $(t,x) \in \mathrm{Dom}(\mathbf{M}_{\mu_l})$, we define the function $\kappa_{\overline{\delta}_l,g_l,h_l,x_l,v_l,t,x}(\cdot)$ as:

$$\forall T \in \mathbb{R}_+^*, \;\; \kappa_{\overline{\delta}_l,g_l,h_l,x_l,v_l,t,x}(T) := \left(g_l(t-T-\overline{\delta}_l) + h_l + T\varphi^*\left(\tfrac{x_l+v_l(t-\overline{\delta}_l-T)-x}{T}\right)\right) \tag{2.77}$$

Given this definition, equation (2.74) becomes:

$$\mathbf{M}_{\mu_l}(t,x) = \inf_{T\in\left[\max\left(0,\frac{x_l+v_l(t-\overline{\delta}_l)-x}{-\nu^\flat+v_l},\frac{x_l+v_l(t-\overline{\delta}_l)-x}{\nu^\sharp+v_l},t-\overline{\delta}_{l+1}\right),t-\overline{\delta}_l\right]} \kappa_{\overline{\delta}_l,g_l,h_l,x_l,v_l,t,x}(T) \tag{2.78}$$

Since $\varphi^*(\cdot)$ is convex, the function $h : u \to \varphi^*(u-v_l)$ is convex and its associated perspective function $T \to Th(\frac{x_l+v_l(t-\overline{\delta}_l)-x}{T})$ is also convex for $T>0$ by [18]. Hence the function $\kappa_{\overline{\delta}_l,g_l,h_l,x_l,v_l,t,x}(\cdot)$ is convex as the sum of two convex functions. The subderivative of $\kappa_{\overline{\delta}_l,g_l,h_l,x_l,v_l,t,x}(\cdot)$ is given by:

$$\begin{array}{l}\forall T \in \left[\max\left(0,\frac{x_l+v_l(t-\overline{\delta}_l)-x}{-\nu^\flat+v_l},\frac{x_l+v_l(t-\overline{\delta}_l)-x}{\nu^\sharp+v_l},t-\overline{\delta}_{l+1}\right),t-\overline{\delta}_l\right], \;\; \partial_-\kappa_{\overline{\delta}_l,g_l,h_l,x_l,v_l,t,x}(T) = \\ \left\{w \mid \exists v \in \partial_-\varphi^*(\frac{x_l+v_l(t-\overline{\delta}_l)-x}{T}-v_l), w = -g_l+\varphi^*(\frac{x_l+v_l(t-\overline{\delta}_l)-x}{T}-v_l) - \frac{x_l+v_l(t-\overline{\delta}_l)-x}{T}v\right\}\end{array} \tag{2.79}$$

which can be written using a slight abuse of notation as:

$$\partial_-\kappa_{\overline{\delta}_l,g_l,h_l,x_l,v_l,t,x}(T) := -g_l+\varphi^*(\frac{x_l+v_l(t-\overline{\delta}_l)-x}{T}-v_l) - \frac{x_l+v_l(t-\overline{\delta}_l)-x}{T}\partial_-\varphi^*(\frac{x_l+v_l(t-\overline{\delta}_l)-x}{T}-v_l) \tag{2.80}$$

Because of the higher complexity of this case, we need to define intermediate quantities used in the explicit minimization.

Definition 24. [Densities associated with v_l and g_l]

- We define the function $f_{v_l}(\cdot)$ as $f_{v_l} : \rho \to \psi(\rho) - \rho v_l$. The function f_{v_l} is concave as the sum of concave functions and attains its maximum value $\varphi^*(-v_l)$ (by definition of the function $\varphi^*(\cdot)$) for a given $\rho := \rho_l$.
- Note that since $v_l \in [0,\nu^\flat[$, the function f_{v_l} satisfies $f_{v_l}(0)=0$ and $f_{v_l}(\omega) \leq 0$. By assumption, we also have $g_l \leq \varphi^*(-v_l)$ and since $f_{v_l}(\cdot)$ is concave and continuous, there exist two solutions $\rho_1(v_l,g_l) \in [0,\rho_l]$ and $\rho_2(v_l,g_l) \in [\rho_l,\omega]$ such that $f_{v_l}(\rho_p(v_l,g_l)) = g_l$ for $p \in \{1,2\}$ (see Figure 2.12).

- For $p \in \{1,2\}$, we also define $u_p(v_l, g_l)$ as elements of $-\partial_+\psi(\rho_p(v_l, g_l))$. Note that since f_{v_l} is concave, it is increasing on $[0, \rho_l]$ and decreasing on $[\rho_l, \omega]$, which implies that $u_1(v_l, g_l) \leq -v_l$ and $u_2(v_l, g_l) \geq -v_l$. Note also that the Legendre-Fenchel inversion formula implies that $u_p(v_l, g_l) \in \mathrm{Dom}(\varphi^*)$ for $p \in \{1,2\}$.

Definition 25. [Capture times associated with $u_p(v_l, g_l)$, for $p \in \{1,2\}$]

- We define $T_p(t, x, v_l, g_l)$ for $p \in \{1,2\}$ as:

$$T_p(t,x,v_l,g_l) := \begin{cases} \frac{x_l + v_l(t-\overline{\delta}_l) - x}{u_p(v_l,g_l)+v_l} & \text{if} \quad u_p(v_l,g_l) \neq -v_l \\ +\infty & \text{if} \quad u_p(v_l,g_l) = -v_l \end{cases} \tag{2.81}$$

- The definition of $T_p(\cdot,\cdot,\cdot,\cdot)$ implies that $T_1(t,x,v_l,g_l) \geq 0$ if and only if $x_l + v_l(t-\overline{\delta}_l) - x \leq 0$ and that $T_2(t,x,v_l,g_l) \geq 0$ if and only if $x_l + v_l(t-\overline{\delta}_l) - x \geq 0$.

- Note also that since $u_p(v_l, g_l) \in [-\nu^\flat, \nu^\sharp]$, we have $T_1(t,x,v_l,g_l) \geq \frac{x_l+v_l(t-\overline{\delta}_l)-x}{-\nu^\flat+v_l}$ when $x_l + v_l(t-\overline{\delta}_l) - x \leq 0$ and $T_2(t,x,v_l,g_l) \geq \frac{x_l+v_l(t-\overline{\delta}_l)-x}{\nu^\sharp+v_l}$ when $x_l + v_l(t-\overline{\delta}_l) - x \geq 0$.

The previous definitions can now be used to compute the explicit minimizer.

Proposition 18. [Explicit minimization of $\kappa_{\overline{\delta}_l,g_l,h_l,x_l,v_l,t,x}(\cdot)$] For all $(t,x) \in \mathrm{Dom}(\mathbf{M}_{\mu_l})$, the function $\kappa_{\overline{\delta}_l,g_l,h_l,x_l,v_l,t,x}(\cdot)$ has the following minimizer over $\left[\max\left(0, \frac{x_l+v_l(t-\overline{\delta}_l)-x}{-\nu^\flat+v_l}, \frac{x_l+v_l(t-\overline{\delta}_l)-x}{\nu^\sharp+v_l}, t-\overline{\delta}_{l+1}\right), t-\overline{\delta}_l\right]$:

$$\begin{cases} (i) & T_1(t,x,v_l,g_l) & \text{if } x_l + v_l(t-\overline{\delta}_l) - x \leq 0 \\ & & \text{and } T_1(t,x,v_l,g_l) \in \left[t-\overline{\delta}_{l+1}, t-\overline{\delta}_l\right] \\ (ii) & t-\overline{\delta}_l & \text{if } x_l + v_l(t-\overline{\delta}_l) - x \leq 0 \\ & & \text{and } T_1(t,x,v_l,g_l) \geq t-\overline{\delta}_l \\ (iii) & t-\overline{\delta}_{l+1} & \text{if } x_l + v_l(t-\overline{\delta}_l) - x \leq 0 \\ & & \text{and } T_1(t,x,v_l,g_l) \leq t-\overline{\delta}_{l+1} \\ (iv) & T_2(t,x,v_l,g_l) & \text{if } x_l + v_l(t-\overline{\delta}_l) - x \geq 0 \\ & & \text{and } T_2(t,x,v_l,g_l) \in \left[t-\overline{\delta}_{l+1}, t-\overline{\delta}_l\right] \\ (v) & t-\overline{\delta}_l & \text{if } x_l + v_l(t-\overline{\delta}_l) - x \geq 0 \\ & & \text{and } T_2(t,x,v_l,g_l) \geq t-\overline{\delta}_l \\ (vi) & t-\overline{\delta}_{l+1} & \text{if } x_l + v_l(t-\overline{\delta}_l) - x \geq 0 \\ & & \text{and } T_2(t,x,v_l,g_l) \leq t-\overline{\delta}_{l+1} \end{cases} \tag{2.82}$$

Proof — The function $\kappa_{\overline{\delta}_l,g_l,h_l,x_l,v_l,t,x}(T)$ is minimal for a given $T > 0$ if and only if $0 \in \partial_-\kappa_{\overline{\delta}_l,g_l,h_l,x_l,v_l,t,x}(T)$. Since $u_p(v_l,g_l) \in -\partial_+\psi(\rho_p(v_l,g_l))$ for $p \in \{1,2\}$, we have by the

Legendre-Fenchel inversion formula that $\rho_p(v_l, g_l) \in \partial_- \varphi^*(u_p(v_l, g_l))$. This last formula imply that $0 \in \partial_- \left(\varphi^*(\cdot) - \cdot \rho_p(v_l, g_l)\right)(u_p(v_l, g_l))$ and thus that:

$$\begin{aligned}\psi(\rho_p(v_l, g_l)) &= \inf_{u \in \mathrm{Dom}(\varphi^*)} \left[\varphi^*(u) - \rho_p(v_l, g_l)u\right] \\ &= \varphi^*(u_p(v_l, g_l)) - \rho_p(v_l, g_l)u_p(v_l, g_l)\end{aligned}$$

Since we consider only positive capture times T, we have to consider two situations:

- If $x_l + v_l(t - \overline{\delta}_l) - x \leq 0$, we have that $T_2(t, x, v_l, g_l) \leq 0$ and $T_1(t, x, v_l, g_l) \geq 0$. The relations $\psi(\rho_1(v_l, g_l)) - \rho_1(v_l, g_l)v_l = g_l$, $\rho_1(v_l, g_l) \in \partial_- \varphi^*(u_1(v_l, g_l))$ and $\psi(\rho_1(v_l, g_l)) = \varphi^*(u_1(v_l, g_l)) - \rho_1(v_l, g_l)u_1(v_l, g_l)$ imply that $-g_l + \varphi^*(u_1(v_l, g_l)) - (u_1(v_l, g_l) + v_l)\rho_1(v_l, g_l) = 0$. Hence, using our definition of $T_1(t, x, v_l, g_l) := \frac{x_l + v_l(t - \overline{\delta}_l) - x}{u_1(v_l, g_l) + v_l}$, we have that:

  $$0 = -g_l + \varphi^*\left(\frac{x_l + v_l(t - \overline{\delta}_l) - x}{T_1(t, x, v_l, g_l)} - v_l\right) - \frac{x_l + v_l(t - \overline{\delta}_l) - x}{T_1(t, x, v_l, g_l)}\rho_1(v_l, g_l)$$

  Using equation (2.79), we have $0 \in \partial_- \kappa^-_{\overline{\delta}_l, g_l, h_l, x_l, v_l, t, x}(T_1(t, x, v_l, g_l))$ and thus $T_1(t, x, v_l, g_l)$ minimizes $\kappa^-_{\overline{\delta}_l, g_l, h_l, x_l, v_l, t, x}(T)$ for positive times T.

  The cases (i), (ii) and (iii) in equation (2.82) are obtained using the convexity of $\kappa^-_{\overline{\delta}_l, g_l, h_l, x_l, v_l, t, x}(\cdot)$. Note that in our situation, definition 25 implies that $T_1(t, x, v_l, g_l) \geq \frac{x_l + v_l(t - \overline{\delta}_l) - x}{-\nu^\flat + v_l}$.

  Since $x_l + v_l(t - \overline{\delta}_l) - x \leq 0$, we also have that $\frac{x_l + v_l(t - \overline{\delta}_l) - x}{\nu^\sharp + v_l} \leq 0$. Hence, we have that:

  $$T_1(t, x, v_l, g_l) \geq \max\left(0, \frac{x_l + v_l(t - \overline{\delta}_l) - x}{-\nu^\flat + v_l}, \frac{x_l + v_l(t - \delta_l) - x}{\nu^\sharp + v_l}\right)$$

  Hence, the condition $T_1(t, x, v_l, g_l) \geq \max\left(0, \frac{x_l + v_l(t - \overline{\delta}_l) - x}{-\nu^\flat + v_l}, \frac{x_l + v_l(t - \overline{\delta}_l) - x}{\nu^\sharp + v_l}, t - \overline{\delta}_{l+1}\right)$ is satisfied if and only if $T_1(t, x, v_l, g_l) \geq t - \overline{\delta}_{l+1}$. Note also that if the previous condition is not satisfied, then $\max\left(0, \frac{x_l + v_l(t - \overline{\delta}_l) - x}{-\nu^\flat + v_l}, \frac{x_l + v_l(t - \overline{\delta}_l) - x}{\nu^\sharp + v_l}, t - \overline{\delta}_{l+1}\right) = t - \overline{\delta}_{l+1}$.

- If $x_l + v_l(t - \overline{\delta}_l) - x \geq 0$, we have that $T_1(t, x, v_l, g_l) \leq 0$ and $T_2(t, x, v_l, g_l) \geq 0$. The relations $\psi(\rho_1(v_l, g_l)) - \rho_1(v_l, g_l)v_l = g_l$, $\rho_2(v_l, g_l) \in \partial_- \varphi^*(u_2(v_l, g_l))$ and $\psi(\rho_2(v_l, g_l)) = \varphi^*(u_2(v_l, g_l)) - \rho_2(v_l, g_l)u_2(v_l, g_l)$ imply that $-g_l + \varphi^*(u_1(v_l, g_l)) - (u_1(v_l, g_l) + v_l)\rho_1(v_l, g_l) = 0$. Hence, using our definition of $T_2(t, x, v_l, g_l) := \frac{x_l + v_l(t - \overline{\delta}_l) - x}{u_2(v_l, g_l) + v_l}$, we have that:

  $$0 = -g_l + \varphi^*\left(\frac{x_l + v_l(t - \overline{\delta}_l) - x}{T_2(t, x, v_l, g_l)} - v_l\right) - \frac{x_l + v_l(t - \overline{\delta}_l) - x}{T_2(t, x, v_l, g_l)}\rho_2(v_l, g_l)$$

  Using equation (2.79), we have $0 \in \partial_- \kappa^-_{\overline{\delta}_l, g_l, h_l, x_l, v_l, t, x}(T_2(t, x, v_l, g_l))$ and thus $T_2(t, x, v_l, g_l)$ minimizes $\kappa^-_{\overline{\delta}_l, g_l, h_l, x_l, v_l, t, x}(T)$ for positive times T.

The cases (iv), (v) and (vi) in equation (2.82) are obtained using the convexity of $\kappa_{\overline{\delta}_l,g_l,h_l,x_l,v_l,t,x}(\cdot)$. Note that in our situation, definition 25 implies that $T_2(t,x,v_l,g_l) \geq \frac{x_l+v_l(t-\overline{\delta}_l)-x}{\nu^\sharp+v_l}$.

Since $x_l + v_l(t-\overline{\delta}_l) - x \geq 0$, we also have that $\frac{x_l+v_l(t-\overline{\delta}_l)-x}{-\nu^\flat+v_l} \leq 0$. Hence, we have that:

$$T_2(t,x,v_l,g_l) \geq \max\left(0, \frac{x_l+v_l(t-\overline{\delta}_l)-x}{-\nu^\flat+v_l}, \frac{x_l+v_l(t-\overline{\delta}_l)-x}{\nu^\sharp+v_l}\right)$$

Hence, the condition $T_2(t,x,v_l,g_l) \geq \max\left(0, \frac{x_l+v_l(t-\overline{\delta}_l)-x}{-\nu^\flat+v_l}, \frac{x_l+v_l(t-\overline{\delta}_l)-x}{\nu^\sharp+v_l}, t-\overline{\delta}_{l+1}\right)$ is satisfied if and only if $T_2(t,x,v_l,g_l) \geq t-\overline{\delta}_{l+1}$. Note also that if the previous condition is not satisfied, then $\max\left(0, \frac{x_l+v_l(t-\overline{\delta}_l)-x}{-\nu^\flat+v_l}, \frac{x_l+v_l(t-\overline{\delta}_l)-x}{\nu^\sharp+v_l}, t-\overline{\delta}_{l+1}\right) = t-\overline{\delta}_{l+1}$.

Once the minimizer is computed, it can be used to find the explicit expression of the value function.

Proposition 19. [Computation of $\mathbf{M}_{\mu_l}(\cdot,\cdot)$] For all $(t,x) \in \mathrm{Dom}(\mathbf{M}_{\mu_l})$, the expression $\mathbf{M}_{\mu_l}(t,x)$ can be computed using the following formulae:

$$\mathbf{M}_{\mu_l}(t,x) = \begin{cases} (i) & \psi(\rho_1(v_l,g_l))(t-\overline{\delta}_l) + (x_l-x)\rho_1(v_l,g_l) + h_l \\ & \text{if } x_l + v_l(t-\overline{\delta}_l) \leq x \\ & \text{and } T_1(t,x,v_l,g_l) \in \left[t-\overline{\delta}_{l+1}, t-\overline{\delta}_l\right] \\ (ii) & \psi(\rho_2(v_l,g_l))(t-\overline{\delta}_l) + (x_l-x)\rho_2(v_l,g_l) + h_l \\ & \text{if } x_l + v_l(t-\overline{\delta}_l) \geq x \\ & \text{and } T_2(t,x,v_l,g_l) \in \left[t-\overline{\delta}_{l+1}, t-\overline{\delta}_l\right] \end{cases} \tag{2.83}$$

and

$$\mathbf{M}_{\mu_l}(t,x) = \begin{cases} (iii) & h_l + (t-\overline{\delta}_l)\varphi^*\left(\frac{x_l-x}{t-\overline{\delta}_l}\right) \\ & \text{if } x_l + v_l(t-\overline{\delta}_l) \leq x \text{ and } T_1(t,x,v_l,g_l) \geq t-\overline{\delta}_l \\ & \text{or if } x_l + v_l(t-\overline{\delta}_l) \geq x \text{ and } T_2(t,x,v_l,g_l) \geq t-\overline{\delta}_l \\ (iv) & g_l(\overline{\delta}_{l+1}-\overline{\delta}_l) + h_l + (t-\overline{\delta}_{l+1})\varphi^*\left(\frac{x_l+v_l(\overline{\delta}_{l+1}-\overline{\delta}_l)-x}{t-\overline{\delta}_{l+1}}\right) \\ & \text{if } x_l + v_l(t-\overline{\delta}_l) \leq x \text{ and } T_1(t,x,v_l,g_l) \leq t-\overline{\delta}_{l+1} \\ & \\ & \text{or if } x_l + v_l(t-\overline{\delta}_l) \geq x \text{ and } T_2(t,x,v_l,g_l) \leq t-\overline{\delta}_{l+1} \end{cases} \tag{2.84}$$

Proof — The cases (iii) and (iv) in equation (2.84) are trivially obtained by combining equations (2.78) and (2.82).

The cases (i) and (ii) in equation (2.83) are also obtained by combining equations (2.78) and (2.82). By combining the formula $\varphi^*(\frac{x_l+v_l(t-\overline{\delta}_l-T_p(t,x,v_l,g_l))-x}{T_p(t,x,v_l,g_l)}) = \psi(\rho_p(v_l,g_l)) + \frac{x_l+v_l(t-\overline{\delta}_l-T_p(t,x,v_l,g_l))-x}{T_p(t,x,v_l,g_l)}\rho_p(v_l,g_l)$ and the definition of $\rho_p(v_l,g_l)$, we have:

$$-g_l + \varphi^*\left(\frac{x_l + v_l(t-\overline{\delta}_l - T_p(t,x,v_l,g_l)) - x}{T_p(t,x,v_l,g_l)}\right) = \rho_p(v_l,g_l)\frac{x_l+v_l(t-\overline{\delta}_l)-x}{T_p(t,x,v_l,g_l)}$$

Using again the definition of $\rho_p(v_l, g_l)$, we have $g_l - \rho_p(v_l, g_l)v_l = \psi(\rho_p(v_l, g_l))$, which after some algebra leads to the cases (i) and (ii) in equation (2.83). ■

Figure 2.12 illustrates the domains of equation (2.83) and (2.84), for the solution to an affine internal condition defined by equation (2.73).

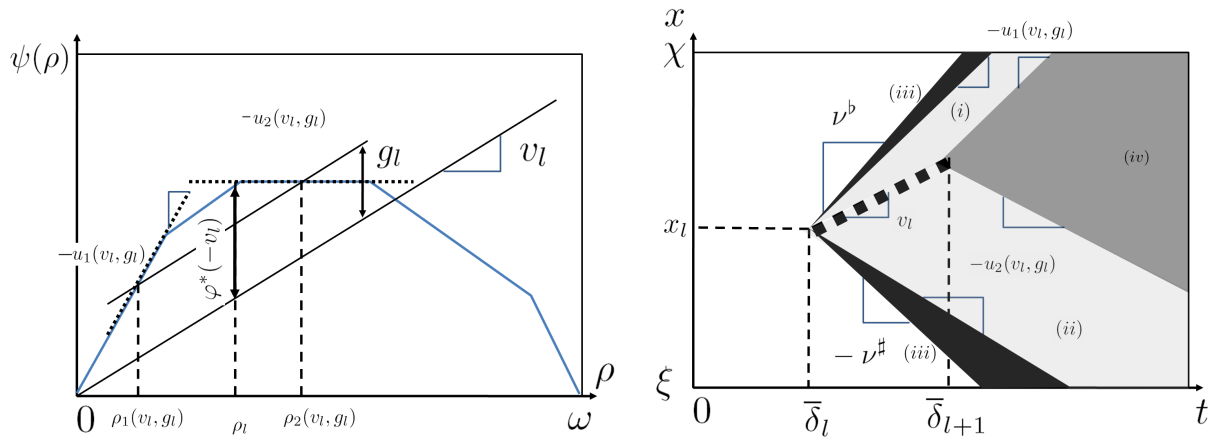

Figure 2.12: **Construction of the solution associated with an affine internal condition.**
Left: Illustration of the construction of a $u_1(v_l, g_l)$ and $u_2(v_l, g_l)$ from known v_l and g_l. **Right:** The (t, x) domain of the solution corresponding to the affine internal condition (2.73) can be separated in four different areas. The domains highlighted in dark gray correspond to the case (iii) in equation (2.84). The domains highlighted in light gray correspond to the cases (i) and (ii) in equation (2.83). The remaining domain in medium gray corresponds to the case (iv) in (2.84). The domain of the internal condition is represented by a dashed line.

2.6 Extension to piecewise affine initial, boundary and internal conditions

2.6.1 Semi-analytic solutions

Using the inf-morphism property (2.36), we can express the solution associated with piecewise affine initial, boundary and internal conditions as a *semi-analytic formula*. A semi-analytic formula is defined here as an operation (in the present case a minimization) on a finite set of closed-form expression functions.

In order to establish the Lax-Hopf algorithm, we first need to establish the following result.

Proposition 20. [Decomposition of piecewise affine functions] Let $\mathbf{c}(\cdot,\cdot)$ be a piecewise affine value condition defined on a finite number of segments of $\mathbb{R}^2$. There exists a finite number of affine functions $\mathbf{c}_i(\cdot,\cdot),\ i \in I$ of $\mathbb{R}^2$ such that:

$$\mathbf{c}(\cdot,\cdot) = \min_{i\in I} \mathbf{c}_i(\cdot,\cdot) \tag{2.85}$$

Proof — Since $\mathbf{c}(\cdot,\cdot)$ is a piecewise affine function defined on segments of $\mathbb{R}^2$, there exist $x_{\min,i}$, $x_{\max,i}$, $t_{\min,i}$, $t_{\max,i}$, $s_{x,i}$, $s_{t,i}$, $s_{p,i}$ such that

$$\mathbf{c}(t,x) = \begin{cases} s_{p,i} + s_{x,i}x + s_{t,i}t & \text{if } \exists i \in I \text{ and } \alpha \in [0,1] \text{ such that } x = x_{\min,i} + \alpha(x_{\max,i} - x_{\min,i}) \\ & \text{and } t = t_{\min,i} + \alpha(t_{\max,i} - t_{\min,i}) \\ +\infty & \text{otherwise} \end{cases} \tag{2.86}$$

Let us define the affine functions $\mathbf{c}_i(\cdot,\cdot)$ for $i \in I$ as follows:

$$\mathbf{c}_i(t,x) = \begin{cases} s_{p,i} + s_{x,i}x + s_{t,i}t & \text{if } \exists \alpha \in [0,1] \text{ such that } x = x_{\min,i} + \alpha(x_{\max,i} - x_{\min,i}) \\ & \text{and } t = t_{\min,i} + \alpha(t_{\max,i} - t_{\min,i}) \\ +\infty & \text{otherwise} \end{cases} \tag{2.87}$$

This definition trivially implies (2.85), which completes the proof. ■

Proposition 20 implies that a set of piecewise affine initial, boundary and internal conditions can be decomposed as the minimum of a finite number of affine initial, boundary and internal conditions. In addition, the solutions associated with affine initial, boundary and internal conditions have a closed form expression by equations (2.48), (2.59), (2.71), (2.83) and (2.84). Hence, using the inf-morphism property (2.36), we can compute the solution associated with a set of piecewise affine initial, boundary and internal conditions semi-analytically. The corresponding *Lax-Hopf algorithm* is presented in the following section.

2.6.2 Lax Hopf algorithm

We now present a specific instantiation of the Lax-Hopf algorithm for a rectangular grid and for the mixed initial-boundary-internal conditions problem. Note that any grid can be used, since each point of the solution is computed using the coefficients of the initial, boundary and internal conditions only. The space and time steps are denoted by Δx and Δt respectively. The grid is defined by the set $\mathcal{G} := \{1,\dots,n_t\} \times \{1,\dots,n_x\}$, where n_t and n_x are positive integers.

LAX-HOPF ALGORITHM FOR THE MOSKOWITZ FUNCTION

INITIALIZATION
$\mathbf{M}(M,N) \longleftarrow +\infty \quad \forall (M,N) \in \mathcal{G}$ [Output matrix containing the Moskowitz function]
MAIN LOOP
For $M := 0$ **to** n_t **do** [time iteration]
  For $N := 0$ **to** n_x **do** [space iteration]
    Definition of $x_N := N\Delta x + \xi$ and $t_M := M\Delta t$ [space and time grid definition]
    For $i \in I$ **do** [iteration on the set of initial conditions]
      Compute $\mathbf{M}_{\mathcal{M}_{\mathbf{0}_i}}(t_M, x_N)$ [using equation (2.48)]
      If $\mathbf{M}_{\mathcal{M}_{0,i}}(t_M, x_N) \leq \mathbf{M}(M,N)$ **then** $\mathbf{M}(M,N) = \mathbf{M}_{\mathcal{M}_{0,i}}(t_M, x_N)$
    For $j \in J$ **do** [iteration on the set of upstream boundary conditions]
      Compute $\mathbf{M}_{\gamma_j}(t_M, x_N)$ [using equation (2.59)]
      If $\mathbf{M}_{\gamma_j}(t_M, x_N) \leq \mathbf{M}(M,N)$ **then** $\mathbf{M}(M,N) = \mathbf{M}_{\gamma_j}(t_M, x_N)$
    For $k \in K$ **do** [iteration on the set of downstream boundary conditions]
      Compute $\mathbf{M}_{\beta_k}(t_M, x_N)$ [using equation (2.71)]
      If $\mathbf{M}_{\beta_k}(t_M, x_N) \leq \mathbf{M}(M,N)$ **then** $\mathbf{M}(M,N) = \mathbf{M}_{\beta_k}(t_M, x_N)$
    For $l \in L$ **do** [iteration on the set of internal conditions]
      Compute $\mathbf{M}_{\mu_l}(t_M, x_N)$ [using equations (2.83) and (2.84)]
      If $\mathbf{M}_{\mu_l}(t_M, x_N) \leq \mathbf{M}(M,N)$ **then** $\mathbf{M}(M,N) = \mathbf{M}_{\mu_l}(t_M, x_N)$
RETURN $\mathbf{M}(M,N)$

The quantity $\mathbf{M}(M,N)$ represents the exact value of the Moskowitz function at (t_M, x_N), up to machine accuracy.

2.7 Extension to scalar conservation laws

In this section, we extend the Lax-Hopf algorithm for solving scalar conservation laws, related to scalar HJ PDEs by a variable change. Indeed, as mentioned in section 2.1, the derivatives of a function modeled by a HJ PDE satisfy a scalar conservation law themselves.

2.7.1 Spatial derivatives of the solutions to affine initial, boundary and internal conditions

The solutions $\mathbf{M}_{\mathcal{M}_{0i}}(\cdot,\cdot)$, $\gamma_j(\cdot,\cdot)$, $\beta_k(\cdot,\cdot)$ and $\mathbf{M}_{\mu_l}(\cdot,\cdot)$ are convex since they are associated with convex target functions defined on a compact subset of $\mathbb{R}_+ \times X$. Hence, these functions are differentiable almost everywhere on their domains of definition. The spatial derivatives of the above functions can be computed (whenever $\varphi^*(\cdot)$ is differentiable and using $\varphi^{*'}(\cdot)$ as the notation for the derivative of $\varphi^*(\cdot)$) explicitly as:

$$\frac{\partial \mathbf{M}_{\mathcal{M}_{0i}}(t,x)}{\partial x} = \begin{cases} a_i & \text{if } u_0(a_i) \in]\frac{\overline{\alpha}_i - x}{t}, \frac{\overline{\alpha}_{i+1} - x}{t}[\\ -\varphi^{*'}(\frac{\overline{\alpha}_i - x}{t}) & \text{if } u_0(a_i) < \frac{\overline{\alpha}_i - x}{t} \\ -\varphi^{*'}(\frac{\overline{\alpha}_{i+1} - x}{t}) & \text{if } u_0(a_i) > \frac{\overline{\alpha}_{i+1} - x}{t} \end{cases} \tag{2.88}$$

In the previous formula, $u_0(a_i)$ is an element of $-\partial_+\psi(-a_i)$.

$$\frac{\partial \mathbf{M}_{\gamma_j}(t,x)}{\partial x} = \begin{cases} -\rho_j & \text{if } T_0(\rho_j, x) \in [t - \overline{\beta}_{j+1}, t - \overline{\beta}_j] \\ -\varphi^{*'}(\frac{\xi - x}{t - \overline{\beta}_j}) & \text{if } t - \overline{\beta}_j < T_0(\rho_j, x) \\ -\varphi^{*'}(\frac{\xi - x}{t - \overline{\beta}_{j+1}}) & \text{if } T_0(\rho_j, x) < t - \overline{\beta}_{j+1} \end{cases} \tag{2.89}$$

In the previous formula, ρ_j and T_0 are computed by definition 18.

$$\frac{\partial \mathbf{M}\beta_k(t,x)}{\partial x} = \begin{cases} -\rho_k & \text{if } T_0(\rho_k, x) \in]t - \overline{\gamma}_{k+1}, t - \overline{\gamma}_k[\\ -\varphi^{*'}(\frac{\chi - x}{t - \overline{\gamma}_k}) & \text{if } t - \overline{\gamma}_k < T_0(\rho_k, x) \\ -\varphi^{*'}(\frac{\chi - x}{t - \overline{\gamma}_{k+1}}) & \text{if } T_0(\rho_k, x) < t - \overline{\gamma}_{k+1} \end{cases} \tag{2.90}$$

In the previous formula, ρ_k and T_0 are computed by definition 21.

$$\frac{\partial \mathbf{M}_{\mu_l}(t,x)}{\partial x} = \begin{cases} -\rho_1(v_l, g_l) & \text{if } x_l + v_l(t - \overline{\delta}_l) < x \\ & \text{and } T_1(t, x, v_l, g_l) \in \left]t - \overline{\delta}_{l+1}, t - \overline{\delta}_l\right[\\ -\rho_2(v_l, g_l) & \text{if } x_l + v_l(t - \overline{\delta}_l) > x \\ & \text{and } T_2(t, x, v_l, g_l) \in \left]t - \overline{\delta}_{l+1}, t - \overline{\delta}_l\right[\\ -\varphi^{*'}\left(\frac{x_l - x}{t - \overline{\delta}_l}\right) & \text{if } x_l + v_l(t - \overline{\delta}_l) < x \\ & \text{and } T_1(t, x, v_l, g_l) > t - \overline{\delta}_l \\ & \text{or if } x_l + v_l(t - \overline{\delta}_l) > x \\ & \text{and } T_2(t, x, v_l, g_l) > t - \overline{\delta}_l \\ -\varphi^{*'}\left(\frac{x_l + v_l(\overline{\delta}_{l+1} - \overline{\delta}_l) - x}{t - \overline{\delta}_{l+1}}\right) & \text{if } x_l + v_l(t - \overline{\delta}_l) < x \\ & \text{and } T_1(t, x, v_l, g_l) < t - \overline{\delta}_{l+1} \\ & \text{or if } x_l + v_l(t - \overline{\delta}_l) > x \\ & \text{and } T_2(t, x, v_l, g_l) < t - \overline{\delta}_{l+1} \end{cases} \tag{2.91}$$

In the previous formula, ρ_1, ρ_2, T_1 and T_2 are computed by definition 25.

2.7.2 Computation of the density function

In order to provide a similar algorithm for the density, we now assume that the Moskowitz function is Lipschitz-continuous on $\mathbb{R}_+ \times X$ in order to define a measurable-integrable density function by equation (2.92). Note that this assumption is only required for the computation of ρ and not for the computation of the Moskowitz function $\mathbf{M}(\cdot, \cdot)$. For instance, the solution to the HJ PDE (2.5) associated with any Lipschitz-continuous initial, left and downstream boundary condition functions (but not internal conditions) is itself Lipschitz-continuous [35, 41, 42].

Whenever the Moskowitz function is differentiable in (t, x), we compute the density function $\rho(t, x)$ by:

$$\rho(t, x) = -\frac{\partial \mathbf{M}(t, x)}{\partial x} \tag{2.92}$$

Proposition 21. [Computation of the spatial derivative of $\mathbf{M}(\cdot, \cdot)$] Let us consider $(t, x) \in \mathbb{R}_+ \times X$ such that $\mathbf{M}(\cdot, \cdot)$ is differentiable at (t, x). Since the Moskowitz function $\mathbf{M}(\cdot, \cdot)$ is the minimum of the convex functions $\mathbf{M}_{\mathcal{M}_{0,i}}(\cdot, \cdot)$, $\mathbf{M}_{\gamma_j}(\cdot, \cdot)$, $\mathbf{M}_{\beta_k}(\cdot, \cdot)$ and $\mathbf{M}_{\mu_l}(\cdot, \cdot)$ for $(i, j, k, l) \in I \times J \times K \times L$, there exists a solution $\mathbf{M}_{\mathbf{a}}(\cdot, \cdot)$ associated with a value condition $\mathbf{a}(\cdot, \cdot)$ which is equal to the Moskowitz function at (t, x), *i.e.* $\mathbf{M}(t, x) = \mathbf{M}_a(t, x)$. We assume that $\mathbf{M}_{\mathbf{a}}(\cdot, \cdot)$ is differentiable at (t, x). Given these assumptions, we have the following property:

$$\frac{\partial \mathbf{M}(t, x)}{\partial x} = \frac{\partial \mathbf{M}_{\mathbf{a}}(t, x)}{\partial x} \tag{2.93}$$

Proof — Let us define the function $g(\cdot, \cdot)$ as $g(\cdot, \cdot) := \mathbf{M}_{\mathbf{a}}(\cdot, \cdot) - \mathbf{M}(\cdot, \cdot)$. Since $\mathbf{M}(\cdot, \cdot)$ and $\mathbf{M}_{\mathbf{a}}(\cdot, \cdot)$ are both differentiable at (t, x), $g(\cdot, \cdot)$ is also differentiable at (t, x). By definition of $\mathbf{M}(\cdot, \cdot)$, the function $g(\cdot, \cdot)$ is positive and satisfies $g(t, x) = 0$. Hence, (t, x) minimizes $g(\cdot, \cdot)$ and we have $\frac{\partial g(t,x)}{\partial x} = 0$, which implies equation (2.93). ■

Since $\mathbf{M}(\cdot, \cdot)$ is the minimum of convex functions, it is differentiable almost everywhere [18]. Hence, its associated density function $\rho(\cdot, \cdot)$ is defined almost everywhere on $\mathbb{R}_+ \times X$. We use equation (2.93) to compute the density function $\rho(\cdot, \cdot)$ exactly whenever it is defined using the following algorithm, extending the Lax-Hopf algorithm.

2.7.3 Extension of the Lax-Hopf algorithm for scalar conservation laws

We consider the specific instantiation of the extension of the Lax-Hopf algorithm for a rectangular grid and for the mixed initial-boundary-internal conditions problem. Note again that any grid can be used, since each point of the solution is computed using the coefficients of the initial, boundary and internal conditions only. The space and time steps are denoted by Δx and Δt respectively. The grid is defined by the set $\mathcal{G} := \{1, \ldots, n_t\} \times \{1, \ldots, n_x\}$, where n_t and n_x are positive integers.

LAX-HOPF ALGORITHM FOR THE DENSITY FUNCTION

INITIALIZATION
$\mathbf{M}(M,N) \longleftarrow +\infty \quad \forall (M,N) \in \mathcal{G}$ [Output matrix containing the Moskowitz function]
$\mathbf{D}(M,N) \longleftarrow \text{NaN} \quad \forall (M,N) \in \mathcal{G}$ [Output matrix containing the Density function]
MAIN LOOP
For $M := 1$ **to** n_t **do** [time iteration]
  For $N := 1$ **to** n_x **do** [space iteration]
    $x_N := N\Delta x + \xi$ and $t_M := M\Delta t$ [space and time grid definition]
    For $i \in I$ **do** [iteration on the set of initial conditions]
      Computation of $\mathbf{M}_{\mathcal{M}_{0,i}}(t_M, x_N)$ [using equation (2.48)]
      If $\mathbf{M}_{\mathcal{M}_{0,i}}(t_M, x_N) \leq \mathbf{M}(M,N)$ **then**
      $\mathbf{M}(M,N) = \mathbf{M}_{\mathcal{M}_{0,i}}(t_M, x_N)$
        If $\mathbf{M}_{\mathcal{M}_{0,i}}$ is differentiable at (t_M, x_N)
        then
        $\mathbf{D}(M,N) = -\frac{\partial \mathbf{M}_{\mathcal{M}_{0,i}}(t_M, x_N)}{\partial x}$ [using equation (2.88)]
    For $j \in J$ **do** [iteration on the set of upstream boundary conditions]
      Computation of $\mathbf{M}_{\gamma_j}(t_M, x_N)$ [using equation (2.59)]
      If $\mathbf{M}_{\gamma_j}(t_M, x_N) \leq \mathbf{M}(M,N)$ **then**
      $\mathbf{M}(M,N) = \mathbf{M}_{\gamma_j}(t_M, x_N)$
        If $\mathbf{M}_{\gamma_j}$ is differentiable at (t_M, x_N) **then**
        $\mathbf{D}(M,N) = -\frac{\partial \mathbf{M}_{\gamma_j}(t_M, x_N)}{\partial x}$ [using equation (2.89)]
    For $k \in K$ **do** [iteration on the set of downstream boundary conditions]
      Computation of $\mathbf{M}_{\beta_k}(t_M, x_N)$ [using equation (2.71)]
      If $\mathbf{M}_{\beta_k}(t_M, x_N) \leq \mathbf{M}(M,N)$ **then**
      $\mathbf{M}(M,N) = \mathbf{M}_{\beta_k}(t_M, x_N)$
        If $\mathbf{M}_{\beta_k}$ is differentiable at (t_M, x_N) **then**
        $\mathbf{D}(M,N) = -\frac{\partial \mathbf{M}_{\beta_k}(t_M, x_N)}{\partial x}$ [using equation (2.90)]
    For $l \in L$ **do** [iteration on the set of internal conditions]
      Computation of $\mathbf{M}_{\mu_l}(t_M, x_N)$ [using equations (2.83) and (2.84)]
      If $\mathbf{M}_{\mu_l}(t_M, x_N) \leq \mathbf{M}(M,N)$ **then**
      $\mathbf{M}(M,N) = \mathbf{M}_{\mu_l}(t_M, x_N)$
        If $\mathbf{M}_{\mu_l}$ is differentiable at (t_M, x_N) **then**
        $\mathbf{D}(M,N) = -\frac{\partial \mathbf{M}_{\mu_l}(t_M, x_N)}{\partial x}$ [using equation (2.91)]
RETURN $\mathbf{D}(M,N)$

The quantity $\mathbf{D}(M,N)$ represents the exact value of the density function associated with the Moskowitz function at (t_M, x_N), up to machine accuracy.

2.8 Numerical examples

2.8.1 Integration of internal conditions into Hamilton-Jacobi equations

In this implementation, we consider a triangular Hamiltonian as defined in example 2, with parameters $\nu^\flat = 1$, $\gamma = 1$, $\omega = 6$, $\nu^\sharp = \frac{1}{5}$ and $\delta = \varphi^*(0) = 1$. We also consider piecewise affine initial, upstream, downstream and internal condition functions defined by equation (2.94):

$$\mathcal{M}_0(t,x) = \begin{cases} a_i x + b_i & \text{if } t = 0, \\ & \text{and } \exists i \in I \text{ such that } x \in [\overline{\alpha}_i, \overline{\alpha}_{i+1}] \\ +\infty & \text{otherwise} \end{cases}$$

$$\gamma(t,x) = \begin{cases} c_j t + d_j & \text{if } x = \xi \\ & \text{and } \exists j \in J \text{ such that } t \in [\overline{\gamma}_j, \overline{\gamma}_{j+1}] \\ +\infty & \text{otherwise} \end{cases}$$

$$\beta(t,x) = \begin{cases} e_k t + f_k & \text{if } x = \chi \\ & \text{and } \exists k \in K \text{ such that } t \in [\overline{\beta}_k, \overline{\beta}_{k+1}] \\ +\infty & \text{otherwise} \end{cases} \tag{2.94}$$

$$\mu_p(t,x) = \begin{cases} g_{pl}(t - \overline{\delta_{pl}}) + h_{pl} & \text{if } \exists l \in L_p \text{ such that} \\ & x = v_{pl}(t - \overline{\delta_{pl}}) + x_{pl} \\ & \text{and } t \in [\overline{\delta_{pl}}, \overline{\delta_{pl+1}}] \\ +\infty & \text{otherwise} \end{cases}$$

In this numerical application, we choose the following set of coefficients a_i, b_i, $\overline{\alpha}_i$, c_j, d_j, $\overline{\gamma}_j$, e_k, f_k, $\overline{\beta}_k$:

$$\begin{cases} a := (-1, -7/2, -1/10, -7/5) \\ b := (0, -\frac{25}{2}, -\frac{43}{2}, \frac{9}{2}) \\ \overline{\alpha} := (0, 5, 10, 20, 25) \end{cases} \begin{cases} c := (1, 1/2, 4/5, 7/10) \\ d := (0, \frac{3}{2}, -\frac{9}{5}, -\frac{3}{10}) \\ \overline{\gamma} := (0, 3, 11, 15, 20) \end{cases} \begin{cases} e := (0, 2/5, 0, 4/5) \\ f := (-\frac{61}{2}, -\frac{289}{10}, -\frac{221}{10}, -\frac{365}{10}) \\ \overline{\beta} := (0, 4, 17, 18, 20) \end{cases} \tag{2.95}$$

We first compute the solution to equation (2.5) associated with (2.95) numerically using the Lax-Hopf algorithm. The results are shown in Figure 2.13.

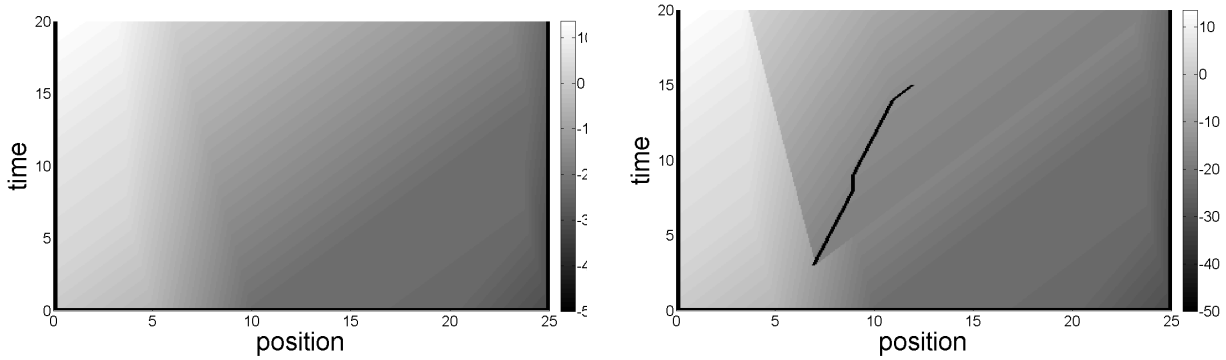

Figure 2.13: **Example of integration of an internal condition into the solution of the HJ PDE (2.5).**
Left: Computation of the solution to the mixed initial-boundary conditions problem with parameters listed in (2.95). **Right:** Computation of the solution to the mixed initial-boundary-internal conditions problem (2.95) and (2.96). The initial, boundary and internal conditions are represented by solid lines.

We then incorporate a single internal condition, defined by the following coefficients.

$$\begin{cases} v_1 := (2/5, 0, 1/2, 1/2) \\ g_1 := (1/5, 1, 1/4, 0) \\ h_1 := (-18, -19, -20, -21, -21) \\ \overline{\delta_1} := (3, 8, 9, 14, 15) \end{cases} \tag{2.96}$$

As can be seen in Figure 2.13, the incorporation of the internal condition modifies the value of the solution around it and enables us to add new information.

2.8.2 Numerical validation of the Lax-Hopf algorithm (density function)

We compare the Lax-Hopf algorithm and the Godunov scheme [91, 54, 48] (and its specific instantiation as the Daganzo cell transmission model [39, 40]), which is widely used by the transportation research community.

In this implementation, we consider a (non piecewise affine) Greenshields Hamiltonian defined as in example 1, where $\nu = 1$ and $\rho^* = 4$ (dummy values). We consider the following initial and upstream boundary condition functions:

$$\begin{cases} a := (-2, -4, -1) \\ b := (0, 20, -40) \\ \overline{\alpha} := (0, 10, 20, 30) \end{cases} \quad \begin{cases} c := (2) \\ d := (0) \\ \overline{\gamma} := (0, 20) \end{cases} \tag{2.97}$$

These initial and upstream boundary conditions were used previously in the article [91].

We compute the Moskowitz and density functions solution to the initial and upstream boundary conditions problem (2.97) using the Lax-Hopf algorithm and compare the results with the analytical formula derived in [91]. The results are illustrated in Figure 2.14.

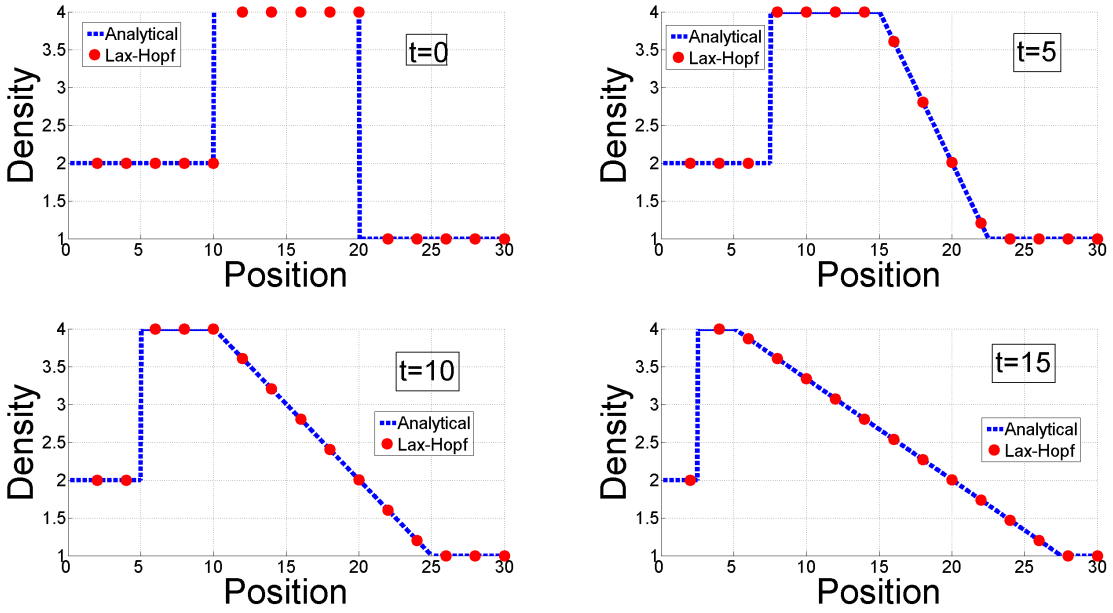

Figure 2.14: **Comparison between the Lax-Hopf algorithm and the analytical solution of problem (2.97).**
The solutions at times $t = 0$, $t = 5$, $t = 10$ and $t = 15$ are represented in the upper left, upper right, lower left and lower right subfigures respectively. In each of these subfigures, the analytical solution is represented by a dashed line and the solution yielded by the Lax-Hopf algorithm is represented using dots. The difference between the two solutions is of the order of machine error and thus not visible on these figures.

As can be seen in Figure 2.14, the numerical solution of the LWR PDE using the Lax-Hopf algorithm is identical to the analytical solution computed by the method of characteristics in [16]. In addition to its high accuracy, the Lax-Hopf algorithm is not limited by the *Courant Friedrichs Lewy* (CFL) time step size condition inherent to many finite difference schemes and can thus compute the solution at a given time faster than finite difference schemes, such as the Godunov scheme.

The Godunov scheme is only stable when the CFL condition $\nu\Delta t \leq \Delta x$ is satisfied, where Δt and Δx represent the discretized time and space steps. We consider the mixed initial-boundary-internal conditions problem (2.97) as previously and compute the solution at time $t = 15$ using the Godunov scheme and the Lax-Hopf algorithm, for different space

resolutions Δx. The computational times are shown in Figure 2.15. For fairness of the comparison, all algorithms presented here have been implemented in the same programming language (`Matlab`) and run on the same platform (`Thinkpad T61` running `Windows XP`).

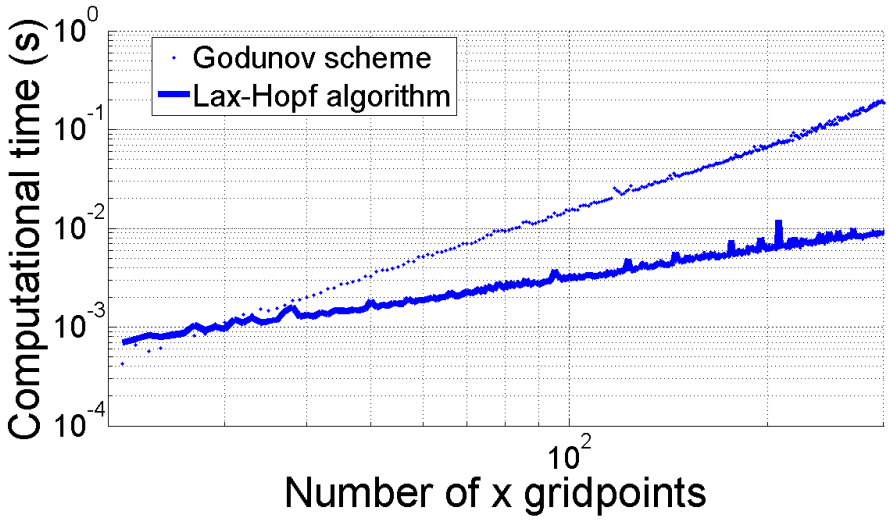

Figure 2.15: **Computational time comparison between the Lax-Hopf algorithm and the Godunov scheme (2.97).**
This figure represents the time required to compute the solution of problem (2.97) at time $t = 15$, using both the Godunov scheme (dots) and the Lax-Hopf algorithm (dashed line).

Figure 2.15 shows that the Lax-Hopf algorithm is significantly faster than the Godunov scheme when high accuracy is required. Indeed, the Lax-Hopf algorithm can compute the solution at time $t = 15$ using only the knowledge of the initial and boundary conditions. In contrast, the Godunov scheme has to compute the solution for each time step Δt, which is upper-constrained by the CFL condition and thus cannot be arbitrary large.

2.8.3 Comparison with standard numerical schemes

The striking difference in terms of computational cost between the Lax-Hopf algorithm and any finite difference scheme, such as the Lax-Friedrichs scheme, is that one does not need intermediate computations for times $M \in \{1, \dots, n_t\}$ to compute the solution at time step n_t. In other words, no iteration is needed to compute the value of the solution at any given time.

Another difference is that the computational cost of the Lax-Hopf algorithm is related to the number of piecewise affine elements in the initial, boundary and internal conditions only. In particular, the computational time required to solve a given problem depends

upon its complexity (*i.e.* the total number of piecewise affine elements in the definition of the piecewise affine initial, boundary and internal conditions). In finite difference schemes however, the computational time is independent of the complexity of the problem to solve.

Unlike finite difference schemes, the solution computed using the Lax-Hopf algorithm is (up to machine accuracy) exact. Indeed, the formulae (2.48), (2.59), (2.71), (2.83) and (2.84) are closed form and the minimization process used in the Lax-Hopf algorithm yields exact results.

Note that other computational methods such as front tracking methods [19, 38, 61] can also be used to explicitly compute solutions to conservation laws, from which the HJ PDE (2.5) is derived. However, the Lax-Hopf algorithm is different, since it can be applied to a general concave Hamiltonian, is not event-based and does not require the explicit computation of shockwaves propagation.

Chapter 3

Convex formulations of the model constraints in Hamilton-Jacobi partial differential equations

3.1 Model constraints for well-posedness

In this section, we investigate the constraints that must apply on a general set of value conditions to ensure that the solution to the HJ PDE satisfies all prescribed value conditions. One of the specificities of the HJ PDE (2.5) investigated in this dissertation is the fact that the solution itself may not reflect the value conditions that are imposed on it. Indeed, an arbitrary set of value conditions is said to apply in the *strong sense* if the solution is identical to the set of value conditions (on their respective domains of definition) and in the *weak sense* if at least one of the value conditions does not apply everywhere. In the following, we determine the conditions on the value conditions and on the Hamiltonian $\psi(\cdot)$ that ensure that *all* value conditions apply in the strong sense.

For this, we first have to define an binary relation that characterizes the order between general concave or convex functions.

Definition 26. [Hypographical and epigraphical characterizations of pointwise inequality between functions] Let $\mathcal{H}yp(\cdot)$ denote the hypograph of a function and $\mathcal{E}pi(\cdot)$ its epigraph. Let two concave functions $\psi_1(\cdot)$ and $\psi_2(\cdot)$ be given. The binary relation of inequality between these functions is defined by:

$$\psi_1(\cdot) \leq \psi_2(\cdot) \Longleftrightarrow \mathcal{H}yp(\psi_1) \subset \mathcal{H}yp(\psi_2) \Longleftrightarrow \left\{ \begin{array}{l} \mathrm{Dom}(\psi_1) \subset \mathrm{Dom}(\psi_2) \ \text{ and} \\ \forall p \in \mathrm{Dom}(\psi_1), \ \ \psi_1(p) \leq \psi_2(p) \end{array} \right. \tag{3.1}$$

Let two convex functions $\varphi_1(\cdot)$ and $\varphi_2(\cdot)$ be given. The binary relation of inequality

between these functions is defined by:

$$\varphi_1(\cdot) \leq \varphi_2(\cdot) \Longleftrightarrow \mathcal{E}pi(\varphi_1) \supset \mathcal{E}pi(\varphi_2) \Longleftrightarrow \begin{cases} \text{Dom}(\varphi_1) \supset \text{Dom}(\varphi_2) \text{ and} \\ \forall u \in \text{Dom}(\varphi_2), \ \ \varphi_1(u) \leq \varphi_2(u) \end{cases} \tag{3.2}$$

We now define the concept of *true state*, *i.e.* the actual value of the Moskowitz function, which plays a particular role in our estimation problem.

Definition 27. [True state] The true state $\overline{\mathbf{M}}(\cdot,\cdot)$ represents the state of the system, which could be obtained if measured by errorless sensors covering the entire space-time domain $[0, t_{\max}] \times X$.

Some experimental data sets such as the *NGSIM* data [102] enable us to derive the true state function $\overline{\mathbf{M}}(\cdot,\cdot)$. An example of true state function $\overline{\mathbf{M}}(\cdot,\cdot)$ derived from the NGSIM data is illustrated in Figure 3.1.

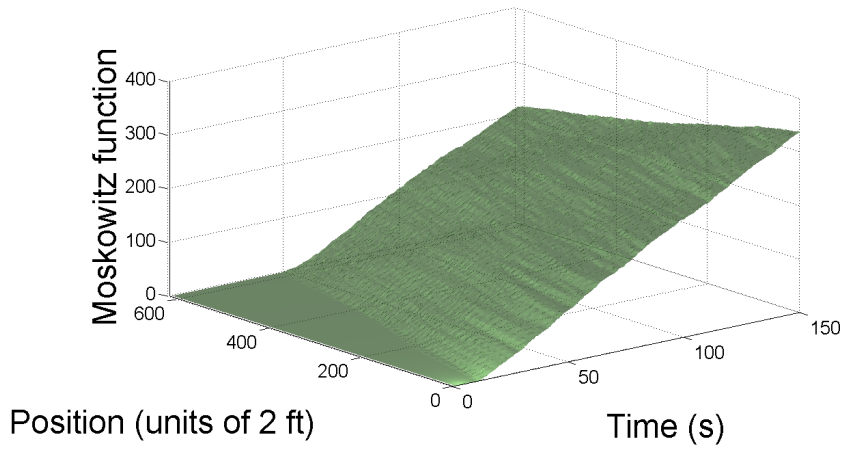

Figure 3.1: **NGSIM experimental data.**
This figure represents of the experimental Moskowitz surface obtained from the NGSIM data.

In most real time applications, $\overline{\mathbf{M}}(\cdot,\cdot)$ is not known, since measuring it requires a sensor observing the state of traffic on the whole spatial domain and for all times. In the NGSIM dataset [102] for instance, the true state $\overline{\mathbf{M}}(\cdot,\cdot)$ was observed by using a camera filming a highway section from above. This data however required post-processing and was not available in real time.

Our data assimilation framework requires the following assumption on the true state function $\overline{\mathbf{M}}(\cdot,\cdot)$.

Fact 1. [**Mathematical properties of the state**] The true state $\overline{\mathbf{M}}(\cdot,\cdot)$ is assumed to be Lipschitz-continuous [41, 42].

Note that the Lipschitz continuity of $\overline{\mathbf{M}}(\cdot,\cdot)$ implies the existence almost everywhere and boundedness of the flow $\frac{\partial\overline{\mathbf{M}}(t,x)}{\partial t}$ and the density $-\frac{\partial\overline{\mathbf{M}}(t,x)}{\partial x}$. This assumption is true for most physical systems, including highway traffic modeling [41]. Note also that no assumption is made that $\overline{\mathbf{M}}(\cdot,\cdot)$ satisfies the HJ PDE (2.5) exactly, which is in general true for most physical systems (*i.e.* their state does not satisfy a model perfectly).

The true state function enables the definition of corresponding *true value conditions*, which will be later shown to satisfy specific constraints.

Definition 28. [**True value condition**] Let $\overline{\mathbf{M}}(\cdot,\cdot)$ denote the true state of the system. A *true value condition* $\overline{\mathbf{c}}(\cdot,\cdot)$ is a function defined on a subset of $[0,t_{\max}]\times X$ and satisfying:

$$\overline{\mathbf{c}}(t,x) := \begin{cases} \overline{\mathbf{M}}(t,x) & \text{if}(t,x)\in \text{Dom}(\overline{\mathbf{c}}) \\ +\infty & \text{otherwise} \end{cases} \tag{3.3}$$

The following property holds:

Proposition 22. [**Minimum of true value conditions**] Let $\overline{\mathbf{c}}_j(\cdot,\cdot)_{j\in J}$ be a finite family of true value conditions, as in definition 28. The minimum $\overline{\mathbf{c}}(\cdot,\cdot) := \min_{j\in J}(\overline{\mathbf{c}}_j(\cdot,\cdot))$ of the true value conditions $\overline{\mathbf{c}}_j(\cdot,\cdot)$ is also a true value condition, whose domain of definition is given by:

$$\text{Dom}(\overline{\mathbf{c}}) := \bigcup_{j\in J}\text{Dom}(\overline{\mathbf{c}}_j) \tag{3.4}$$

In addition, we have the following property:

$$\forall j\in J,\ \ \forall (t,x)\in \text{Dom}(\overline{\mathbf{c}}_j),\ \ \overline{\mathbf{c}}(t,x) = \overline{\mathbf{c}}_j(t,x) \tag{3.5}$$

Proof — The proof of this proposition is straightforward and follows directly from definition 28. ■

A value condition represents some knowledge of the true state of the system, which is used in conjunction with the HJ PDE (2.5) to construct an *estimated state* of the system.

Definition 29. [**Estimated state**] Let a value condition $\mathbf{c}(\cdot,\cdot)$ be defined as in definition 2. The estimated state is defined as the solution (2.20) associated with $\overline{\mathbf{c}}(\cdot,\cdot)$ and the Hamiltonian $\psi(\cdot)$ and denoted by $\mathbf{M}_{\overline{\mathbf{c}},\psi}(\cdot,\cdot)$.

Note the $\psi(\cdot)$ index in the definition above, which as previously indicates that the value of the solution $\mathbf{M}_{\mathbf{c},\psi}(\cdot,\cdot)$ associated with the value condition $\mathbf{c}(\cdot,\cdot)$ depends (implicitly) on the Hamiltonian of the HJ PDE. As a consequence of theorem 1, the estimated state $\mathbf{M}_{\mathbf{c},\psi}(\cdot,\cdot)$ is a solution to (2.5) in the B-J/F sense. However, the estimated state does not necessarily satisfy the true value condition that we want to impose on it [31, 32].

In the following section, we find the conditions on a finite set of value conditions $(\mathbf{c}_j(\cdot,\cdot))_{j\in J}$ such that all of these value conditions apply in the strong sense when solving (2.5). In this case, we say that the value conditions are *compatible with the model*. The corresponding constraints on the value conditions are called *model compatibility constraints*. The value conditions $(\mathbf{c}_j(\cdot,\cdot))_{j\in J}$ satisfy the model compatibility constraints if and only if the following equality is true:

$$\forall j \in J,\ \forall (t,x) \in \mathrm{Dom}(\mathbf{c}_j),\ \ \mathbf{M}_{\mathbf{c}_j,\psi}(t,x) = \mathbf{c}_j(t,x) \tag{3.6}$$

The following section presents an equivalent formulation of (3.6), based on the properties of the solution (2.20), which results in algebraic conditions to be verified for (3.6) to be satisfied.

3.1.1 Compatibility conditions

Because of the inf-morphism property (2.36) and the Lax-Hopf formula (2.20), the equality (3.6) can be decomposed as a set of inequalities known as *compatibility conditions*, which we now express.

Proposition 23. [Compatibility conditions] Let us define a finite family of value condition functions $\mathbf{c}_j(\cdot,\cdot),\ \ j \in J$ as in definition 2 and their minimum $\mathbf{c}(\cdot,\cdot) := \min_{j\in J} \mathbf{c}_j(\cdot,\cdot)$. The estimated state $\mathbf{M}_{\mathbf{c},\psi}(\cdot,\cdot)$ associated with $\overline{\mathbf{c}}(\cdot,\cdot)$ satisfies the property (3.6) if and only if the following set of inequalities is satisfied:

$$\mathbf{M}_{\mathbf{c}_i,\psi}(t,x) \geq \mathbf{c}_j(t,x),\ \ \forall (t,x) \in \mathrm{Dom}(\mathbf{c}_j),\ \ \forall i \in J,\ \ \forall j \in J \tag{3.7}$$

Proof — Let us first start from (3.6). By definition of $\mathbf{c}(\cdot,\cdot)$, we have that $(t,x) \in \mathrm{Dom}(\mathbf{c})$ if and only if $(t,x) \in \mathrm{Dom}(\mathbf{c}_j)$ for some $j \in J$. Hence, using equation (3.5), we can equivalently rewrite (3.6) as:

$$\forall j \in J,\ \ \forall (t,x) \in \mathrm{Dom}(\mathbf{c}_j),\ \ \mathbf{M}_{\mathbf{c},\psi}(t,x) = \mathbf{c}_j(t,x) \tag{3.8}$$

We now prove that (3.8) implies (3.7). The inf-morphism property (2.36) implies that the estimated state $\mathbf{M}_{\mathbf{c},\psi}(\cdot,\cdot)$ associated with the value condition $\mathbf{c}(\cdot,\cdot)$ is the minimum of the estimated states $\mathbf{M}_{\mathbf{c}_i,\psi}(\cdot,\cdot)$ associated with the value conditions $\mathbf{c}_i(\cdot,\cdot)$:

$$\mathbf{M}_{\mathbf{c},\psi}(t,x) = \min_{i\in J} \mathbf{M}_{\mathbf{c}_i,\psi}(t,x) \tag{3.9}$$

Hence, the condition (3.8) implies the constraints (3.7).

Reciprocally, we prove that (3.7) implies the equality (3.8). When (3.7) is satisfied, equation (3.9) implies that $\mathbf{M}_{\mathbf{c},\psi}(t,x) \geq \mathbf{c}_j(t,x)$ for all $j \in J$ and for all $(t,x) \in \mathrm{Dom}(\mathbf{c}_j)$. The converse inequality is obtained from the Lax-Hopf formula (2.20):

$$\mathbf{M}_{\mathbf{c}_j,\psi}(t,x) = \inf_{(u,T)\in \mathrm{Dom}(\varphi^*)\times\mathbb{R}_+} (\mathbf{c}_j(t-T, x+Tu) + T\varphi^*(u)) \tag{3.10}$$

By taking $T = 0$ and $u \in \mathrm{Dom}(\varphi^*)$ in (3.10), we have that $\forall j \in J, \quad \forall (t,x) \in \mathrm{Dom}(\mathbf{c}_j), \quad \mathbf{M}_{\mathbf{c}_j,\psi}(t,x) \leq \mathbf{c}_j(t,x)$. By the inf-morphism property, this last inequality implies $\forall j \in J, \ \forall (t,x) \in \mathrm{Dom}(\mathbf{c}_j), \ \mathbf{M}_{\mathbf{c},\psi}(t,x) \leq \mathbf{c}_j(t,x)$ which completes the proof. ■

We assumed in this section that $\psi(\cdot)$ was given. In the next section, we define conditions on $\psi(\cdot)$ and the true state $\overline{\mathbf{M}}(\cdot,\cdot)$ which ensure that the compatibility conditions (3.7) associated with true value condition $\overline{\mathbf{c}}_j(\cdot,\cdot)$ are automatically satisfied, *i.e.* the equality (3.6) is satisfied. In general, the true state $\overline{\mathbf{M}}(\cdot,\cdot)$ not given, but some of its properties are known. Thus, the following results amount to finding the proper Hamiltonian $\psi(\cdot)$ such that the compatibility conditions (3.7) are satisfied.

3.1.2 Sufficient conditions on the Hamiltonian for compatibility of true value conditions

While the true state is generally unknown, the properties of its derivatives have been extensively studied in the literature [56, 72, 86]. Note that by (2.4), the derivatives of the true state function represent the true density and true flow functions. We assume that we can measure some values of the derivatives of $\overline{\mathbf{M}}(\cdot,\cdot)$ which are representative of the range of physical measurements of the system. Using these measurements, we define a particular class of Hamiltonians as follows.

Proposition 24. [Upper estimate of the Hamiltonian]. For a given true state $\overline{\mathbf{M}}(\cdot,\cdot)$, we define the set $B(\overline{\mathbf{M}})$ as follows:

$$B(\overline{\mathbf{M}}) := \left\{ \left(-\tfrac{\partial \overline{\mathbf{M}}(t,x)}{\partial x}, \tfrac{\partial \overline{\mathbf{M}}(t,x)}{\partial t} \right), \ (t,x) \in [0, t_{\max}] \times X \ \text{ such that } \ \overline{\mathbf{M}}(\cdot,\cdot) \ \text{ is differentiable} \right\}$$

There exists a concave and upper semicontinuous function $\psi_0(\cdot)$ such that:

$$B(\overline{\mathbf{M}}) \subset \mathcal{H}yp(\psi_0) \tag{3.11}$$

Proof — Recall that the true state is Lipschitz-continuous by assumption. Thus, its derivatives are defined almost everywhere and bounded, which implies the boundedness of $B(\overline{\mathbf{M}})$. Hence, we can choose for $\psi_0(\cdot)$ any concave function greater than the upper concave envelope of $B(\overline{\mathbf{M}})$. ■

Note that the choice of a function $\psi_0(\cdot)$ compatible with (3.11) is not unique. An example of choice of $\psi_0(\cdot)$ satisfying (3.11) is illustrated in Figure 3.2 later.

The conditions (3.7) are necessarily satisfied for a true value condition $\overline{\mathbf{c}}(\cdot,\cdot)$ and for a Hamiltonian $\psi_0(\cdot)$ satisfying (3.11), as shown in the following proposition.

Proposition 25. [Compatibility property for true value conditions] Let us define a finite set of true value condition functions $\overline{\mathbf{c}}_j(\cdot,\cdot),\ \ j \in J$ as in definition 28, a concave and upper semicontinuous Hamiltonian $\psi_0(\cdot)$ satisfying (3.11) and its associated convex transform φ_0^* as in (2.7). Let us also define the set of solutions $\mathbf{M}_{\overline{\mathbf{c}}_j,\psi_0}(\cdot,\cdot)$ associated with $\overline{\mathbf{c}}_j(\cdot,\cdot)$ as in (2.20). Given these assumptions, the set of inequalities (3.7) are satisfied.

Proof — In the present case, the compatibility conditions (3.7) can be written as:

$$\mathbf{M}_{\overline{\mathbf{c}}_i,\psi_0}(t,x) \geq \overline{\mathbf{c}}_j(t,x),\ \ \forall (t,x) \in \mathrm{Dom}(\overline{\mathbf{c}}_j),\ \ \forall i \in J,\ \ \forall j \in J \tag{3.12}$$

Let us fix $i \in J$, $j \in J$ and $(t,x) \in \mathrm{Dom}(\overline{\mathbf{c}}_j)$.
We first express $\mathbf{M}_{\overline{\mathbf{c}}_i,\psi_0}(t,x)$ in terms of $\overline{\mathbf{c}}_i(\cdot,\cdot)$ using the Lax-Hopf formula (2.20):

$$\mathbf{M}_{\overline{\mathbf{c}}_i,\psi_0}(t,x) = \inf_{(u,T)\in \mathrm{Dom}(\varphi_0^*)\times\mathbb{R}_+} \left(\overline{\mathbf{c}}_i(t-T,x+Tu) + T\varphi_0^*(u)\right) \tag{3.13}$$

Since $(t,x) \in \mathrm{Dom}(\overline{\mathbf{c}}_j)$, we have by definition 28 that $\overline{\mathbf{c}}_j(t,x) = \overline{\mathbf{M}}(t,x)$. Hence, we can write the inequality (3.12) which we want to prove as:

$$\inf_{(T,u)\in[0,t_{\max}]\times \mathrm{Dom}(\varphi_0^*)} \left(\overline{\mathbf{c}}_i(t-T,x+Tu) + T\varphi_0^*(u)\right) \geq \overline{\mathbf{M}}(t,x) \tag{3.14}$$

By definition 28, we have that $\overline{\mathbf{c}}_i(t-T,x+Tu) \geq \overline{\mathbf{M}}(t-T,x+Tu)$ for all $(T,u) \in [0,t_{\max}]\times \mathrm{Dom}(\varphi_0^*)$. Indeed, $\overline{\mathbf{c}}_i(t-T,x+Tu) = \overline{\mathbf{M}}(t-T,x+Tu)$ if $(t-T,x+Tu) \in \mathrm{Dom}(\overline{\mathbf{c}}_i)$ and that $\overline{\mathbf{c}}_i(t-T,x+Tu) = +\infty$ otherwise. Hence, if the equation (3.15) below is satisfied, then inequality (3.14) will be automatically true:

$$\inf_{(T,u)\in[0,t_{\max}]\times \mathrm{Dom}(\varphi_0^*)} \left(\overline{\mathbf{M}}(t-T,x+Tu) + T\varphi_0^*(u)\right) \geq \overline{\mathbf{M}}(t,x) \tag{3.15}$$

We now prove that (3.15) holds. Since $\overline{\mathbf{M}}(\cdot,\cdot)$ is Lipschitz-continuous by assumption and assuming that $\overline{\mathbf{M}}(\cdot,\cdot)$ is differentiable almost everywhere on $\{(t-\tau,x+\tau u),\ \ \tau \in [0,T]\}$, we can write:

$$\overline{\mathbf{M}}(t-T,x+Tu) + T\varphi_0^*(u) - \overline{\mathbf{M}}(t,x) = \int_0^T \left(-\tfrac{\partial \overline{\mathbf{M}}(t-\tau,x+\tau u)}{\partial t} + u\tfrac{\partial \overline{\mathbf{M}}(t-\tau,x+\tau u)}{\partial x} + \varphi_0^*(u)\right) d\tau \tag{3.16}$$

Since $\psi_0(\cdot)$ is concave and upper semicontinuous, it is equal to its Legendre-Fenchel biconjugate [8]. Hence, we have that $\psi_0(\rho) = \inf_{u\in\mathrm{Dom}(\varphi_0^*)} (-\rho u + \varphi_0^*(u))$ and thus that $\psi_0(\rho) \leq -\rho u + \varphi_0^*(u)$ for all $u \in \mathrm{Dom}(\varphi_0^*)$. This result enables us to derive the following inequality from equation (3.16):

$$\overline{\mathbf{M}}(t-T,x+Tu) + T\varphi_0^*(u) - \overline{\mathbf{M}}(t,x) \geq \int_0^T \left(-\tfrac{\partial \overline{\mathbf{M}}(t-\tau,x+\tau u)}{\partial t} + \psi_0\left(-\tfrac{\partial \overline{\mathbf{M}}(t-\tau,x+\tau u)}{\partial x}\right)\right) d\tau \tag{3.17}$$

Using (3.11), we have that $-\frac{\partial \overline{\mathbf{M}}(t-\tau,x+\tau u)}{\partial t}+\psi_0\left(-\frac{\partial \overline{\mathbf{M}}(t-\tau,x+\tau u)}{\partial x}\right)\geq 0$ for all $(\tau,u)\in[0,T]\times \mathrm{Dom}(\varphi_0^*)$. Since $T>0$, the right hand side of equation (3.17) is nonnegative, which implies the following inequality:

$$\forall (T,u)\in\mathbb{R}_+\times\mathrm{Dom}(\varphi_0^*),\quad \overline{\mathbf{M}}(t-T,x+Tu)+T\varphi_0^*(u)-\overline{\mathbf{M}}(t,x)\geq 0 \tag{3.18}$$

Equation (3.15) is obtained from equation (3.18) by taking the infimum over $(T,u)\in\mathbb{R}_+\times\mathrm{Dom}(\varphi_0^*)$, which completes the proof. Note that if $\overline{\mathbf{M}}(\cdot,\cdot)$ is not differentiable almost everywhere on the set $\{(t-\tau,x+\tau u),\ \ \tau\in[0,T]\}$, it will be differentiable on the set $\{(t-\tau,x+\delta x+\tau u),\ \ \tau\in[0,T]\}$ for a small δx, by Lipschitz-continuity. Hence, we have that $\overline{\mathbf{M}}(t-T,x+\delta x+Tu)+T\varphi_0^*(u)-\overline{\mathbf{M}}(t,x+\delta x)\geq 0$, which implies $\overline{\mathbf{M}}(t-T,x+\delta x+Tu)+T\varphi_0^*(u)-\overline{\mathbf{M}}(t,x+\delta x)\geq 0$ by (Lipschitz) continuity of $\overline{\mathbf{M}}(\cdot,\cdot)$. ■

Proposition 25 thus implies that the estimated state $\mathbf{M}_{\overline{\mathbf{c}},\psi_0}(\cdot,\cdot)$ associated with any true value condition $\overline{\mathbf{c}}(\cdot,\cdot)$ satisfies the imposed true value condition when the Hamiltonian $\psi_0(\cdot)$ satisfies (3.11).

Because of the order-preserving property of (2.7), the constraints (3.7) are satisfied for a given Hamiltonian $\psi_1(\cdot)$ only if they are also satisfied for any Hamiltonian $\psi_2(\cdot)$ greater than $\psi_1(\cdot)$, as expressed by the following proposition.

Proposition 26. [Hamiltonian inequality property] Let us define a finite set of true value conditions $\overline{\mathbf{c}}_j(\cdot,\cdot),\quad j\in J$ as in definition 28. Let us also define two concave and upper semicontinuous Hamiltonians $\psi_1(\cdot)$ and $\psi_2(\cdot)$, satisfying $\psi_1(\cdot)\leq\psi_2(\cdot)$. The associated solutions $\mathbf{M}_{\overline{\mathbf{c}}_j,\psi_1}(\cdot,\cdot)$ and $\mathbf{M}_{\overline{\mathbf{c}}_j,\psi_2}(\cdot,\cdot)$ associated with the true value condition $\overline{\mathbf{c}}_j(\cdot,\cdot)$ are defined by (2.20). We have the following property:

$$\mathbf{M}_{\overline{\mathbf{c}}_i,\psi_1}(t,x)\geq\overline{\mathbf{c}}_j(t,x),\ \ \forall(t,x)\in\mathrm{Dom}(\overline{\mathbf{c}}_j),\ \ \forall i\in J,\ \ \forall j\in J \tag{3.19}$$

implies

$$\mathbf{M}_{\overline{\mathbf{c}}_i,\psi_2}(t,x)\geq\overline{\mathbf{c}}_j(t,x),\ \ \forall(t,x)\in\mathrm{Dom}(\overline{\mathbf{c}}_j),\ \ \forall i\in J,\ \ \forall j\in J \tag{3.20}$$

Proof — The proof of this proposition is a direct consequence of the following property:

$$\mathbf{M}_{\overline{\mathbf{c}}_i,\psi_1}(t,x)\leq\mathbf{M}_{\overline{\mathbf{c}}_i,\psi_2}(t,x),\ \ \forall(t,x)\in[0,t_{\max}]\times X,\ \ \forall i\in J \tag{3.21}$$

Indeed, since $\psi_1(\cdot)\leq\psi_2(\cdot)$, we have that $pu+\psi_1(p)\leq pu+\psi_2(p)\ \ \forall(p,u)\in\mathbb{R}^2$. Hence, the convex transforms $\varphi_1^*(\cdot)$ and $\varphi_2^*(\cdot)$ respectively associated with $\psi_1(\cdot)$ and $\psi_2(\cdot)$ satisfy $\varphi_1^*(\cdot)\leq\varphi_2^*(\cdot)$.

Let us fix $(t,x,j)\in[0,t_{\max}]\times X\times J$. The solutions $\mathbf{M}_{\overline{\mathbf{c}}_i,\psi_1}(t,x)$ and $\mathbf{M}_{\overline{\mathbf{c}}_i,\psi_2}(t,x)$ can be expressed using the following Lax-Hopf formulae:

$$\begin{aligned}\mathbf{M}_{\overline{\mathbf{c}}_i,\psi_1}(t,x) &= \inf_{(u,T)\in \mathrm{Dom}(\varphi_1^*)\times\mathbb{R}_+} (\overline{\mathbf{c}}_i(t-T,x+Tu)+T\varphi_1^*(u))\\ \mathbf{M}_{\overline{\mathbf{c}}_i,\psi_2}(t,x) &= \inf_{(u,T)\in \mathrm{Dom}(\varphi_2^*)\times\mathbb{R}_+} (\overline{\mathbf{c}}_i(t-T,x+Tu)+T\varphi_2^*(u))\end{aligned} \tag{3.22}$$

Since $\varphi_1^*(\cdot) \leq \varphi_2^*(\cdot)$, we have that $\mathrm{Dom}(\varphi_2^*) \subset \mathrm{Dom}(\varphi_1^*)$. Hence, equation (3.22) implies (3.21) and thus, (3.19) implies (3.20). ■

In consequence, the smallest concave function satisfying (3.11), illustrated in Figure 3.2 plays a particular role in our problem.

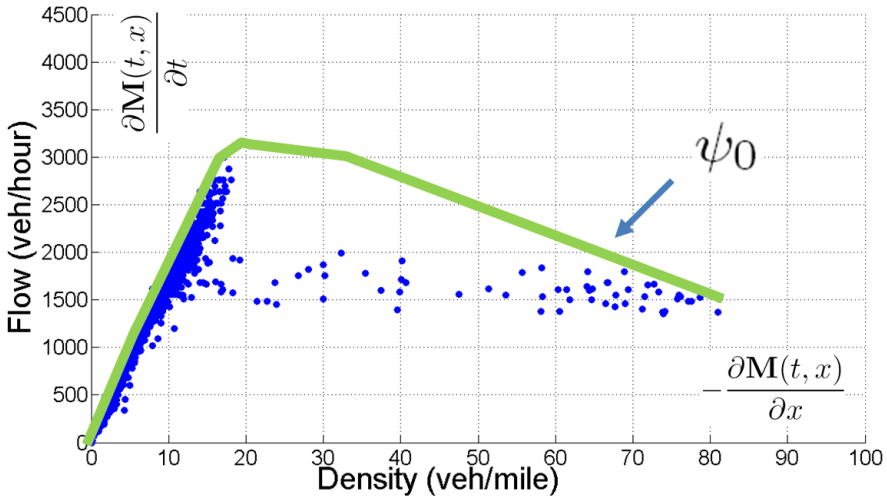

Figure 3.2: **Illustration of an upper estimate function $\psi_0(\cdot)$.**
In this figure, the horizontal axis represents the density and the vertical axis the flow. The scatter plot represents the values of flow and density obtained from experimental traffic flow data [103]. Each point in this plot is a given $\left(-\frac{\partial \overline{\mathbf{M}}(t,x)}{\partial x}, \frac{\partial \overline{\mathbf{M}}(t,x)}{\partial t}\right)$ for some $(t,x) \in [0, t_{\max}]\times X$. A typical example of upper estimate function $\psi_0(\cdot)$ is the upper concave envelope of the points, represented by a dashed line and which satisfies (3.11).

Proposition 27. [Smallest concave upper estimate] Let $\overline{\mathbf{M}}$ be given and let $B(\overline{\mathbf{M}})$ be defined as in proposition 24. Let $\mathcal{C}$ be the set of upper semicontinuous concave functions from $\mathbb{R}$ to $\mathbb{R}$ and let us define the set of functions $\mathcal{A}$ by:

$$\mathcal{A} := \left\{\psi \in \mathcal{C} \text{ such that } B(\overline{\mathbf{M}}) \subset \mathcal{H}yp(\psi)\right\} \tag{3.23}$$

Let us define the function $\psi_{\inf}(\cdot)$ as:

$$\mathcal{H}yp(\psi_{\inf}) := \bigcap_{\psi\in\mathcal{A}} \mathcal{H}yp(\psi) \tag{3.24}$$

The function $\psi_{\inf}(\cdot)$ defined by (3.24) is the smallest element of $\mathcal{A}$.

Proof — The set $\mathcal{A}$ is not empty by proposition 24 and thus the function $\psi_{\inf}(\cdot)$ defined by (3.24) exists. We now prove that $\psi_{\inf}(\cdot)$ is the smallest element of $\mathcal{A}$. Let $\psi(\cdot) \in \mathcal{A}$. Since $\psi(\cdot)$ is concave, upper semicontinuous and satisfies (3.11), its hypograph is closed, convex and contains the set $B(\overline{\mathbf{M}})$. By (3.24), the hypograph of $\psi_{\inf}(\cdot)$ is thus closed, convex and contains $B(\overline{\mathbf{M}})$ since it is the (infinite) intersection of closed and convex sets containing $B(\overline{\mathbf{M}})$. Hence, $\psi_{\inf}$ is concave, upper semicontinuous and satisfies (3.11), which implies $\psi_{\inf} \in \mathcal{A}$. The function $\psi_{\inf}(\cdot)$ is also the smallest element of $\mathcal{A}$, since any element $\psi(\cdot)$ of $\mathcal{A}$ satisfies $\mathcal{H}yp(\psi_{\inf}(\cdot)) \subset \mathcal{H}yp(\psi(\cdot))$ by (3.24). ■

Proposition 28. [Minimal conditions] Let $\mathcal{A}$ be defined as in proposition 27 and let $\psi_{\inf}(\cdot)$ be defined as in as in (3.24). Let $\psi(\cdot) \in \mathcal{A}$ and let us define a finite set of true value conditions $\overline{\mathbf{c}}_j(\cdot,\cdot)$, $j \in J$ and their associated solutions $\mathbf{M}_{\overline{\mathbf{c}}_j,\psi_{\inf}}(\cdot,\cdot)$ and $\mathbf{M}_{\overline{\mathbf{c}}_j,\psi}(\cdot,\cdot)$ as in (2.20). Given the above definitions, we have the following property:

$$\mathbf{M}_{\overline{\mathbf{c}}_i,\psi}(t,x) \geq \overline{\mathbf{c}}_j(t,x), \quad \forall (t,x) \in \mathrm{Dom}(\overline{\mathbf{c}}_j), \quad \forall i \in J, \quad \forall j \in J, \quad \forall \psi(\cdot) \in \mathcal{A} \tag{3.25}$$

if and only if

$$\mathbf{M}_{\overline{\mathbf{c}}_i,\psi_{\inf}}(t,x) \geq \overline{\mathbf{c}}_j(t,x), \quad \forall (t,x) \in \mathrm{Dom}(\overline{\mathbf{c}}_j), \quad \forall i \in J, \quad \forall j \in J \tag{3.26}$$

Proof — The conditions (3.25) imply (3.26), since $\psi_{\inf}(\cdot) \in \mathcal{A}$ by proposition 27. Conversely, the conditions (3.26) imply (3.25), by proposition 26, remarking that $\mathcal{H}yp(\psi_{\inf}) \subset \mathcal{H}yp(\psi)$. ■

Proposition 28 enables the verification of the conditions (3.25) for a true value condition $\overline{\mathbf{c}}(\cdot,\cdot)$ and for all Hamiltonians $\psi(\cdot)$ satisfying (3.11) using the conditions (3.26) only.

We now present some important properties of the model compatibility constraints.

3.2 Properties of the model compatibility constraints

3.2.1 Concavity property of the solutions with respect to their coefficients

Because of the Lax-Hopf formula (2.20), the solutions associated with affine initial, boundary and internal conditions have a concavity property with respect to some of their coefficients, which we now present.

Proposition 29. [Concavity property of the solution associated with an affine initial condition] The solution $\mathbf{M}_{\mathcal{M}_{0,i}}(\cdot,\cdot)$ associated with the affine initial condition (2.39) is a concave function of the coefficients a_i and b_i.

Proof — The Lax-Hopf formula (2.20) associated with the solution $\mathbf{M}_{\mathcal{M}_{0,i}}(\cdot,\cdot)$ can be written as:

$$\mathbf{M}_{\mathcal{M}_{0,i}}(t,x) \;=\; \inf_{u\in \mathrm{Dom}(\varphi^*) \text{ s. t. } (x+tu)\in[\overline{\alpha}_i,\overline{\beta}_i]} (a_i(x+tu)+b_i+t\varphi^*(u)) \tag{3.27}$$

Let us fix $(t,x,u)\in[0,t_{\max}]\times X\times \mathrm{Dom}(\varphi^*)$. The function $f(\cdot,\cdot)$ defined as $f(a_i,b_i) = a_i(x+tu)+b_i+t\varphi^*(u)$ is concave (indeed, affine). Hence, the solution $\mathbf{M}_{\mathcal{M}_{0,i}}(t,x)$ is a concave function of (a_i,b_i), since it is the infimum of concave functions of (a_i,b_i) [18, 87]. ■

Proposition 30. [Concavity property of the solution associated with an affine upstream boundary condition] The solution $\mathbf{M}_{\gamma_j}(\cdot,\cdot)$ associated with the affine upstream boundary condition (2.49) is a concave function of the coefficients c_j and d_j.

Proof — The Lax-Hopf formula (2.20) associated with the solution $\mathbf{M}_{\gamma_j}(\cdot,\cdot)$ can be written as:

$$\mathbf{M}_{\gamma_j}(t,x) \;=\; \inf_{T\in\left[-\frac{\xi-x}{\nu^\flat},+\infty\right[\cap\left[t-\overline{\gamma}_{j+1},t-\overline{\gamma}_j\right]} \left(c_j(t-T)+d_j+T\varphi^*\left(\frac{\xi-x}{T}\right)\right) \tag{3.28}$$

Let us fix $(t,x,T)\in[0,t_{\max}]\times X\times\left[-\frac{\xi-x}{\nu^\flat},+\infty\right[\cap\left[t-\overline{\gamma}_{j+1},t-\overline{\gamma}_j\right]$. The function $g(\cdot,\cdot)$ defined as $f(c_j,d_j) = c_j(t-T)+d_j+T\varphi^*\left(\frac{\xi-x}{T}\right)$ is concave (indeed, affine). Hence, the solution $\mathbf{M}_{\gamma_j}(t,x)$ is a concave function of (c_j,d_j), since it is the infimum of concave functions of (c_j,d_j) [18, 87]. ■

Proposition 31. [Concavity property of the solution associated with an affine downstream boundary condition] The solution $\mathbf{M}_{\beta_k}(\cdot,\cdot)$ associated with the affine downstream boundary condition (2.61) is a concave function of the coefficients e_k and f_k.

Proof — The Lax-Hopf formula (2.20) associated with the solution $\mathbf{M}_{\beta_k}(\cdot,\cdot)$ can be written as:

$$\mathbf{M}_{\beta_k}(t,x) \;=\; \inf_{T\in\left[\frac{\chi-x}{\nu^\sharp},+\infty\right[\cap\left[t-\overline{\beta}_{k+1},t-\overline{\beta}_k\right]} \left(e_k(t-T)+f_k+T\varphi^*\left(\frac{\chi-x}{T}\right)\right) \tag{3.29}$$

Let us fix $(t,x,T)\in[0,t_{\max}]\times X\times\left[\frac{\chi-x}{\nu^\sharp},+\infty\right[\cap\left[t-\overline{\beta}_{k+1},t-\overline{\beta}_k\right]$. The function $h(\cdot,\cdot)$ defined as $f(e_k,f_k) = e_k(t-T)+f_k+T\varphi^*\left(\frac{\chi-x}{T}\right)$ is concave (indeed, affine). Hence, the solution $\mathbf{M}_{\beta_k}(t,x)$ is a concave function of (e_k,f_k), since it is the infimum of concave functions of (e_k,f_k) [18, 87]. ■

Proposition 32. [Concavity property of the solution associated with an affine internal condition] The solution $\mathbf{M}_{\mu_l}(\cdot,\cdot)$ associated with the internal condition (2.73) is a concave function of the coefficients g_l and h_l.

Proof — The Lax-Hopf formula (2.20) associated with the solution $\mathbf{M}_{\mu_l}(\cdot,\cdot)$ can be written [31, 32] as:

$$\mathbf{M}_{\mu_l}(t,x) = \inf_{T\in\mathbb{R}_+\cap[t-\overline{\delta}_l,t-\overline{\gamma}_l]} g_l(t-T-\overline{\gamma}_l) + h_l + T\varphi^*\left(\frac{x_l+v_l(t-\overline{\gamma}_l-T)-x}{T}\right) \tag{3.30}$$

Let us fix $(t,x,T)\in[0,t_{\max}]\times X\times\mathbb{R}_+$. The function $d(\cdot,\cdot)$ defined as $d(g_l,h_l) := g_l(t-T-\overline{\gamma}_l)+h_l+T\varphi^*\left(\frac{x_l+v_l(t-\overline{\gamma}_l-T)-x}{T}\right)$ is concave (indeed, affine). Hence, the solution $\mathbf{M}_{\mu_l}(t,x)$ is a concave function of (g_l,h_l), since it is the infimum of concave functions [18, 87]. ■

3.2.2 Convex formulation of the model compatibility constraints

For the initial, boundary and internal conditions defined by (2.39), (2.49), (2.61) and (2.73), the model compatibility constraints (3.7) define constraints on the coefficients a_i, b_i, c_j, d_j, e_k, f_k, g_l, h_l. We now prove that these constraints are convex.

Proposition 33. [Convexity property of the model constraints] Let initial, boundary and internal conditions be defined as in (2.39), (2.49), (2.61) and (2.73), for $i\in I$, $j\in J$, $k\in K$ and $l\in L$ where I, J, K and L are finite sets. The model compatibility constraints (3.7) are convex inequalities in the coefficients a_i, b_i, c_j, d_j, e_k, f_k, g_l and h_l.

Proof — The constraints (3.7) are of the form:

$$\mathbf{M}_{\mathbf{c}_n}(t,x)\geq\mathbf{c}_m(t,x),\ \ \forall(t,x)\in\mathrm{Dom}(\mathbf{c}_m),\ \ \forall n\in N,\ \ \forall m\in N \tag{3.31}$$

Let $(n,m)\in N^2$ and $(t,x)\in\mathrm{Dom}(\mathbf{c}_m)$. The quantity $\mathbf{c}_m(t,x)$ is an affine function of the coefficients a_i, b_i, c_j, d_j, e_k, f_k, g_l and h_l. In addition, $\mathbf{M}_{\mathbf{c}_n}(t,x)$ is a concave function of a_i, b_i, c_j, d_j, e_k, f_k, g_l and h_l. The constraint $\mathbf{M}_{\mathbf{c}_n}(t,x)\geq\mathbf{c}_m(t,x)$ can be written as $-\mathbf{M}_{\mathbf{c}_n}(t,x)+\mathbf{c}_m(t,x)\leq 0$ where $-\mathbf{M}_{\mathbf{c}_n}(t,x)+\mathbf{c}_m(t,x)$ is a convex function (as the sum of convex functions) of a_i, b_i, c_j, d_j, e_k, f_k, g_l and h_l. Hence, $\mathbf{M}_{\mathbf{c}_n}(t,x)\geq\mathbf{c}_m(t,x)$ is a convex constraint [18] in a_i, b_i, c_j, d_j, e_k, f_k, g_l and h_l. ■

Proposition 33 states that the inequality constraints (3.7) define a convex set in the space $(a_i,b_i,c_j,d_j,e_k,f_k,g_l,h_l)$. Using this property, we pose inverse modeling problems as convex optimization programs in chapter 4.

3.2.3 Monotonicity property of the model compatibility conditions

An important property of the model compatibility constraints (3.7) is their monotonicity with respect to new data, outlined in the following proposition.

Proposition 34. [**Monotonicity property**] Let a set of affine initial, boundary and internal conditions be defined as in (2.39), (2.49), (2.61) and (2.73) for $i \in I$, $j \in J$, $k \in K$ and $l \in L$ where I, J, K and L are finite sets. The convex set defined by the inequality constraints (3.31) is decreasing (in the sense of inclusion) as new initial, boundary or internal conditions are added.

Proof — The model compatibility constraints can be written as:

$$\mathbf{M}_{\mathbf{c}_n}(t,x) \geq \mathbf{c}_m(t,x), \ \ \forall (t,x) \in \mathrm{Dom}(\mathbf{c}_m), \ \ \forall n \in N, \ \ \forall m \in N \tag{3.32}$$

Let $\mathcal{N} \subset \mathbb{R}^{|N|}$ be the convex set defined by (3.32). We now add a finite number of new value conditions $\mathbf{c}_p$, defined for $p \in P$. The model compatibility constraints become:

$$\mathbf{M}_{\mathbf{c}_n}(t,x) \geq \mathbf{c}_m(t,x), \ \ \forall (t,x) \in \mathrm{Dom}(\mathbf{c}_m), \ \ \forall n \in N \cup P, \ \ \forall m \in N \cup P \tag{3.33}$$

Let $\mathcal{M} \subset \mathbb{R}^{|N|+|P|}$ be the convex set defined by (3.33). Since the constraints (3.33) imply (3.32), we the projection of $\mathcal{M}$ on $\mathbb{R}^{|N|}$ is a subset of $\mathcal{N}$, which completes the proof. ■

The above property is very important in practice, since it ensures that the feasible sets decreases in size when new data is added. Hence, the results of the estimation problems derived in the next chapter necessarily improve when new data is added, which is not the case for Monte-Carlo based estimation methods.

Chapter 4

Applications

In chapter 3, we established the convexity of the model compatibility constraints. We now use this result to solve different estimation problems arising in traffic-flow engineering. For this, we first derive the relationship between value condition coefficients and measurement data. We then instantiate the convex model compatibility constraints as linear inequalities for triangular Hamiltonians defined by example 2. Similarly, we show that the measurement data yields data compatibility constraints, which can also be formulated as linear inequalities.

4.1 Traffic flow measurement data and value conditions

In the context of traffic flow monitoring, measurement data traditionally originates from *Eulerian* (*i.e.* fixed) sensors. This is in contrast with new *Lagrangian* (*i.e.* mobile) sensors, which sense traffic conditions while moving alongside it.

4.1.1 Fixed detector data

Fixed sensors are currently the backbone of traffic monitoring. They measure various quantities related to traffic flow at a fixed location and for all times. Current fixed-sensor technology includes:

- Inductive loop detectors, such as the *Performance Measurement System* PeMS [103] in California and magnetometers [24] are based on measurements of the inductance of an electromagnetic loop. They can measure two quantities: the flow of vehicles above the sensor and the occupancy which can be related to the density of vehicles above the sensor. Dual loop detector arrangements [103], as well as some classes of magnetometers [24] can also directly measure traffic speed.
- Speed radars, which are measuring the doppler shift as well as the time of flight of electromagnetic waves. They can measure three quantities: the flow and density of vehicles around the sensor, as well as the average traffic speed.

- Speed cameras, which are paired with image recognition systems. They usually measure flow, density and average traffic speed.

One of the biggest problems associated with the fixed sensing infrastructure is their deployment and maintenance costs. Since this sensing infrastructure is dedicated (*i.e.* the infrastructure cannot be used to sense other physical phenomena besides traffic flow), these high costs are limiting the deployment of new sensors. In practice, the Departments of Transportation (DOTs) are operating these sensors, and usually have to spend their funding on more urgent issues.

4.1.2 Mobile sensor data

The emergence of new portable computational platforms with communication and sensing capabilities, provides the engineering community with unprecedented opportunities for sensing. In the context of traffic flow, cellular phones [97, 57] located onboard vehicles and equipped with positioning systems such as the GPS can act as traffic sensors. Other possible mobile sensing systems exist, including *toll tag readers* such as the FasTrak system in California.

All mobile sensing systems pose an additional mathematical and computational challenge with respect to fixed sensors. Since most of the current traffic sensing systems are fixed, most of the estimation techniques for traffic-flow engineering are not specifically designed to incorporate mobile measurements.

In order to estimate the state of traffic based on Eulerian and Lagrangian sensor measurements, we first need to establish the relation between the measurement data and the value conditions which incorporate the measurement constraints into the HJ PDE (2.5). This will be explained later in the thesis

4.1.3 Experimental setup

In the following sections, we pose different problems arising in transportation engineering as *Linear Programs* (LPs) or series of LPs and test their performance using experimental data from the Mobile Century [57] experiment.

In all numerical applications, we consider a 3.858 km long spatial domain, located between the PeMS [103] stations 400536 and 400284 on Highway $I-880$ N in Hayward, California. The measurement data comes from two sources. The flow data $q_{\text{in}}^{\text{meas}}(\cdot)$ and $q_{\text{out}}^{\text{meas}}(\cdot)$ is generated by the PeMS stations 400536 and 400284 respectively. The probe location and timing data comes from GPS measurements generated by Nokia $N95$ cellphones located onboard probe vehicles. The layout is illustrated in Figure 4.1.

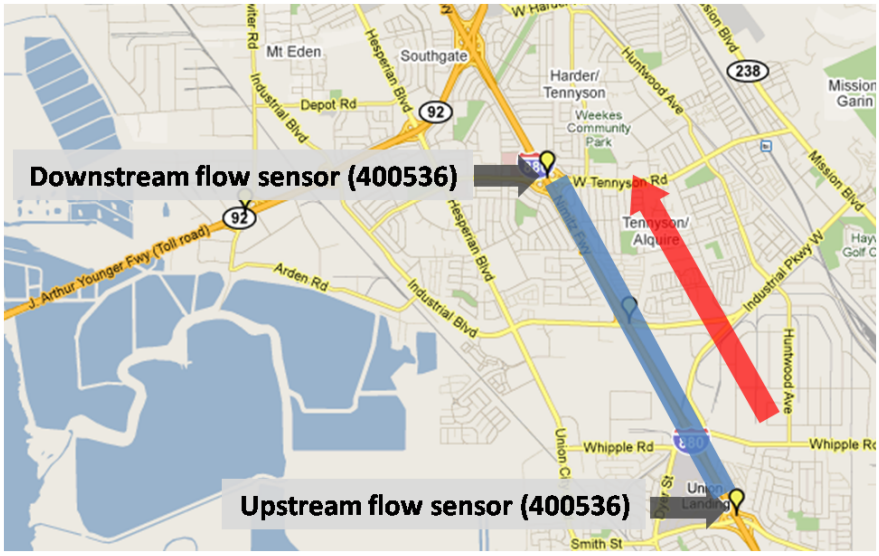

Figure 4.1: **Experiment site layout.**
The upstream and downstream PeMS stations are delimiting a 3.858 km spatial domain, outlined by a solid line. The direction of traffic flow is represented by an arrow.

The complete experimental setting is described in [57]. The data set used in all numerical applications of this dissertation can be freely downloaded from [101].

All LPs have been implemented in `Matlab`, using the package `CVX` [55]. The problems solved in this dissertation are relatively tractable: they typically involve thousands of variables and constraints and can be solved numerically in a few seconds on a typical laptop computer.

4.1.4 Link between measurement data and value conditions

In our specific application, the sensor data does not provide the initial condition of the problem, since this would require us instrumenting the entire spatial domain. Fixed traffic sensors traditionally measure the inflow and outflow of vehicles on the spatial domain, which are related to the upstream and downstream boundary conditions. In addition to fixed sensors, mobile sensors onboard vehicles track the vehicle trajectory and thus generate *internal conditions* [31]. The formal link between traffic measurement data and value condition (boundary and internal conditions) blocks is shown in the following definition.

Definition 30. [Affine upstream, downstream and internal conditions] Let us define $\mathbb{N} = \{0, \ldots, n_{\max}\}$ and $\mathbb{M} = \{0, \ldots, m_{\max}\}$. For all $n \in \mathbb{N}$ and $m \in \mathbb{M}$, we define the following

upstream, downstream and internal conditions:

$$\gamma_n(t,x) = \begin{cases} \sum_{i=0}^{n-1} q_{\text{in}}(i)T + q_{\text{in}}(n)(t-nT) & \text{if } x = \xi \\ & \text{and } t \in [nT,(n+1)T] \\ +\infty & \text{otherwise} \end{cases} \tag{4.1}$$

$$\beta_n(t,x) = \begin{cases} \sum_{i=0}^{n-1} q_{\text{out}}(i)T + q_{\text{out}}(n)(t-nT) - \Delta & \text{if } x = \chi \text{ and } t \in [nT,(n+1)T] \\ +\infty & \text{otherwise} \end{cases} \tag{4.2}$$

$$\mu_m(t,x) = \begin{cases} L_m + r_m(t - t_{\min}(m)) & \text{if } x = x_{\min}(m) + v^{\text{meas}}(m)(t - t_{\min}(m)) \\ & \text{and } t \in [t_{\min}(m), t_{\max}(m)] \\ +\infty & \text{otherwise} \end{cases} \tag{4.3}$$

where $v^{\text{meas}}(m) = \frac{x_{\max}(m) - x_{\min}(m)}{t_{\max}(m) - t_{\min}(m)}$.

The domains of definitions of these functions are illustrated in Figure 4.2.

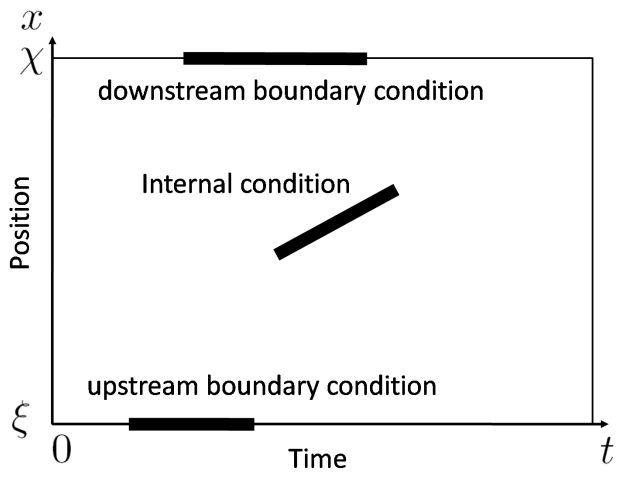

Figure 4.2: **Illustration of the domains of the possible value conditions used to construct the solution of the Moskowitz HJ PDE.**
The time is represented by the horizontal axis, while the location is represented by the vertical axis. The coefficients ξ and χ represent respectively the upstream and downstream boundaries of the highway segment of interest.

The coefficients in equations (4.1), (4.2) and (4.3) can be physically interpreted as follows:

$$\begin{cases} q_{\text{in}}(n) & \text{average inflow between times nT and (n+1)T} \\ q_{\text{out}}(n) & \text{average outflow between times nT and (n+1)T} \\ \Delta & \text{initial number of vehicles on the highway section} \end{cases}$$

$$\begin{cases} t_{\min}(m) & \text{initial time at which the internal condition } m \text{ applies} \\ t_{\max}(m) & \text{final time at which the internal condition } m \text{ applies} \\ x_{\min}(m) & \text{initial location at which the internal condition } m \text{ applies} \\ x_{\max}(m) & \text{final location at which the internal condition } m \text{ applies} \\ v^{\text{meas}}(m) & \text{speed of the internal condition } m \\ L_m & \text{label of the vehicle } m \text{ at time } t_{\min}(m) \\ r_m & \text{rate of change of the label of vehicle } m \end{cases} \tag{4.4}$$

Since the Moskowitz function is increasing in time and decreasing in space, the coefficients of (4.1), (4.2) and (4.3) satisfy the following conditions:

$$\begin{cases} \Delta \geq 0 \quad \text{positivity of the initial number of vehicles} \\ \forall n \in \mathbb{N}, \;\; q_{\text{in}}(n) \geq 0 \quad \text{positivity of the inflow} \\ \forall n \in \mathbb{N}, \;\; q_{\text{out}}(n) \geq 0 \quad \text{positivity of the outflow} \\ \forall m \in \mathbb{M}, \;\; r_m \geq 0 \quad \text{positivity of the passing rate} \end{cases} \tag{4.5}$$

The monotonicity properties of the Moskowitz function with respect to its variables follow directly from the positivity of flow and density functions (2.4) and are derived in [80].

Some of the above coefficients can be obtained (with some error) through traffic measurement data. Inductive loop detectors [103] and speed radars located in ξ and χ can measure the inflow $q_{\text{in}}(n)$ and outflow $q_{\text{out}}(n)$ for all time intervals $[nT, (n+1)T]$. The coefficients $t_{\min}(m)$, $t_{\max}(m)$, $x_{\min}(m)$ and $x_{\max}(m)$ can be obtained using vehicle positioning systems, such as GPS-enabled cellphones onboard vehicles [101]. In contrast, the coefficients L_m and r_m cannot be measured using conventional traffic sensors. Similarly, the initial number of vehicles Δ cannot be measured using conventional sensors. Hence, the available measurements do not enable us to define the upstream (4.1), downstream (4.2) and internal conditions (4.3) univocally. In order to estimate the state $\mathbf{M}(\cdot, \cdot)$ of the system, one has to estimate the coefficients (4.4), which are constrained both by the model and the measurement data.

In the applications of this dissertation, the coefficients $x_{\min}(m)$, $x_{\max}(m)$, $t_{\min}(m)$ and $t_{\max}(m)$ are measured by are measured by GPS systems, which are very accurate. Hence, we assume that these coefficients are fixed. Given this assumption, we define the decision variable of our estimation problems as follows.

Definition 31. The coefficients of the upstream, downstream and internal conditions to be estimated are defined by the following decision variable:

$$y := (q_{\text{in}}(1), \ldots, q_{\text{in}}(n_{\max}), q_{\text{out}}(1), \ldots, q_{\text{out}}(n_{\max}), L_1, \ldots, L_{m_{\max}}, r_1, \ldots, r_{m_{\max}}) \tag{4.6}$$

4.2 Explicit instantiation of the model compatibility conditions for triangular Hamiltonians

We now instantiate (3.31) explicitly so it can be applied to traffic flow engineering problems. Following common assumptions in transportation engineering [41, 42], we assume that the Hamiltonian $\psi(\cdot)$ is a continuous triangular function defined by:

$$\psi(\rho) = \begin{cases} v\rho & \text{if } \rho \leq k_c \\ w(\rho - k_m) & \text{otherwise} \end{cases} \tag{4.7}$$

where v, w, k_c and k_m are model parameters satisfying $vk_c = w(k_c - k_m)$ and representing the *free flow speed* (v), the *critical density* (k_c), the *congestion speed* (w) and the *maximal density* (k_m).

Explicit expression of the solutions to the affine value conditions

In this section, we compute the solutions associated with the value conditions (4.1), (4.2) and (4.3) explicitly using the specific Hamiltonian (4.7). The results below are the instantiation of equations (2.59), (2.71), (2.83) and (2.84) for (4.7).

$$\mathbf{M}_{\gamma_n}(t,x) = \begin{cases} +\infty & \text{if } t \leq nT + \frac{x-\xi}{v} \\ \sum_{i=0}^{n-1} q_{\text{in}}(i)T + q_{\text{in}}(n)(t - \frac{x-\xi}{v} - nT) & \text{if } nT + \frac{x-\xi}{v} \leq t \\ & \text{and } t \leq (n+1)T + \frac{x-\xi}{v} \\ \sum_{i=0}^{n} q_{\text{in}}(i)T + k_c v(t - (n+1)T - \frac{x-\xi}{v}) & \text{otherwise} \end{cases}$$

$$\mathbf{M}_{\beta_n}(t,x) = \begin{cases} +\infty & \text{if } t \leq nT + \frac{x-\chi}{w} \\ -\Delta + \sum_{i=0}^{n-1} q_{\text{out}}(i)T + q_{\text{out}}(n)(t - \frac{x-\chi}{w} - nT) & \text{if } nT + \frac{x-\chi}{w} \leq t \\ & \text{and } t \leq (n+1)T + \frac{x-\chi}{w} \\ -\Delta + \sum_{i=0}^{n} q_{\text{out}}(i)T + k_c v(t - (n+1)T - \frac{x-\chi}{w}) & \text{otherwise} \end{cases} \tag{4.8}$$

$$\mathbf{M}_{\mu_m}(t,x) = \begin{cases} L_m + r_m\left(t - \frac{x - x_{\min}(m) - v^{\text{meas}}(m)(t - t_{\min}(m))}{v - v^{\text{meas}}(m)} - t_{\min}(m)\right) \\ \text{if } x \geq x_{\min}(m) + v^{\text{meas}}(m)(t - t_{\min}(m)) \\ \text{and } x \geq x_{\max}(m) + v(t - t_{\max}(m)) \\ \text{and } x \leq x_{\min}(m) + v(t - t_{\min}(m)) \\ L_m + r_m\left(t - \frac{x - x_{\min}(m) - v^{\text{meas}}(m)(t - t_{\min}(m))}{w - v^{\text{meas}}(m)} - t_{\min}(m)\right) \\ + k_c(v - w)\frac{x - x_{\min}(m) - v^{\text{meas}}(m)(t - t_{\min}(m))}{w - v^{\text{meas}}(m)} \\ \text{if } x \leq x_{\min}(m) + v^{\text{meas}}(m)(t - t_{\min}(m)) \\ \text{and } x \leq x_{\max}(m) + w(t - t_{\max}(m)) \\ \text{and } x \geq x_{\min}(m) + w(t - t_{\min}(m)) \\ L_m + r_m\left(t_{\max}(m) - t_{\min}(m)\right) + (t - t_{\max}(m))\, k_c\left(v - \frac{x - x_{\max}(m)}{t - t_{\max}(m)}\right) \\ \text{if } x \leq x_{\max}(m) + v(t - t_{\max}(m)) \\ \text{and } x \geq x_{\max}(m) + w(t - t_{\max}(m)) \\ +\infty \text{ otherwise} \end{cases} \tag{4.9}$$

Explicit instantiation of the model constraints

For the specific boundary and internal conditions (4.1), (4.2) and (4.3), the model compatibility constraints (3.31) are:

$$\begin{cases} \mathbf{M}_{\gamma_n}(t,\xi) \geq \gamma_p(t,\xi) & \forall t \in [pT,(p+1)T], \forall (n,p) \in \mathbb{N}^2 \quad (i) \\ \mathbf{M}_{\gamma_n}(t,\chi) \geq \beta_p(t,\chi) & \forall t \in [pT,(p+1)T], \forall (n,p) \in \mathbb{N}^2 \quad (ii) \\ \mathbf{M}_{\gamma_n}(t,x) \geq \mu_m(t,x) & \forall (t,x) \in \mathrm{Dom}(\mu_m), \forall n \in \mathbb{N}, \forall m \in \mathbb{M} \quad (iii) \\ \mathbf{M}_{\beta_n}(t,\xi) \geq \gamma_p(t,\xi) & \forall t \in [pT,(p+1)T], \forall (n,p) \in \mathbb{N}^2 \quad (iv) \\ \mathbf{M}_{\beta_n}(t,\chi) \geq \beta_p(t,\chi) & \forall t \in [pT,(p+1)T], \forall (n,p) \in \mathbb{N}^2 \quad (v) \\ \mathbf{M}_{\beta_n}(t,x) \geq \mu_m(t,x) & \forall (t,x) \in \mathrm{Dom}(\mu_m), \forall n \in \mathbb{N}, \forall m \in \mathbb{M} \quad (vi) \\ \mathbf{M}_{\mu_m}(t,\xi) \geq \gamma_p(t,\xi) & \forall t \in [pT,(p+1)T], \forall (m,p) \in \mathbb{M} \times \mathbb{N} \quad (vii) \\ \mathbf{M}_{\mu_m}(t,\chi) \geq \beta_p(t,\chi) & \forall t \in [pT,(p+1)T], \forall (m,p) \in \mathbb{M} \times \mathbb{N} \quad (viii) \\ \mathbf{M}_{\mu_m}(t,x) \geq \mu_p(t,x) & \forall (t,x) \in \mathrm{Dom}(\mu_p), \forall (m,p) \in \mathbb{M}^2 \quad (ix) \end{cases} \tag{4.10}$$

Although inequalities (4.10) are a function of the decision variable (4.6), they cannot necessarily be expressed as linear inequalities (in terms of the decision variable) in general. However, because of the specific structure of the solutions (4.8) for triangular Hamiltonians, the inequalities (4.10) can be rewritten as a finite number of linear inequality constraints, as shown in the following proposition.

Proposition 35. [Model constraints for triangular Hamiltonians] For triangular Hamiltonians defined by (4.7), the inequality constraints (4.10) can be expressed as a finite number of inequality constraints:

$$\begin{cases} \mathbf{M}_{\gamma_n}(pT,\xi) \geq \gamma_p(pT,\xi) & \forall (n,p) \in \mathbb{N}^2 \quad (i) \\ \mathbf{M}_{\gamma_n}(pT,\chi) \geq \beta_p(pT,\chi) & \forall (n,p) \in \mathbb{N}^2 \quad (ii)(a) \\ \mathbf{M}_{\gamma_n}(nT + \frac{\chi-\xi}{v},\chi) \geq \beta_p(nT + \frac{\chi-\xi}{v},\chi) & \forall (n,p) \in \mathbb{N}^2 \text{ such that} \\ & nT + \frac{\chi-\xi}{v} \in [pT,(p+1)T] \quad (ii)(b) \end{cases} \tag{4.11}$$

$$\begin{cases} \mathbf{M}_{\gamma_n}(t_{\min}(m),x_{\min}(m)) \geq \mu_m(t_{\min}(m),x_{\min}(m)) & \forall n \in \mathbb{N}, \forall m \in \mathbb{M} \quad (iii)(a) \\ \mathbf{M}_{\gamma_n}(t_{\max}(m),x_{\max}(m)) \geq \mu_m(t_{\max}(m),x_{\max}(m)) & \forall n \in \mathbb{N}, \forall m \in \mathbb{M} \quad (iii)(b) \\ \mathbf{M}_{\gamma_n}(t_1(m,n),x_1(m,n)) \geq \mu_m(t_1(m,n),x_1(m,n)) & \forall n \in \mathbb{N}, \forall m \in \mathbb{M} \text{ such that} \\ & t_1(m,n) \in [t_{\min}(m);t_{\max}(m)] \quad (iii)(c) \end{cases} \tag{4.12}$$

$$\begin{cases} \mathbf{M}_{\beta_n}(pT,\xi) \geq \gamma_p(pT,\xi) & \forall (n,p) \in \mathbb{N}^2 \quad (iv)(a) \\ \mathbf{M}_{\beta_n}(nT + \frac{\xi-\chi}{w},\xi) \geq \gamma_p(nT + \frac{\xi-\chi}{w},\xi) & \forall (n,p) \in \mathbb{N}^2 \text{ such that} \\ & nT + \frac{\xi-\chi}{w} \in [pT,(p+1)T] \quad (iv)(b) \\ \mathbf{M}_{\beta_n}(pT,\chi) \geq \beta_p(pT,\chi) & \forall (n,p) \in \mathbb{N}^2 \quad (v) \end{cases} \tag{4.13}$$

$$\begin{cases} \mathbf{M}_{\beta_n}(t_{\min}(m),x_{\min}(m)) \geq \mu_m(t_{\min}(m),x_{\min}(m)) & \forall n \in \mathbb{N}, \forall m \in \mathbb{M} \quad (vi)(a) \\ \mathbf{M}_{\beta_n}(t_{\max}(m),x_{\max}(m)) \geq \mu_m(t_{\max}(m),x_{\max}(m)) & \forall n \in \mathbb{N}, \forall m \in \mathbb{M} \quad (vi)(b) \\ \mathbf{M}_{\beta_n}(t_2(m,n),x_2(m,n)) \geq \mu_m(t_2(m,n),x_2(m,n)) & \forall n \in \mathbb{N}, \forall m \in \mathbb{M} \text{ such that} \\ & t_2(m,n) \in [t_{\min}(m);t_{\max}(m)] \quad (vi)(c) \end{cases} \tag{4.14}$$

$$\begin{cases} \mathbf{M}_{\mu_m}(pT,\xi) \geq \gamma_p(pT,\xi) & \forall (m,p) \in \mathbb{M}\times\mathbb{N} \quad (vii)(a) \\ \mathbf{M}_{\mu_m}(t_3(m),\xi) \geq \gamma_p(t_3(m),\xi) & \forall (m,p) \in \mathbb{M}\times\mathbb{N} \\ & \text{such that } t_3(m) \in [pT,(p+1)T] \quad (vii)(b) \\ \mathbf{M}_{\mu_m}(t_4(m),\xi) \geq \gamma_p(t_4(m),\xi) & \forall (m,p) \in \mathbb{M}\times\mathbb{N} \\ & \text{such that } t_4(m) \in [pT,(p+1)T] \quad (vii)(c) \end{cases} \tag{4.15}$$

$$\begin{cases} \mathbf{M}_{\mu_m}(pT,\chi) \geq \beta_p(pT,\chi) & \forall (m,p) \in \mathbb{M}\times\mathbb{N} \quad (viii)(a) \\ \mathbf{M}_{\mu_m}(t_5(m),\chi) \geq \beta_p(t_5(m),\chi) & \forall (m,p) \in \mathbb{M}\times\mathbb{N} \\ & \text{such that } t_5(m) \in [pT,(p+1)T] \quad (viii)(b) \\ \mathbf{M}_{\mu_m}(t_6(m),\chi) \geq \beta_p(t_6(m),\chi) & \forall (m,p) \in \mathbb{M}\times\mathbb{N} \\ & \text{such that } t_6(m) \in [pT,(p+1)T] \quad (viii)(c) \end{cases} \tag{4.16}$$

$$\begin{cases} \mathbf{M}_{\mu_m}(t_{\min}(p),x_{\min}(p)) \geq \mu_p(t_{\min}(p),x_{\min}(p)) & \forall (m,p) \in \mathbb{M}^2 \quad (ix)(a) \\ \mathbf{M}_{\mu_m}(t_{\min}(p),x_{\max}(p)) \geq \mu_p(t_{\max}(p),x_{\max}(p)) & \forall (m,p) \in \mathbb{M}^2 \quad (ix)(b) \\ \mathbf{M}_{\mu_m}(t_7(m,p),x_7(m,p)) \geq \mu_p(t_7(m,p),x_7(m,p)) & \forall (m,p) \in \mathbb{M}^2 \text{ such that} \\ & t_7(m,p) \in [t_{\min}(p),t_{\max}(p)] \quad (ix)(c) \\ \mathbf{M}_{\mu_m}(t_8(m,p),x_8(m,p)) \geq \mu_p(t_8(m,p),x_8(m,p)) & \forall (m,p) \in \mathbb{M}^2 \text{ such that} \\ & t_8(m,p) \in [t_{\min}(p),t_{\max}(p)] \quad (ix)(d) \\ \mathbf{M}_{\mu_m}(t_9(m,p),x_9(m,p)) \geq \mu_p(t_9(m,p),x_9(m,p)) & \forall (m,p) \in \mathbb{M}^2 \text{ such that} \\ & t_9(m,p) \in [t_{\min}(p),t_{\max}(p)] \quad (ix)(e) \\ \mathbf{M}_{\mu_m}(t_{10}(m,p),x_{10}(m,p)) \geq \mu_p(t_{10}(m,p),x_{10}(m,p)) & \forall (m,p) \in \mathbb{M}^2 \text{ such that} \\ & t_{10}(m,p) \in [t_{\min}(p),t_{\max}(p)] \quad (ix)(f) \\ \mathbf{M}_{\mu_m}(t_{11}(m,p),x_{11}(m,p)) \geq \mu_p(t_{11}(m,p),x_{11}(m,p)) & \forall (m,p) \in \mathbb{M}^2 \text{ such that} \\ & t_{11}(m,p) \in [t_{\min}(p),t_{\max}(p)] \quad (ix)(g) \end{cases} \tag{4.17}$$

where

$$\begin{cases} t_1(m,n) = \frac{nTv - v^{\text{meas}}(m)t_{\min}(m) + x_{min}(m) - \xi}{v - v^{\text{meas}}(m)} \\ x_1(m,n) = v^{\text{meas}}(m)\left(\frac{nTv - v^{\text{meas}}(m)t_{\min}(m) + x_{\min}(m) - \xi}{v - v^{\text{meas}}(m)} - t_{\min}(m)\right) + x_{\min}(m) \\ t_2(m,n) = \frac{nTw - v^{\text{meas}}(m)t_{\min}(m) + x_{\min}(m) - \chi}{w - v^{\text{meas}}(m)} \\ x_2(m,n) = v^{\text{meas}}(m)\left(\frac{nTw - v^{\text{meas}}(m)t_{\min}(m) + x_{\min}(m) - \chi}{w - v^{\text{meas}}(m)} - t_{\min}(m)\right) + x_{\min}(m) \\ t_3(m) = \frac{\xi - x_{\min}(m) + wt_{\min}(m)}{w} \\ t_4(m) = \frac{\xi - x_{\max}(m) + wt_{\max}(m)}{w} \\ t_5(m) = \frac{\chi - x_{\min}(m) + vt_{\min}(m)}{v} \\ t_6(m) = \frac{\chi - x_{\max}(m) + vt_{\max}(m)}{v} \end{cases} \tag{4.18}$$

and

$$\begin{cases} t_7(m,p) = \frac{x_{\min}(m)-x_{\min}(p)+v^{\text{meas}}(p)t_{\min}(p)-v^{\text{meas}}(m)t_{\min}(m)}{v^{\text{meas}}(p)-v^{\text{meas}}(m)} \\ x_7(m,p) = v^{\text{meas}}(p)\left(\frac{x_{\min}(m)-x_{\min}(p)+v^{\text{meas}}(p)t_{\min}(p)-v^{\text{meas}}(m)t_{\min}(m)}{v^{\text{meas}}(p)-v^{\text{meas}}(m)} - t_{\min}(p)\right) + x_{\min}(p) \\ t_8(m,p) = \frac{x_{\max}(m)-x_{\min}(p)+v^{\text{meas}}(p)t_{\min}(p)-vt_{\max}(m)}{v^{\text{meas}}(p)-v} \\ x_8(m,p) = v^{\text{meas}}(p)\left(\frac{x_{\max}(m)-x_{\min}(p)+v^{\text{meas}}(p)t_{\min}(p)-vt_{\max}(m)}{v^{\text{meas}}(p)-v} - t_{\min}(p)\right) + x_{\min}(p) \\ t_9(m,p) = \frac{x_{\min}(m)-x_{\min}(p)+v^{\text{meas}}(p)t_{\min}(p)-vt_{\min}(m)}{v^{\text{meas}}(p)-v} \\ x_9(m,p) = v^{\text{meas}}(p)\left(\frac{x_{\min}(m)-x_{\min}(p)+v^{\text{meas}}(p)t_{\min}(p)-vt_{\min}(m)}{v^{\text{meas}}(p)-v} - t_{\min}(p)\right) + x_{\min}(p) \\ t_{10}(m,p) = \frac{x_{\max}(m)-x_{\min}(p)+v^{\text{meas}}(p)t_{\min}(p)-vt_{\max}(m)}{v^{\text{meas}}(p)-w} \\ x_{10}(m,p) = v^{\text{meas}}(p)\left(\frac{x_{\max}(m)-x_{\min}(p)+v^{\text{meas}}(p)t_{\min}(p)-vt_{\max}(m)}{v^{\text{meas}}(p)-w} - t_{\min}(p)\right) + x_{\min}(p) \\ t_{11}(m,p) = \frac{x_{\min}(m)-x_{\min}(p)+v^{meas}(p)t_{\min}(p)-vt_{\min}(m)}{v^{\text{meas}}(p)-w} \\ x_{11}(m,p) = v^{\text{meas}}(p)\left(\frac{x_{\min}(m)-x_{\min}(p)+v^{meas}(p)t_{\min}(p)-vt_{\min}(m)}{v^{\text{meas}}(p)-w} - t_{\min}(p)\right) + x_{\min}(p) \end{cases} \tag{4.19}$$

Proof — The inequality constraints (4.10) are of the following form:

$$\mathbf{M}_{\mathbf{c}_j}(t,x) \geq \mathbf{c}_i(t,x), \quad \forall (t,x) \in \text{Dom}(\mathbf{c}_i) \tag{4.20}$$

where $\text{Dom}(\mathbf{c}_i)$ is a line segment of $\mathbb{R}^2$, $\mathbf{c}_i(\cdot,\cdot)$ is an affine function of the form (4.1), (4.2) or (4.3) and $\mathbf{M}_{\mathbf{c}_j}(\cdot,\cdot)$ is a piecewise affine function of the form (4.8). Hence, $\mathbf{M}_{\mathbf{c}_j}(\cdot,\cdot) - \mathbf{c}_i(\cdot,\cdot)$ is a piecewise affine function, defined on $\text{Dom}(\mathbf{M}_{\mathbf{c}_j}) \cap \text{Dom}(\mathbf{c}_i)$. Note that $\text{Dom}(\mathbf{M}_{\mathbf{c}_j})$ is convex by proposition 3 and that $\text{Dom}(\mathbf{c}_i)$ is a line segment of $\mathbb{R}^2$. Hence, $\text{Dom}(\mathbf{M}_{\mathbf{c}_j}) \cap \text{Dom}(\mathbf{c}_i)$ is also a line segment of $\mathbb{R}^2$, which can thus be written as $\text{Dom}(\mathbf{M}_{\mathbf{c}_j}) \cap \text{Dom}(\mathbf{c}_i) = \{u + \alpha v, \alpha \in [0,1]\}$ for some $(u,v) \in \mathbb{R}^4$.

Let us define $f(\cdot)$ on $[0,1]$ as $f : \alpha \to \mathbf{M}_{\mathbf{c}_j}(u+\alpha v)$. With this definition, inequality (4.20) can be written as:

$$f(\alpha) \geq 0, \quad \forall \alpha \in [0,1] \tag{4.21}$$

Since $\mathbf{M}_{\mathbf{c}_j}(\cdot,\cdot) - \mathbf{c}_i(\cdot,\cdot)$ is piecewise affine and continuous, so is $f(\cdot)$. Let us define the intervals in which $f(\cdot)$ is affine by $[0,\alpha_1], \ldots, [\alpha_p, 1]$. Since $f(\cdot)$ is monotonic on the intervals $[0,\alpha_1], \ldots, [\alpha_p, 1]$, inequality (4.21) is satisfied if and only if $f(0) \geq 0$, $f(\alpha_1) \geq 0, \ldots, f(\alpha_p) \geq 0$ and $f(1) \geq 0$, which yields the finite number of inequalities (4.11), (4.12), (4.13), (4.14), (4.15), (4.16) and (4.17). ■

Since the model inequality constraints (4.5), (4.11), (4.12), (4.13), (4.14), (4.15), (4.16) and (4.17) are all linear inequalities in the decision variable y defined by (4.6), we can write them in a compact form as follows:

$$A_{\text{model}}(\psi) y \leq b_{\text{model}}(\psi) \tag{4.22}$$

Note that the model constraints are a function of the parameters of the Hamiltonian.

4.3 Data constraints

Similarly to the model constraints shown above, measurement data also restricts the possible values that the coefficients (4.4) can take. The values of $t_{\min}(\cdot)$, $t_{\max}(\cdot)$, $x_{\min}(\cdot)$, $x_{\max}(\cdot)$, $q_{\text{in}}(\cdot)$ and $q_{\text{out}}(\cdot)$ can be directly measured, though we assume that $t_{\min}(\cdot)$, $t_{\max}(\cdot)$, $x_{\min}(\cdot)$ and $x_{\max}(\cdot)$ are perfectly known. The measured values of $q_{\text{in}}(\cdot)$ and $q_{\text{out}}(\cdot)$ are denoted by $q_{\text{in}}^{\text{meas}}(\cdot)$ and $q_{\text{out}}^{\text{meas}}(\cdot)$ respectively. In the remainder of this dissertation, we choose the following error model for $q_{\text{in}}(\cdot)$ and $q_{\text{out}}(\cdot)$:

$$\begin{array}{l} \left|\left|\frac{q_{\text{in}}(\cdot)-q_{\text{in}}^{\text{meas}}(\cdot)}{q_{\text{in}}^{\text{meas}}(\cdot)}\right|\right|_p \leq e_{\max} \\ \left|\left|\frac{q_{\text{out}}(\cdot)-q_{\text{out}}^{\text{meas}}(\cdot)}{q_{\text{out}}^{\text{meas}}(\cdot)}\right|\right|_p \leq e_{\max} \end{array} \tag{4.23}$$

where $||\cdot||_p$ is the standard L_p norm:

$$||f(\cdot)||_p = (\sum_{n=1}^{n_{\max}} |f(n)|^p)^{\frac{1}{p}} \tag{4.24}$$

Different choices of norm are possible, but all choices of $p \geq 1$ yield convex constraints by convexity of the norm. In particular, the choices $p = 1$ and $p = +\infty$ yield linear constraints, which can be written as:

$$A_{\text{data}} y \leq b_{\text{data}} \quad \text{for } p = 1 \text{ or } p = +\infty \tag{4.25}$$

The choice $q = 2$ yields quadratic convex constraints, which can be written as:

$$y^T Q(i) y \leq b_{\text{data}}(i), \;\; (Q(i) \geq 0), \;\; \forall i \in [1, i_{\max}] \;\; \text{for } p = 2 \tag{4.26}$$

Note that the error model (4.23), for $p = +\infty$ is commonly used in practice. It corresponds to a situation in which we assume that the relative error on each measurement of the sensor is bounded by a constant value. In the remainder of this dissertation, we assume that the error model yields linear inequalities of the form (4.25) for simplicity. Note that the results presented below could be trivially extended for quadratic constraints (4.26), yielding quadratically constrained convex programs.

4.4 Compatibility and consistency problems

We now define two fundamental convex feasibility problems which will play an important role in the subsequent sections.

4.4.1 Data and model compatibility problem

Let y denote the decision variable (4.6), and let the model and data constraints be defined as in (4.22) and (4.25) respectively. The data and model compatibility constraints can be satisfied at the same time if and only if the following problem is feasible:

$$\begin{aligned} &\textbf{Find } y \\ &\textbf{such that } \begin{cases} A_{\text{model}}(\psi)y \leq b_{\text{model}}(\psi) \\ A_{\text{data}}y \leq b_{\text{data}} \end{cases} \end{aligned} \tag{4.27}$$

When the above problem is feasible, one can estimate the minimum (respectively maximum) of a piecewise affine convex (respectively concave) function of the decision variable using a LP. One can thus estimate lower and upper bounds on linear functions of the decision variable using LPs. We apply this property in section 4.5 to estimate upper and lower bounds on linear functions of the decision variable.

In contrast, when (4.27) is infeasible, no set of value conditions satisfying both the model and data constraints can exist. However, by relaxing alternatively the model or data constraints, one can define [30] two problems of interest, which are the subject of section 4.6. The data reconciliation problem consists in finding the set of value conditions satisfying the model constraints, that is as close as possible (in some norm sense) to satisfy the data constraints. In contrast, the data assimilation problem consists in finding the set of value conditions satisfying the data constraints, that is as close as possible to satisfy the model constraints.

4.4.2 Data consistency problem

The problem (4.27) must be feasible when the following conditions are satisfied:

1 - The Hamiltonian $\psi(\cdot)$ satisfies (3.11) (that is, the hypograph of the Hamiltonian contains all experimental flow-density values, as in Figure 3.2.
2 - The coefficients $\overline{y}$ associated with the actual value condition satisfy the data constraints (4.25)

(4.28)

Indeed, if the conditions (4.28) are met, the coefficients $\overline{y}$ associated with the true value condition will satisfy (4.25) and (4.22) by proposition 25. The problem of checking the feasibility of (4.27) under the constraints (4.28) is referred to as *consistency check*. This problem is used in section 4.7 to detect cyberattacks and in section 4.5 to give guaranteed bounds on some traffic-related quantities.

4.5 Estimation problems

4.5.1 Definition for general functions of traffic-related coefficients

A number of traffic-flow related quantities can be written as linear functions of the decision variable (4.29) and can be estimated using Linear Programming, as shown in the following proposition.

$$y := (q_{\text{in}}(1), \ldots, q_{\text{in}}(n_{\max}), q_{\text{out}}(1), \ldots, q_{\text{out}}(n_{\max}), L_1, \ldots, L_{m_{\max}}, r_1, \ldots, r_{m_{\max}}) \tag{4.29}$$

Proposition 36. [Estimation of linear functions] Let $f(\cdot)$ be a linear function of (4.6), defined as $f(y) = c^T y$. The possible values that $f(\cdot)$ can take under the linear model (4.22) and data (4.23) constraints (for the L_1 or L_∞ norms) is the interval $[f_{\min}, f_{\max}]$, where $f_{\min}$ and $f_{\max}$ are solutions to the following LPs:

$$\begin{aligned} &\textbf{Minimize (}\text{respectively } \textbf{Maximize)} \;\; c^T y \\ &\textbf{such that} \;\; \begin{cases} A_{\text{model}}(\psi) y \leq b_{\text{model}}(\psi) \\ A_{\text{data}} y \leq b_{\text{data}} \end{cases} \end{aligned} \tag{4.30}$$

Note that the above estimation problem has a sense only if the compatibility problem (4.27) is feasible. Not also that when the conditions (4.28) are satisfied, (4.27) is feasible and the true value condition $\overline{y}$ is an element of the feasible set. Hence the actual value $f(\overline{y})$ of $f(\cdot)$ is guaranteed to be in the interval $[f_{\min}, f_{\max}]$.

4.5.2 Lower and upper bounds on traffic coefficients

Estimation of the initial number of vehicles using linear programming

The initial number of vehicles Δ on the highway section can be estimated through Linear Programming. Indeed, Δ appears linearly in the decision variable (4.6), while the model (4.22) and data constraints (4.25) are linear inequalities in (4.6). Since the feasible set is convex by the constraints of (4.30), the possible values of Δ such that the model and data constraints are satisfied are $\Delta_{\min} \leq \Delta \leq \Delta_{\max}$, where $\Delta_{\min}$ and $\Delta_{\max}$ are solutions to the following optimization programs:

$$\begin{aligned} &\textbf{minimize (}\text{respectively } \textbf{maximize)} \;\; \Delta \\ &\textbf{such that} \;\; \begin{cases} A_{\text{model}}(\psi) y \leq b_{\text{model}}(\psi) \\ A_{\text{data}} y \leq b_{\text{data}} \end{cases} \end{aligned} \tag{4.31}$$

We illustrate the estimation process in Figure 4.3, in which we show the evolution of the interval $[\Delta_{\min}, \Delta_{\max}]$ as we increase the quantity of measurement data. In this problem, we consider the spatial domain defined in section 4.1.3, between the times 11:40 AM

and 12:10 PM. We solve (4.40) using 60 blocks of upstream boundary conditions (4.1) and downstream boundary conditions (4.2), and a variable number of internal conditions (4.3).

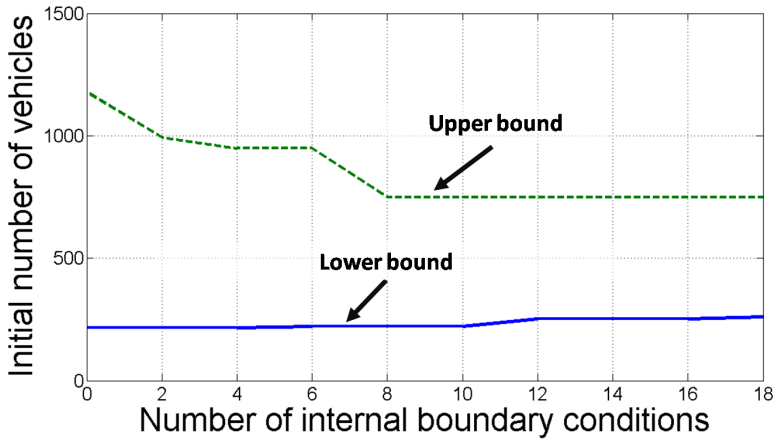

Figure 4.3: **Initial number of vehicles estimation using linear programming.** This figure represents the evolution of the upper and lower bounds on the initial number of vehicles Δ as new internal condition data is added into the estimation problem. The horizontal axis represents the number of probe measurement data blocks $\mu_m(\cdot,\cdot)$ as defined in (4.3). As predicted by proposition 34, the upper bound (dashed) on Δ decreases and the lower bound (solid line) on Δ increases when additional data is added into the estimation problem.

The same framework can also be applied for estimating other functions of the decision variable (4.6), such as the travel time across the highway section. Unlike the initial number of vehicles, the travel time is a nonlinear and nonconvex function of the decision variable (4.6), which makes the estimation problem more challenging.

Travel time estimation using convex programming

In order to properly define a travel time function, we first need to assume [80] that no vehicles can pass each other, which implies in particular $r_m = 0$ for all $m \in \mathbb{M}$. In this situation, known in the transportation engineering as *First In First Out* (FIFO), the vehicle trajectories are the isolines of the state function. In order to properly define the travel time function, we also have to assume that the function $\beta(\cdot,\cdot) = \min_{n\in\mathbb{N}} \beta_n(\cdot,\cdot)$ is strictly increasing. Note that by (4.2), imposing this last condition amounts to impose $q_{\text{out}}(\cdot) > 0$ instead of the inequality $q_{\text{out}}(\cdot) \geq 0$ in (4.5). With these two assumptions, the travel time can be defined as follows. Let t be given, and $i = \lfloor \frac{t}{T} \rfloor$. The travel time $\sigma(t)$ is defined as $\tau - t$, where $\gamma_i(t,\xi) = \beta(\tau,\chi)$. Since $\beta(\cdot,\chi)$ is strictly increasing, we can also define the travel time as:

$$\sigma(y,t) = \min_{s\in\mathbb{R}_+ \text{ s. t. } \beta(s,\chi)\geq\gamma_i(t,\xi)} (s-t) \tag{4.32}$$

or alternatively:

$$\sigma(y,t) = \max_{s\in\mathbb{R}_+ \text{ s. t. } \beta(s,\chi)\leq\gamma_i(t,\xi)} (s-t) \tag{4.33}$$

Since $\beta_j(s,\chi)$ and $\gamma_i(t,\chi)$ are functions of the decision variable (4.6), the travel time function $\sigma(\cdot,\cdot)$ hereby defined is a function of the decision variable (4.6), though not linear. While we cannot estimate the travel time using a LP of the form (4.30), we can still obtain valuable information on upper and lower bounds of the travel time function using LPs, as outlined in the following proposition.

Proposition 37. [Upper and lower bounds on travel time function] Let us assume that (4.27) is feasible, that is, the model and data constraints are compatible. Let two times t and τ be given, and let $i = \lfloor \frac{t}{T} \rfloor$ and $j = \lfloor \frac{\tau}{T} \rfloor$. We have that $\tau - t$ is a lower bound on the travel time $\sigma(y,t)$ (under the model and data constraints) if and only if the following problem is infeasible:

$$\textbf{find} \quad y$$

$$\textbf{such that} \quad \begin{cases} A_{\text{model}}(\psi)y \leq b_{\text{model}}(\psi) \\ A_{\text{data}}y \leq b_{\text{data}} \\ \beta_j(\tau,\chi) - \gamma_i(t,\xi) \geq 0 \end{cases} \tag{4.34}$$

Similarly, $\tau - t$ is an upper bound on the travel time $\sigma(y,t)$ under the model and data constraints if and only if the following problem is infeasible:

$$\textbf{find} \quad y$$

$$\textbf{such that} \quad \begin{cases} A_{\text{model}}(\psi)y \leq b_{\text{model}}(\psi) \\ A_{\text{data}}y \leq b_{\text{data}} \\ \beta_j(\tau,\chi) - \gamma_i(t,\xi) \leq 0 \end{cases} \tag{4.35}$$

Proof — We prove that $\tau - t$ is a lower bound on the travel time function if and only if (4.34) is infeasible. Let us assume that (4.34) is infeasible. This amounts to saying that $\beta_j(\tau,\chi) < \gamma_i(t,\xi)$ whenever the model and data constraints $A_{\text{model}}(\psi)y \leq b_{\text{model}}(\psi)$ and $A_{\text{data}}y \leq b_{\text{data}}$ are both satisfied. Hence, since $\beta(\tau,\chi) = \beta_j(\tau,\chi)$ by construction, this is equivalent to saying that $\beta(\tau,\chi) < \gamma_i(t,\xi)$ whenever the model and data constraints are both satisfied. By the definition (4.33) of $\sigma(y,t)$, this is equivalent to $\sigma(y,t) > \tau - t$, whenever y satisfies the model and data constraints, which completes the proof. The proof relative to the upper bound is similar, and involves the definition (4.32) of $\sigma(y,t)$. ■

Note that the feasibility programs (4.34) and (4.35) enable us to compute the largest lower bound $\sigma_{\text{d}}(t)$ and the smallest upper bound $\sigma_{\text{u}}(t)$ on the travel time by trial and error.

We illustrate the above results by computing the upper and lower bounds on the travel time function, using the experimental setup of section 4.1.3, between times 11:40 AM and 12:10 PM. For this, we check the feasibility of problems (4.34) and (4.35) for $\tau = jT$, and plot in Figure 4.4 respectively the lowest and highest value of jT such that (4.35) and (4.34) are respectively infeasible. The lowest value $j_{\max}T$ for which (4.35) is infeasible implies that $\sigma_{\mathrm{u}}(t)$ is in the interval $[(j_{\max}-1)T - t, j_{\max}T - t]$. Similarly, the highest value $j_{\min}T$ for which (4.34) is infeasible implies that $\sigma_{\mathrm{d}}(t)$ is in the interval $[j_{\min}T - t, (j_{\min}+1)T - t]$. As stated in proposition 34, the distance between the upper and lower bounds decreases as more data is added into the estimation problem.

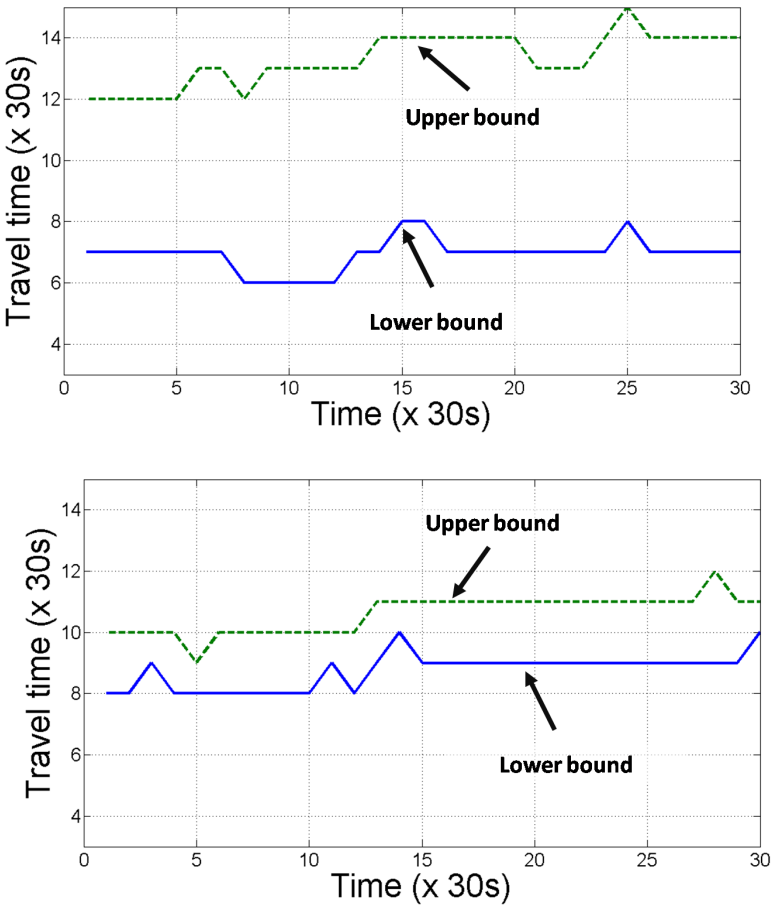

0.7

Figure 4.4: **Travel time estimation using linear programming.** In this figure, the horizontal axis represents the time, while the vertical axis represents the travel time. The upper and lower bounds on the travel time function are represented by a dashed and solid line respectively. **Top:** In this figure, we consider 60 upstream and downstream boundary conditions blocks and 20 internal condition blocks. **Bottom:** In this figure, we increase the number of internal condition blocks to 45. As can be seen, the corresponding bounds on the travel time function are improved since more data is added into the estimation problem, following proposition 34.

Remark — The largest lower bound (or smallest upper bound) on travel time cannot be directly estimated using convex programming. Indeed, by checking the feasibility of (4.34) for increasing values of $\tau = nT$, we can find the integer j such that $\sigma_{\mathrm{d}}(t) \in [jT-t, (j+1)T-t]$ (in this situation, (4.34) is infeasible for $\tau = jT$, and becomes feasible for $\tau = jT+1$). When such a j is identified, $\sigma_{\mathrm{d}}(t)$ is the solution to the following optimization program:

$$\textbf{minimize } \frac{z}{q_{\text{out}}(j)}$$

$$\textbf{such that } \begin{cases} A_{\text{model}}(\psi)y \leq b_{\text{model}}(\psi) \\ A_{\text{data}}y \leq b_{\text{data}} \\ \beta_j(\frac{z}{q_{\text{out}}(j)}, \chi) - \gamma_i(t, \xi) \leq 0 \end{cases} \tag{4.36}$$

The decision variable of (4.36) can be written as (y, z), where y is the decision variable defined by (4.6). The constraints $A_{\text{model}}(\psi)y \leq b_{\text{model}}(\psi)$ and $A_{\text{data}}y \leq b_{\text{data}}$ are both linear in the new decision variable (they indeed depend only upon y). The constraint $\beta_j(\frac{z}{q_{\text{out}}(j)}, \chi) - \gamma_i(t, \xi) \leq 0$ is also linear, since it can be written as:

$$\begin{aligned} &\sum_{k=0}^{j-1} q_{\text{out}}(k)T + q_{\text{out}}(j)(\frac{z}{q_{\text{out}}(j)} - jT) \\ &-\Delta - \sum_{k=0}^{i-1} q_{\text{in}}(k)T - q_{\text{in}}(i)(t - iT) \leq 0 \end{aligned} \tag{4.37}$$

The choice of $\frac{z}{q_{\text{out}}(j)}$ in the objective function is made to enforce the linearity of the constraints (and it plays the role of τ in the previous equations). The objective is however nonconvex, since $(z, q) \to \frac{z}{q}$ is not convex. Problem (4.36) thus cannot be solved using convex programming, but may still be solved numerically using other optimization methods. ■

4.5.3 Guaranteed ranges for traffic coefficients estimation

The upper and lower bounds on functions of the decision variable investigated above do not necessarily hold in practice, since the true value $\overline{y}$ of the decision variable (4.6) may not satisfy the model and data constraints. However, when the conditions (4.28) hold, the values of the upper and lower bounds are guaranteed. Indeed, when (4.28) is satisfied, $\overline{y}$ belongs to the set $\{y | A_{\text{model}}(\psi)y \leq b_{\text{model}}(\psi)\} \cap \{A_{\text{data}}y \leq b_{\text{data}}\}$, which implies

$$f(\overline{y}) \geq \begin{array}{ll} \textbf{minimize} & f(y) \\ \textbf{such that} & \begin{cases} A_{\text{model}}(\psi)y \leq b_{\text{model}}(\psi) \\ A_{\text{data}}y \leq b_{\text{data}} \end{cases} \end{array} \tag{4.38}$$

and

$$f(\overline{y}) \leq \begin{array}{ll} \textbf{maximize} & f(y) \\ \textbf{such that} & \begin{cases} A_{\text{model}}(\psi)y \leq b_{\text{model}}(\psi) \\ A_{\text{data}}y \leq b_{\text{data}} \end{cases} \end{array} \tag{4.39}$$

In order to obtain guaranteed bounds in practice, one has to choose the model parameter such that the condition (4.28) holds. In the context of traffic flow, the typical values of the

model parameter are accurately known, and do not vary significantly between experimental sites. They are available from [75] for instance. In order to impose (4.28) on all practical traffic scenarios, one simply has to overapproximate these values to define the model parameters.

4.6 Data assimilation and data reconciliation problems

4.6.1 Problem definition

In the field of distributed parameters system estimation, the problems of *data assimilation* [47] and *data reconciliation* [37] are closely linked. The data assimilation process consists in finding the value of the state of the system that satisfies the observations, and that is the closest to being a solution to the evolution model. In contrast, the data reconciliation process consists in finding a solution to the evolution model that is the closest to the observations. Given the framework detailed above, the data assimilation and reconciliation problems are related to the solutions of the following convex optimization program.

$$\begin{aligned} &\textbf{minimize} \;\; ||y_1 - y_2||_q \\ &\textbf{such that} \;\; \begin{cases} A_{\text{model}}(\psi) y_1 \leq b_{\text{model}}(\psi) \\ A_{\text{data}} y_2 \leq b_{\text{data}} \end{cases} \end{aligned} \tag{4.40}$$

In the above optimization program, we have to choose $q = 1$ or $q = +\infty$ to obtain a linear objective. Two situations can arise:

- If the optimal value of (4.40) is 0, the model and data constraints can be satisfied at the same time. In this situation, the data assimilation and data reconciliation problems coincide in a setting in which data and model are compatible. The solution is not necessarily unique.

- If the optimal value of (4.40) is nonzero, the optimal solutions y_1^{optimal} and y_2^{optimal} enable us to compute the upstream, downstream and internal conditions respectively associated with the data reconciliation and data assimilation problems. Note that these solutions may not be unique. The value conditions associated with y_1^{optimal} satisfy the model constraints by construction, *i.e.* all upstream boundary, downstream boundary and internal conditions blocks apply in the strong sense [8, 13]. They however do not satisfy the data constraints, but are as close as possible in the $||\cdot||_q$ sense to satisfy them. In contrast, the value conditions associated with y_2^{optimal} satisfy the data constraints by construction, but do not satisfy the model constraints (they are as close as possible to satisfy them in the $||\cdot||_q$ sense).

4.6.2 Numerical example

In this application, we consider the spatial domain defined in section 4.1.3, between the times 11:40 AM and 12:05 PM for data collected on February 8th, 2008. We use the following Hamiltonian parameters: $k_c = 0.048\ m^{-1}$, $v = 24.6\ m/s$, $w = -4.5\ m/s$, and a maximal relative error level of $e_{\max} = 0.01$. We solve (4.40) for $q = 1$, using 604 variables and 17415 linear constraints. For this specific application, the optimal value of (4.40) is +8.58, which ensures that the data assimilation and data reconciliation problems are well defined. As mentioned above, y_1^{optimal} and y_2^{optimal} enable us to compute the value conditions associated with the data assimilation and data reconciliation problems. We compute the solutions to (2.5) associated with these value conditions, and display them in Figure 4.5. The solution to the *data reconciliation problem* at the top of Figure 4.5 satisfies all the boundary and internal conditions that are prescribed on it. The model applies in the strong sense, however the decision variable violates the data constraints (4.25). In contrast, the upstream and downstream boundary conditions do not apply everywhere in the solution to the *data assimilation problem* (Figure 4.5, center). In the illustrated data assimilation example, the data constraints some internal conditions to be set in a way that is incompatible with the upstream and downstream boundary conditions. This can be seen for instance around time $t = 1100s$: a back propagating wave hits the upstream boundary condition at $x = 11000m$, which prevents it from applying between times $t = 1100s$ and $t = 1400s$.

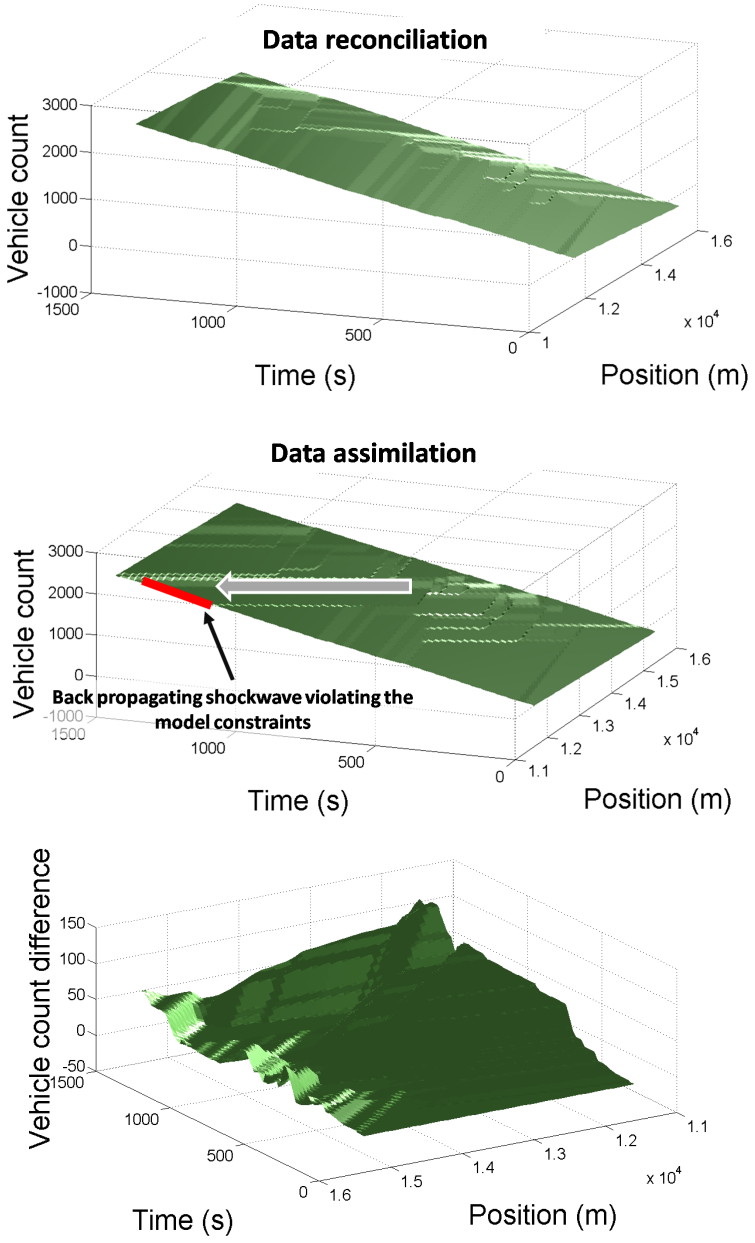

Figure 4.5: **Solutions to data assimilation and data reconciliation problems. Top:** Solution to the data reconciliation problem, in which the model constraints are satisfied, but the data constraints are not. **Center:** Solution to the data assimilation problem, in which the data constraints are satisfied, but the model constraints are not. Both problems are solved simultaneously by (4.40). **Bottom:** Difference (in number of vehicles) between the solution to the data reconciliation problem and the solution to the data assimilation problem.

4.7 Cybersecurity, sensor fault detection and privacy analysis problems

4.7.1 Consistency problems applied to sensor failure detection

The framework developed in section 4.4 can also be applied to detect failures in sensor networks. In this section, we are interested in checking the consistency of the data generated by sensors of the PeMS system [103], which is a network of loop detectors measuring traffic on California highways. The PeMS system is one of the data feeds currently integrated in the *Mobile Millennium* traffic monitoring system [98, 101], operated jointly by Nokia and UC Berkeley. One of the main challenges arising when using data from the PeMS system is the automated identification of the mislocated or faulty sensors. Previous approaches such as [67] have successfully implemented sensor fault detection algorithms based on statistical correlation with adjacent sensors. Our approach is different though, since it can guarantee using the PDE model that at least one of the sensors in an array of sensors is failing.

We solve the fault detection problem either by checking the feasibility of the consistency problem (4.27) using a Hamiltonian satisfying (4.28) on all pairs of consecutive sensors present on the highway network.

We assume that the maximal allowable error of a PeMS sensor is $e_{\max} = 0.3$ in (4.23). There are multiple sources of uncertainty arising when dealing with loop detectors, such as pavement depth, loop layout, which typically creates maximal errors of this magnitude. We also choose an Hamiltonian $\psi(\cdot)$ satisfying (4.28) by overapproximating the tabulated values of [75]: $k_c = 0.05\ m^{-1}$, $v = 30\ m/s$, $w = -7\ m/s$.

As an application, we consider five consecutive PeMS sensors, labeled 401339, 401714, 401376, 400609 and 400835 respectively, as illustrated in Figure 4.6. For each one of the four adjacent pairs of sensors, we compute the minimal value of the error $e_{\max}$ such that the consistency problem (4.27) is feasible during a one month period at the frequency of one day. The distribution of these results is shown in Figure 4.6. Note that since $e_{\max}$ appears linearly in the data constraints, the minimal value of the error $e_{\max}$ such that (4.27) is feasible is also a LP.

Figure 4.6 shows that there is no indication of malfunction for the first and the last pairs of sensors. Note that the success to the minimal error test does not guarantee that a pair of sensors is working, since the actual error of the pair of sensors can be above the maximal allowable error.

The second and third pairs exhibit errors that are higher than 0.3, which indicates a malfunction of the corresponding pairs. Further analysis has shown that the pair $401714 - 400609$ is passing the minimal error test and thus that sensor 401376 is likely incorrectly mapped.

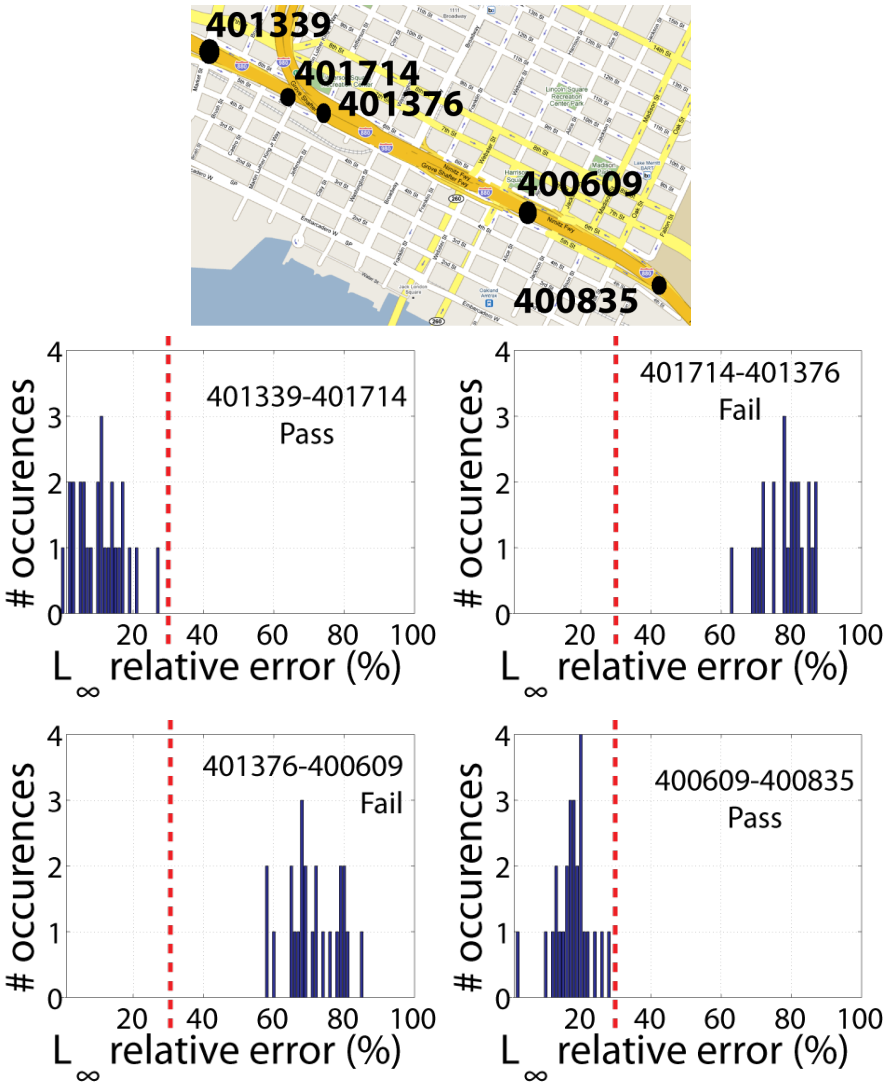

Figure 4.6: **Faulty sensor detection.**
We consider here the traffic flow on highway I880-S near Oakland, CA. The minimal error estimation problem (a LP) is run each day on a one-month period. The sensors of interests are highlighted in the top figure and their corresponding minimal error distribution over the one-month period is represented in the four bottom figures. **Bottom:** The top left and bottom right subfigures represents the minimal errors of the pair $401339 - 401714$ and $40609 - 400835$. These minimal errors fall in the allowable range. In contrast, the minimal errors of the pair $401714 - 401376$ and $401376 - 400609$ are above the allowable range. This means that there must exist a fault in one of the sensors 401714, 401376, or 400609.

4.7.2 Consistency problems applied to cybersecurity

One type of cyberattack [4] consists in faking sensor data and sending it to the monitoring system as if it was originating from valid sensors. Detecting this form of cyberattack is a complex problem in general. Detecting fake data that follows some pattern (for instance if the faked data is periodic) or that falls out of physically reasonable bounds is easy. However, detecting fake data that is both random and consistent with the expected value of sensor measurements is difficult.

A possible approach for solving this problem is to check if (4.27) is feasible, under the assumption (4.28). If (4.27) is feasible, this implies that the data is consistent with our model and data assumptions. Note that this does not guarantee that no cyberattack occurs. Indeed, an attacker can send fake data in a way that is consistent with the model and error levels assumptions. However, if (4.27) is infeasible, at least one of the assumptions (4.28) is false. Either the Hamiltonian does not satisfy (4.28), or the error model (4.28) is wrong. Any of these two situations can denote a cyber-attack if the conditions (4.28) are known to hold. However, note that other phenomena such as sensor failures can also cause (4.27) to be infeasible. The same framework can be applied to sensor fault detection.

We illustrate the cyberattack detection method (4.27) by simulating an attacker sending fake random values of $x_{\min}(\cdot)$, $x_{\max}(\cdot)$, $t_{\min}(\cdot)$ and $t_{\max}(\cdot)$, leading to the construction of new fake internal conditions using (4.3). The values of $x_{\min}(\cdot)$, $x_{\max}(\cdot)$, $t_{\min}(\cdot)$ and $t_{\max}(\cdot)$ are chosen randomly as follows. The speed $\frac{x_{\max}(\cdot)-x_{\min}(\cdot)}{t_{\max}(\cdot)-t_{\min}(\cdot)}$ associated with the internal condition is chosen uniformly in an interval $[v_{\min}, v_{\max}]$. The coefficients satisfy $x_{\min}(\cdot) \geq \xi$, $x_{\max}(\cdot) \leq \chi$, $t_{\min}(\cdot) \geq 0$ and $t_{\max}(\cdot) \leq n_{\max}T$. In the numerical applications, we consider the experimental setup described in section 4.1.3, between times 11:40 AM and 12:00 PM. We use 30 experimental internal conditions (4.3), 40 experimental upstream boundary conditions (4.1) and 40 experimental downstream boundary conditions (4.2). We progressively add fake internal conditions (4.3) and solve problem (4.40) for $q = 1$, and for a Hamiltonian satisfying (4.28). Note that (4.27) is feasible if and only if the solution to (4.40) is zero. Thus, the solution to (4.40) is a measure of the "distance" or incompatibility between data and model. In order to facilitate comparisons and reproduce the results, each result in Figure 4.7 top and bottom was averaged over 10 different choices of fake internal conditions.

As illustrated in Figure 4.7 top, adding fake speed measurements increases the incompatibility between data and model. The incompatibility between data and model is 0 when no fake measurements are added, which is consistent with the fact that (4.28) holds. Note that adding fake speeds does not have a significant impact on the level of incompatibility between data and model when the fake speeds are close to the average speed on the highway section (20 mph in this experiment) which is also consistent with the physics of the problem.

Figure 4.7 bottom shows that the configuration of the measurement data plays a critical role. In this figure, we study the influence of the measurement data on the detection of cyberattacks. For this, we consider four different subsets of 30 internal conditions each, extracted from our measurement data. An example of subset of 12 internal conditions among

28 available measurements is illustrated in Figure 4.8. We fix the fake speeds range to [30 mph, 35 mph], and show the solution to (4.27) for these four configurations, represented on the horizontal axis. As can be seen from this figure, depending on the configuration of our measurement data, we can have very different ranges of level of incompatibility between data and model, for identical number of actual measurements, number of fake internal conditions and range of fake speeds. In the configurations ♯1 and ♯4, it is very difficult to detect that a spoofing attack occurs, since no change in the optimal value of (4.40). However, the spoofing attack is easily detected in the configuration ♯2, even though all configurations contain the same amount of measurement data. These results thus show that it is almost impossible to determine if detecting a cyberattack is easy based on the amount of measurement data alone.

4.7.3 Privacy analysis problems

Another possible application of the framework defined in section 4.5 is the analysis of user privacy using linear programming. The label of the vehicle represented by the internal condition $\mu_m(\cdot,\cdot)$ defined by (4.3) is L_m. In practical problems, the same vehicle sends different packets of information, representing different internal conditions (4.3). To what extent is it possible to "reidentify" one vehicle, *i.e.* to track it by identifying the pieces of data that came from the same vehicle?

Standard methods [60] do not take into account the model constraints: they usually try to reidentify vehicles under the assumption that vehicles maintain a relatively constant speed. While this is true for a large number of traffic scenarios, it does not take into account the underlying model, and can fail if the the traffic speeds change significantly through the computational domain.

If we assume that vehicles do not pass each other (this implies $r_m = 0$ for all $m \in \mathbb{M}$), the minimal and maximal number of vehicles between two different internal condition blocks $\mu_i(\cdot,\cdot)$ and $\mu_j(\cdot,\cdot)$ is solution to the following LP:

$$\textbf{minimize (or maximize)} \quad |L_i - L_j|$$

$$\textbf{such that} \quad \begin{cases} A_{\text{model}}(\psi) y \leq b_{\text{model}}(\psi) \\ A_{\text{data}} y \leq b_{\text{data}} \\ r_m = 0 \ \ \forall m \in \mathbb{M} \end{cases} \tag{4.41}$$

The above LP enables us to identify situations in which the privacy of users could be breached. Indeed, when the maximal number of vehicles between $\mu_i(\cdot,\cdot)$ and $\mu_j(\cdot,\cdot)$ is zero, these boundary conditions represent the same vehicle. In contrast, when the minimal number of vehicles between $\mu_i(\cdot,\cdot)$ and $\mu_j(\cdot,\cdot)$ is nonzero, these boundary conditions cannot originate from the same vehicle. We thus have three cases:

1. If the optimal value $|L_i - L_j|^{\max}$ of the maximization problem (4.41) is zero, then $\mu_i(\cdot,\cdot)$ and $\mu_j(\cdot,\cdot)$ have been generated by the same vehicle.

2. If the optimal value $|L_i - L_j|^{\min}$ of the minimization problem (4.41) is nonzero, then $\mu_i(\cdot,\cdot)$ and $\mu_j(\cdot,\cdot)$ cannot have been generated from the same vehicle.

3. Other cases are inconclusive

We show an example of vehicle reidentification in Figure 4.9, using the experimental setup of section 4.1.3.

In practical computations, given an internal condition $\mu_i(\cdot,\cdot)$, there may exist multiple $j \in \mathbb{M}$ such that the solution to the minimization problem (4.41) is zero. If this happen, we lost track of vehicle i, which can be desirable in the context of traffic flow engineering (see [60] for an analysis of user privacy in mobile traffic sensing systems).

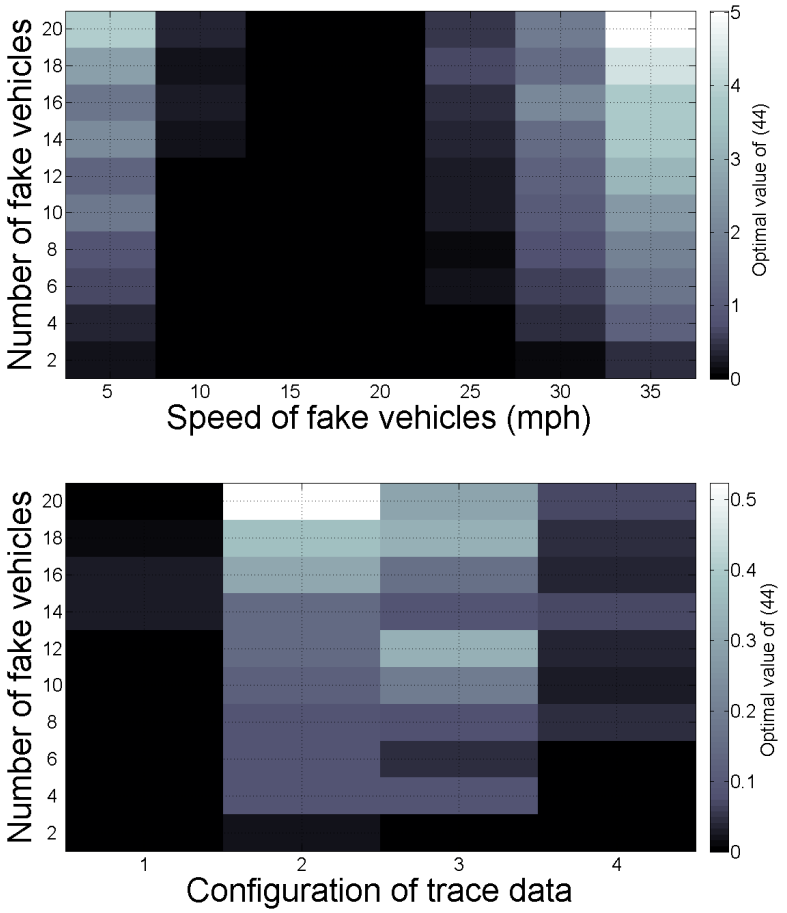

Figure 4.7: **Cyberattack detection using linear programming.** In these figures, we represent the solution to (4.40) as a color map. Low values are represented as dark areas, and correspond to situations in which the "compatibility" between model and data is "good", *i.e.* lower values of $||y_2 - y_i||$ in (4.27). High values are represented as light-colored areas, and denote a higher degree of incompatibility between the model and data constraints. **Top:** The horizontal axis in this figure represents the lower bound k of the interval [k mph, k+5 mph] in which the fake speed data is drawn. The vertical axis represents the number of fake internal conditions added. For instance, the cell $(15, 12)$ corresponds to 12 fake internal conditions for which the speed is in the interval [15 mph, 20 mph]. As can be seen from this figure, the distance increases when more fake measurements are added into the estimation problem, and when they correspond to a speed that is far away from the true average speed (around 20 mph in this application). **Bottom:** This figure illustrates the high sensitivity of the solution to (4.40) with respect to the available measurement data. In this figure, we consider four different sets of 30 actual internal boundary conditions each. The procedure used for choosing a random subset of the available measurement data is illustrated in Figure 4.8. For each of these subsets (configurations), we add an increasing quantity of fake internal conditions, associated with random speeds ranging in [30 mph, 35 mph]. As can be seen, the results vary dramatically depending on which subset of the available data was chosen, even if the number of fake internal conditions is identical.

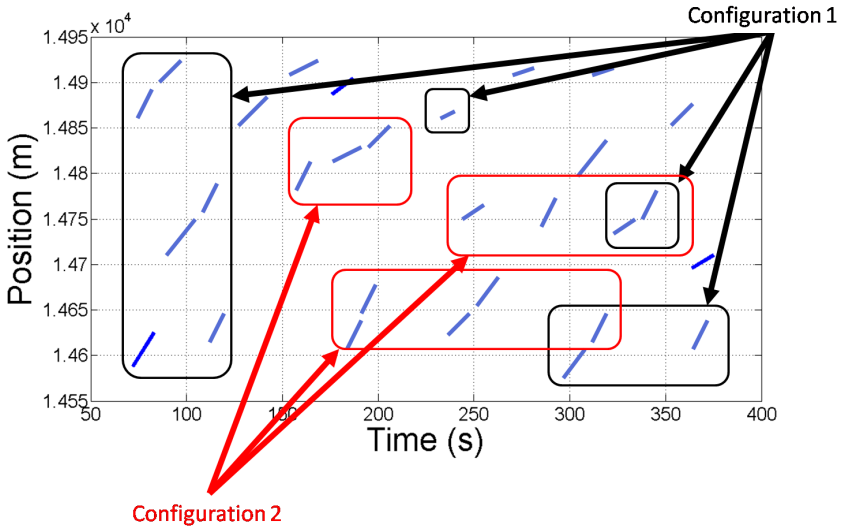

Figure 4.8: **Illustration of the choice of a subset of measurement data.** In this figure, each segment represents the domain of an internal condition (4.3), obtained using experimental data. We illustrate the choice of two subsets of 12 internal conditions among 28 speed measurements, which we call "configuration". The same process applies for Figure 4.7, bottom, with four different configurations involving 30 internal conditions each among 94 available speed measurements.

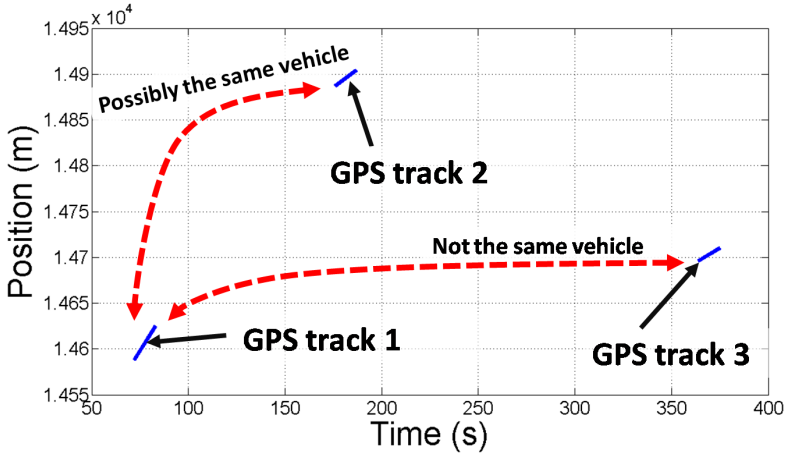

Figure 4.9: **Vehicle reidentification using linear programming.** This figure represents the domains of definition of three internal conditions of the form (4.3). The horizontal axis represents the time, while the vertical axis represents the spatial domain. For this specific problem, the solutions to (4.41) are as follows: the minimal value of $|L_1 - L_2|$ is zero, the maximal value of $L_1 - L_2$ is 196, and the minimal value of $|L_1 - L_3|$ is 164. This thus guarantees that the block ♯3 cannot originate from the same vehicle as the block ♯1. The block ♯2 can possibly come from the same vehicle as the block ♯1 (and indeed is), but we have no guarantee of this since the maximal possible value of $L_1 - L_3$ is nonzero.

Chapter 5

Conclusion

5.1 Contributions

This dissertation presented a new computational method for solving the Hamilton Jacobi (HJ) partial differential equation (PDE), as well as a new convex optimization-based estimation framework based on this computational method. Using the control framework of viability theory, we characterized the solutions to the HJ PDE by a Lax-Hopf formula and derived an important inf-morphism property. With these properties, we showed that the solution associated with piecewise affine initial, boundary and internal conditions can be computed as the minimum of solutions associated with affine initial, boundary and internal conditions. We then showed that the later can be computed explicitly, which enables the construction of a semi-analytic numerical scheme for computing the solutions to HJ PDEs. The key advantages of this numerical scheme over standard computational methods are its exactness and fast computational speed.

The semi-explicit expression of the solutions enabled us to derive the HJ PDE model constraints explicitly. Using the Lax-Hopf formula, we proved that these model constraints are convex. Given that the measurement data constraints are also convex, a large number of estimation problems for which the model is a HJ PDE can be posed as convex-optimization programs. We presented various practical applications of this framework, which were implemented as Linear Programs. Numerical applications using experimental data sets were performed.

Some of the estimation problems developed in this thesis have been implemented in the *Mobile Millennium* system, a real-time traffic flow monitoring system operated jointly by UC Berkeley and Nokia. The main application of this framework to *Mobile Millennium* has been the detection of faulty sensors. For this specific application, a set of algorithms runs in real time and checks the consistency of the data generated by more than 2000 sensors in Northern California every 30 seconds. These algorithms have already identified a number of faulty and misplaced sensors, which enables the *Mobile Millennium* system to run faster

and with greater confidence.

5.2 Open problems

5.2.1 Mathematical problems

Numerous mathematical and computational problems remain for the general problem of control and estimation of highway networks. The extension of this framework to the highway network as a whole is a very complex problem. Indeed, in networks, the boundary conditions of each computational domain are not necessarily known because sensors are not necessarily located at the edge of each link. Hence, while we assumed that the boundary conditions of the computational domain were known in the numerical examples presented in this thesis, this assumption is not necessarily satisfied in practice. In addition, the coupling between links induces additional mathematical difficulties when relating the model compatibility constraints from link to link. This is a major problem, which only has a partial solution in the case of LWR PDEs [53], and is still open for HJ PDEs.

The framework presented above could also be extended for the case in which we consider the viscosity solutions to the HJ PDE. While Barron-Jensen/Frankowska solutions and viscosity solutions to Hamilton-Jacobi equations can be shown to be equivalent for Lipschitz-continuous initial and boundary conditions, they differ when internal boundary conditions are present. In this case, the solution associated with the scalar conservation counterpart of the HJ PDE is the derivative of the viscosity (and not the B-J/F) solution of the HJ PDE. Hence, in order to extend this estimation framework to scalar conservation laws, one needs to derive the model compatibility constraints for viscosity solutions, which differ from the model constraints established in this dissertation. This extension would enable the estimation of quantities related to the density and flow functions, which are more easily observed than their integrals (the Moskowitz function).

Finally, the explicit mathematical link between weak boundary conditions in HJ PDEs and weak boundary conditions of the associated conservation laws is still not established. Neither is the proper functional space requirement needed to unify both theories.

5.2.2 Application problems

This framework has yet to be extended to other traffic estimation problems, such as queue length estimation, which is of great interest for traffic estimation in urban environments. These problems are usually driven by the periodic forcing of the boundary conditions by traffic lights or stop signs which results in periodic behavior of the flow. Solving such problems requires the identification of free-flow and congested areas, which is usually difficult since it involves the derivatives of the Moskowitz function. Thus, the resulting problems would be non-convex by nature, but may still be computationally tractable. Also, by nature

of the problem, shock waves appear periodically, which need to be incorporated in the method.

5.3 Future work

Future work will be first dedicated to extending the framework presented in this thesis to systems modeled by conservation laws. Preliminary analysis shows that if we consider the viscosity solutions to the HJ PDE, the resulting model compatibility constraints become non-convex, and the estimation problems take the general form of *mixed integer linear programs* (MILPs). MILPs are significantly harder to solve than LPs, but may still be tractable in real time for specific systems.

Estimation on general highway networks will be the second focus, in particular the problem of integrating a set of boundary condition constraints into the estimation problem. The state of networked highway sections is more complex to estimate, since the sections interact at their respective boundaries. Hence, the estimation of the state of traffic on the highway network cannot be decoupled into separate traffic estimation problems on highway sections. Integrating the boundary condition constraints between sections into the respective estimation problems yields a non-convex problem. Again, this problem may still be decomposed into a series of convex problems.

Finally, a promising avenue is to study how flow models can enable us to better estimate pollution levels in urban environments. While pollution can be directly measured and mapped, the integration of traffic flow estimates (with traffic flow emission models) into the problem of estimating urban pollution will improve the quality of the estimation. This problem is mathematically very challenging because of the coupling of both phenomena. It will however open the door to traffic flow control for controlling pollution levels in urban environment to safe limits.

Bibliography

[1] O. M. Aamo, A. Smyshlyaev, P. Rouchon, and P. Martin. Boundary control of a nonlinear Stefan problem. In *Proceedings of the IEEE Conference on Decision and Control*, pages 1309–1314, Maui, HI, Dec. 2003.

[2] P. Abbeel and A. Y. Ng. Apprenticeship learning via inverse reinforcement learning. In *Proceedings of the twenty-first international conference on Machine learning*, page 1. ACM, 2004.

[3] L. Alvarez-Icaza, L. Munoz, X. Sun, and R. Horowitz. Adaptive observer for traffic density estimation. In *Proceedings of the American Control Conference*, pages 2705–2710, Boston, MA, June 2004.

[4] S. Amin, A. Cardenas, and S. Sastry. Safe and Secure Networked Control Systems under Denial-of-Service Attacks. Number 5469 in Lecture Notes in Computer Science, pages 31–45. Springer, San Francisco, CA, 2009.

[5] R. Ansorge. What does the entropy condition mean in traffic flow theory? *Transportation Research*, 24B(2):133–143, 1990.

[6] J.-P. Aubin. *Viability Theory*. Systems and Control: Foundations and Applications. Birkhäuser, Boston, MA, 1991.

[7] J.-P. Aubin. Viability kernels and capture basins of sets under differential inclusions. *SIAM Journal of Control and Optimization*, 40:853–881, 2001.

[8] J.-P. Aubin, A. M. Bayen, and P. Saint-Pierre. Dirichlet problems for some Hamilton-Jacobi equations with inequality constraints. *SIAM Journal on Control and Optimization*, 47(5):2348–2380, 2008. Also available as a technical report, Preprint di Mathematica - n. 4, Scuola Normale Superiore, Pisa, Italy, May, 2006.

[9] J.-P. Aubin and A. Cellina. *Differential inclusions*. Springer-Verlag, New York, NY, 1984.

[10] J.-P. Aubin and H Frankowska. *Set Valued Analysis*. Birkhäuser, Boston, MA, 1990.

[11] A. Aw and M. Rascle. Resurrection of "second order" models of traffic flow. *SIAM journal on applied mathematics*, 60(3):916–938, 2000.

[12] M. Bardi and I. Capuzzo-Dolcetta. *Optimal Control and Viscosity Solutions of Hamilton-Jacobi-Bellman equations*. Birkhäuser, Boston, MA, 1997.

[13] C. Bardos, A. Y. Leroux, and J. C. Nedelec. First order quasilinear equations with boundary conditions. *Communications in partial differential equations*, 4(9):1017–1034, 1979.

[14] E. N. Barron and R. Jensen. Semicontinuous viscosity solutions for Hamilton-Jacobi equations with convex Hamiltonians. *Comm. Partial Differential Equations*, 15:1713–1742, 1990.

[15] Y. Bar-Shalom, X.R. Li, and T. Kirubarajan. *Estimation with applications to tracking and navigation*. Wiley-Interscience, 2001.

[16] A. M. Bayen, R. L. Raffard, and C. Tomlin. Network congestion alleviation using adjoint hybrid control: Application to highways. Number 1790 in Lecture Notes in Computer Science, pages 95–110. Springer Verlag, 2004.

[17] S. Blandin, D. Work, P. Goatin, B. Piccoli, and A. Bayen. A general phase transition model for vehicular traffic. *Preprint*, 2009.

[18] S. Boyd and L. Vandenberghe. *Convex Optimization*. Cambridge University Press, Cambridge, UK, 2004.

[19] A. Bressan. *Hyperbolic systems of conservation laws: the one dimensional Cauchy problem*. Oxford Lecture Series in Mathematics and its Applications, 20. Oxford University Press, Oxford, UK, 2000.

[20] A. Bressan, G. Crasta, and B. Piccoli. *Well-posedness of the Cauchy problem for nxn systems of conservation laws*. American Mathematical Society, 2000.

[21] W. Burghout. Hybrid microscopic-mesoscopic traffic simulation. *Royal Institute of Technology Doctoral Dissertation*, 2004.

[22] P. Cardaliaguet, M. Quincampoix, and P. Saint-Pierre. Optimal times for constrained nonlinear control problems without local controllability. *Applied Mathematics and Optimization*, 36:21–42, 1997.

[23] P. Cardaliaguet, M. Quincampoix, and P. Saint-Pierre. Set-valued numerical analysis for optimal control and differential games. In M. Bardi, T.E.S. Raghavan, and T. Parthasarathy, editors, *Stochastic and Differential Games: Theory and Numerical Methods*, Annals of the International Society of Dynamic Games, pages 177–247. Birkhäuser, 1999.

[24] S. Y. Cheung, S. C. Ergen, and P. Varaiya. Traffic surveillance with wireless magnetic sensors. In *Proceedings of the 12th ITS World Congress*, 2005.

[25] A. J. Chorin. Numerical solution of Boltzmann's equation. *Communications on Pure and Applied Mathematics*, 25(2):171–186, 1972.

[26] A. J. Chorin and X. Tu. Implicit sampling for particle filters. *Proceedings of the National Academy of Sciences*, 106(41):17249, 2009.

[27] P. D. Christofides. *Nonlinear and robust control of PDE systems: methods and applications to transport-reaction processes*. Birkhauser, 2001.

[28] P. H. Clarke, Y. S. Ledyaev, R. J. Stern, and P. R. Wolenski. Qualitative properties of trajectories of control systems: a survey. *Journal of dynamical and control systems*, 1(1):1–48, 1995.

[29] C. G. Claudel and A. M. Bayen. Solutions to switched Hamilton-Jacobi equations and conservation laws using hybrid components. Number 4981 in Lecture Notes in Computer Science, pages 101–115. Springer Verlag, Saint Louis, MO, 2008.

[30] C. G. Claudel and A. M. Bayen. Convex formulations of data assimilation problems for a class of Hamilton-Jacobi equations. *Submitted to SIAM Journal on Control and Optimization*, 2009.

[31] C. G. Claudel and A. M. Bayen. Lax-Hopf based incorporation of internal boundary conditions into Hamilton-Jacobi equation. Part I: theory. *IEEE Transactions on Automatic Control*, 55(5):1142–1157, 2010. doi:10.1109/TAC.2010.2041976.

[32] C. G. Claudel and A. M. Bayen. Lax-Hopf based incorporation of internal boundary conditions into Hamilton-Jacobi equation. Part II: Computational methods. *IEEE Transactions on Automatic Control*, 55(5):1158–1174, 2010. doi:10.1109/TAC.2010.2045439.

[33] R. M. Colombo. Hyperbolic phase transitions in traffic flow. *SIAM Journal on Applied Mathematics*, 63(2):708–721, 2002.

[34] J. M. Coron, B. d'Andrea-Novel, and G. Bastin. A strict Lyapunov function for boundary control of hypebolic systems of conservation laws. In *Proceedings of the American Control Conference*, pages 3319–3323, Paradise Island, Bahamas, Dec. 2004.

[35] M. G. Crandall, L. C. Evans, and P.-L. Lions. Some properties of viscosity solutions of Hamilton-Jacobi equations. *Transactions of the American Mathematical Society*, 282(2):487–502, 1984.

[36] M. G. Crandall and P.-L. Lions. Viscosity solutions of Hamilton-Jacobi equations. *Transactions of the American Mathematical Society*, 277(1):1–42, 1983.

[37] C. M. Crowe. Data reconciliation-progress and challenges. *Journal of Process Control*, 6(2):89–98, 1996.

[38] C. M. Dafermos. Polygonal approximations of solutions of the initial value problem for a conservation law. *Journal of Mathematical Analysis and Applications*, 38(1):33–41, 1972.

[39] C. Daganzo. The cell transmission model: a dynamic representation of highway traffic consistent with the hydrodynamic theory. *Transportation Research*, 28B(4):269–287, 1994.

[40] C. Daganzo. The cell transmission model, part II: network traffic. *Transportation Research*, 29B(2):79–93, 1995.

[41] C. Daganzo. A variational formulation of kinematic waves: basic theory and complex boundary conditions. *Transporation Research B*, 39B(2):187–196, 2005.

[42] C. Daganzo. On the variational theory of traffic flow: well-posedness, duality and applications. *Networks and Heterogeneous Media*, 1:601–619, 2006.

[43] A. Downs. *Still stuck in traffic: coping with peak-hour traffic congestion.* Brookings Inst Pr, 2004.

[44] L. C. Evans. *Partial Differential Equations.* Graduate Studies in Mathematics. American Mathematical Society, Providence, RI, 1998.

[45] L. C. Evans and P. E. Souganidis. Differential games and representation formulas for solutions of Hamilton-Jacobi-Isaacs equations. *Indiana University Mathematics Journal*, 33(5):773–797, 1984.

[46] G. Evensen. Using the extended Kalman filter with a multilayer quasi-geostrophic ocean model. *Journal of Geophysical Research*, 97(C11):17905–17924, 1992.

[47] G. Evensen. *Data Assimilation: The Ensemble Kalman Filter.* Springer-Verlag, Berlin Heidelberg, Germany, 2007.

[48] M. Falcone and R. Ferretti. Semi-Lagrangian schemes for Hamilton-Jacobi equations, discrete representation formulae and Godunov methods. *Journal of computational physics*, 175(2):559–575, 2002.

[49] M. Fliess, J. Levine, P. Martin, and P. Rouchon. Flatness and defect of nonlinear systems: introductory theory and examples. *International Journal of Control*, 61(6):1327–1361, 1995.

[50] M. Fliess, P. Martin, N. Petit, and P. Rouchon. Active signal restoration for the telegraph equation. In *IEEE Conference on Decision and Control*, volume 2, pages 1107–1111, 1999.

[51] G. F.Newell. A simplified car-following theory: a lower order model. *Transportation Research Part B: Methodological*, 36(3):195–205, 2002.

[52] H. Frankowska. Lower Semicontinuous Solutions of Hamilton-Jacobi-Bellman Equations. *SIAM Journal of Control and Optimization*, 31(1):257–272, 1993.

[53] M. Garavello and B. Piccoli. Traffic flow on networks. *American Institute of Mathematical Sciences, Springfield, MO, USA*, 2006.

[54] S. K. Godunov. A difference method for numerical calculation of discontinuous solutions of the equations of hydrodynamics. *Math. Sbornik*, 47:271–306, 1959.

[55] M. Grant and S. Boyd. CVX: Matlab software for disciplined convex programming, version 1.21. `http://cvxr.com/cvx`, July 2010.

[56] B. D. Greenshields. A study of traffic capacity. *Proceedings of the Highway Research Board*, 14:448–477, 1935.

[57] J. C. Herrera, D. B. Work, R. Herring, X. J. Ban, Q. Jacobson, and A. M. Bayen. Evaluation of traffic data obtained via GPS-enabled mobile phones: The Mobile Century field experiment. *Transportation Research Part C: Emerging Technologies*, 18:568–583, 2010.

[58] J.C. Herrera and A.M. Bayen. Incorporation of Lagrangian measurements in freeway traffic state estimation. *Transportation Research Part B: Methodological*, 44(4):460–481, May 2010.

[59] R. Herring, A. Hofleitner, P. Abbeel, and A. M. Bayen. Estimating arterial traffic conditions using sparse probe data. In *Proceedings of the 13th International IEEE Conference on Intelligent Transportation Systems*, Madeira Island, Portugal, 2010.

[60] B. Hoh, M. Gruteser, R. Herring, J. Ban, D. Work, J. C. Herrera, A. M. Bayen, M. Annavaram, and Q. Jacobson. Virtual trip lines for distributed privacy-preserving traffic monitoring. In *MobiSys*, Breckenridge, CO, June 2008.

[61] H. Holden and N.H. Risebro. *Front tracking for hyperbolic conservation laws*. Springer Verlag, New York, N.Y., 2002.

[62] P. L. Houtekamer and H. L. Mitchell. A sequential ensemble Kalman filter for atmospheric data assimilation. *Monthly Weather Review*, 129:123–137, 2001.

[63] T. Hunter, R. Herring, P. Abbeel, and A.M. Bayen. Path and travel time inference from GPS probe vehicle data. In *Proceedings of the Neural Information Processing Systems foundation (NIPS)*, Vancouver, Canada, 2009.

[64] C. Y. Kao, S. Osher, and J. Qian. Lax-Friedrichs sweeping scheme for static Hamilton-Jacobi equations. *Journal of Computational Physics*, 196(1):367–391, 2004.

[65] M. Krstic and A. Smyshlyaev. Adaptive boundary control for unstable parabolic PDEs. Part I: Lyapunov design. *IEEE Transactions on Automatic Control*, 53(7):1575, 2008.

[66] M. Krstic and A. Smyshlyaev. Backstepping boundary control for first-order hyperbolic PDEs and application to systems with actuator and sensor delays. *Systems & Control Letters*, 57(9):750–758, 2008.

[67] J. Kwon, C. Chen, and P. Varaiya. Statistical methods for detecting spatial configuration errors in traffic surveillance sensors. *Transportation Research Record: Journal of the Transportation Research Board*, 1870(1):124–132, 2004.

[68] P. D. Lax. Hyperbolic systems of conservation laws II. *Selected Papers Volume I*, pages 233–262, 2005.

[69] L. Leclercq. Bounded acceleration close to fixed and moving bottlenecks. *Transportation research. Part B: methodological*, 41(3):309–319, 2007.

[70] P. Le Floch. Explicit formula for scalar non-linear conservation laws with boudary condition. *Mathematical Methods in the Applied Sciences*, 10:265–287, 1988.

[71] R. LeVeque. *Numerical methods for conservation laws*. Birkhäuser, Basel, Switzerland, 1992.

[72] M. J. Lighthill and G. B. Whitham. On kinematic waves. II. A theory of traffic flow on long crowded roads. *Proceedings of the Royal Society of London*, 229(1178):317–345, 1956.

[73] X. Litrico. Robust flow control of single input multiple outputs regulated rivers. *Journal of Irrigation and Drainage Engineering*, 127(5):281–286, 2001.

[74] X. Litrico and V. Fromion. Boundary control of linearized saint-venant equations oscillating modes. In *Proceedings of the American Control Conference*, pages 2131–2136, Paradise Island, Bahamas, Dec. 2004.

[75] Highway Capacity Manual. Special report 209. *Transportation Research Board, Washington, DC*, 1985.

[76] I. Mitchell. A toolbox of level set methods. `http://www.cs.ubc.ca/ mitchell`, 2005.

[77] I. Mitchell. Games of two identical vehicles. Technical Report SUDAAR 740, Department of Aeronautics and Astronautics, Stanford University, Stanford, CA, July 2001.

[78] I. M. Mitchell, A. M. Bayen, and C. J. Tomlin. Computing reachable sets for continuous dynamic games using level set methods. *IEEE Transactions on Automatic Control*, 50(7):947–957, 2005.

[79] K. Moskowitz. Discussion of 'freeway level of service as influenced by volume and capacity characteristics' by D.R. Drew and C. J. Keese. *Highway Research Record*, 99:43–44, 1965.

[80] G. F. Newell. A simplified theory of kinematic waves in highway traffic. *Transporation Research B*, 27B(4):281–303, 1993.

[81] M. Papageorgiou. Some remarks on macroscopic traffic flow modelling. *Transportation Research Part A: Policy and Practice*, 32(5):323–329, 1998.

[82] N. Petit. *Delay Systems. Flatness in Process Control and Control of some Wave Equations*. PhD thesis, Ecole des Mines de Paris, Centre d'Automatique et des Systèmes, Paris, France, 2000.

[83] L.A. Pipes. Car following models and the fundamental diagram of road traffic. *Transportation Research*, 1(1):21–29, 1967.

[84] C. Prieur and J. de Halleux. Stabilization of a 1-D tank containing a fluid modeled by the shallow water equations. *Systems & Control Letters*, 52(3-4):167–178, 2004.

[85] T.S. Rabbani, F. Di Meglio, X. Litrico, and A.M. Bayen. Feed-forward control of open channel flow using differential flatness. *IEEE Transactions on Control Systems Technology*, 18(1):213–221, 2009.

[86] P. I. Richards. Shock waves on the highway. *Operations Research*, 4(1):42–51, 1956.

[87] R.T. Rockafellar. *Convex Analysis*. Princeton University Press, 1970.

[88] P. Saint-Pierre. Approximation of the viability kernel. *Applied Mathematics and Optimization*, 29:187–209, 1994.

[89] J. A. Sethian. *Level Set Methods and Fast Marching Methods*. Cambridge University Press, New York, NY, 1999.

[90] R. C. Smith and M. A. Demetriou. *Research Directions in Distributed Parameter Systems*. SIAM, Philadelphia, PA, 2000.

[91] I. S. Strub and A. M. Bayen. Weak formulation of boundary conditions for scalar conservation laws. *International Journal of Robust and Nonlinear Control*, 16:733–748, 2006.

[92] D. Sun and A. M. Bayen. Multicommodity Eulerian-Lagrangian large-capacity cell transmission model for en route traffic. *Journal of Guidance Control and Dynamics*, 31(3):616, 2008.

[93] X. Sun, L. Munoz, and R. Horowitz. Methodological calibration of the cell transmission model. In *Proceedings of the American Control Conference*, Boston, MA, June 2004.

[94] O. P. Tossavainen, J. Percelay, A. Tinka, Q. Wu, and A.M. Bayen. Ensemble kalman filter based state estimation in 2d shallow water equations using lagrangian sensing and state augmentation. In *47th IEEE Conference on Decision and Control, 2008*, pages 1783–1790, 2008.

[95] P. Varaiya. Reducing highway congestion: an empirical approach. *European Journal of Control*, 11(4-5), 2005.

[96] Y. Wang and M. Papageorgiou. Real-time freeway traffic state estimation based on extended Kalman filter: a general approach. *Transportation Research Part B: Methodological*, 39(2):141–167, 2005.

[97] D. Work, S. Blandin, O. Tossavainen, B. Piccoli, and A. Bayen. A distributed highway velocity model for traffic state reconstruction. *Applied Research Mathematics eXpress (ARMX)*, 1:1–35, April 2010.

[98] D. Work, O.P. Tossavainen, S. Blandin, A. Bayen, T. Iwuchukwu, and K. Tracton. An ensemble Kalman filtering approach to highway traffic estimation using GPS enabled mobile devices. In *Proceedings of the 47th IEEE Conference on Decision and Control*, pages 2141–2147, Cancun, Mexico, December 2008.

[99] Q. Wu, X. Litrico, and A. M. Bayen. Data reconciliation of an open channel flow network using modal decomposition. *Advances in Water Resources*, 32(2):193–204, 2009.

[100] H. M. Zhang. A theory of nonequilibrium traffic flow. *Transportation Research Part B: Methodological*, 32(7):485–498, 1998.

[101] `http://traffic.berkeley.edu/`.

[102] http://www.ngsim.fhwa.dot.gov/.

[103] http://pems.eecs.berkeley.edu.